CHAPTER 5

CHARACTERISTICS OF PARYLENE-C FILM

5.1 Overview

In this chapter, a systematical study of some parylene-C's properties is performed and discussed. To explore parylene-C's mechanical, rheological, and viscoplastic properties, the chapter starts with the introduction of parylene-C's polymer properties: polymerization, densification, and oxidation followed by a detailed study of crystallization/densification and discussions about them. It shows that the crystallization is one of the major effects causing parylene-C to behave differently after thermal treatment.

The mechanical properties, rheological properties and viscoplastic properties of the parylene-C film were studied using TA Instruments DMA Q800. Among many mechanical properties, Young's modulus, tensile strength and elongation are primarily concerning in terms of implantation applications and therefore were considered in this chapter. Mechanical properties can be known by many ways. For example, Young's modulus and residual stress can be obtained simultaneously by load-deflection approach [103, 138]. In our study, mechanical properties were obtained by uniaxial tensile test due to its simplicity and popularity.

Although it has been long since people started to use parylene-C in the implantable devices, its rheological properties and viscoplastic properties have not been

thoroughly studied yet. By using the same testing setup as mentioned above, creep and stress relaxation, and viscoplastic properties were measured as well. These properties provide very important information for parylene-C-based medical devices in terms of their fabrication and later implantation in human bodies. With the knowledge of these properties, the life-time of the devices is predictable, the device fabrication time could be reduced, and the residual stress generation by annealing the device at a proper temperature is avoidable.

It also shows that the rheological testing results of parylene-C film are highly temperature-dependent. To understand this, except the crystallization results, the glass transition temperature was measured by both dynamic mechanical analysis (DMA) approach and a ramping-temperature-dependent modulus experiment. Both obtained results were compared and discussed to explain the rheological testing results.

5.2 Introduction to Parylene-C Polymerization

The current most common way to prepare Parylene-C film is done by chemical vapor deposition invented by W. F. Gorham in 1966 [172]. Gorham's approach is also commonly used to prepare other parylene (poly-para-xylylene) family members, such as parylene-N (poly-para-xylylene), parylene-D (poly-dichloro-para-xylylene), parylene-C (poly-chloro-para-xylylene), or parylene-HT (or parylene-F, poly-tetrafluoro-para-xylylene) to name a few. During the parylene-C preparation, the parylene-C dimer is sublimated at elevated temperature (180°C in our deposition process), and pyrolysed at 690°C. The parylene-C film can conformally deposit onto the substrate and also the temperature of the chamber wall could range from -196°C to room temperature [173,

174]. Because the paylene-C polymerizes right from the gaseous type, the process is also called vapor deposition polymerization (VDP) [175].

It is parylene-N polymerization which was first focused on and studied. Errede published the mechanism of polymerization of prylene-N in 1960 [176]. Rather than using Gorham's vapor deposition approach to get the parylene-N film, Errede prepared p-xylylene monomer liquid solution at -78°C. Polymerization happens when the solution is disturbed by momentary contact with a warm surface. Beach proposed a model for the vapor deposition parylene-N for the first time in 1978 [177]. Gaynor, Rogojevic and Fortin also developed different kinds of models to describe the vapor deposition of parylene-N thin film after Beach [178–180].

Some of previous researchers' important findings are summarized in this section. The molecular weight of parylene-N is found to be 200,000 to 400,000 g/mol, which corresponds to 2000–4000 units per chain length [178]. In addition, the deposition rate of parylene-C is found to decrease as the deposition temperature rises, which is opposite to the regular chemical vapor deposition reaction that shows higher deposition rate as the deposition temperature rises. It is suggested that the higher deposition rates of the parylene family at lower temperature are caused by increased monomer condensation rate on the substrate surfaces [181].

5.3 Densification

Densification means the polymer chain becoming more compact than its original chain structure. Theoretically speaking, densification can be caused by thermal treatment which gives polymer chain energy to move, or by stretch force which causes the polymer chain to align closer. In densification, the polymer chains do not need to be well

organized to form a lamella, but the polymer chains are getting closer to fill in the voids of the material, which usually results in the reduction of the volume. Therefore, the densification can be observed by measuring the materials' dimension. There hasn't been too much research work done to study the densification of the parylene-C film to our best knowledge. The first related study could be found to be done by Wu in 1995 [182]. Wu and the coworkers measured in situ the thickness of parylene-N and parylene-F at elevated temperature up to the sample decomposing. Their results showed no thickness reduction or increment before the samples decomposed, regardless of whether the annealing was done in air, nitrogen or vacuum. In 2005, Huang et al. published a paper studying the glass transition temperature of ultra-thin parylene-C film (21 nm) deposited on silicon substrate by in situ measuring the film's thickness change [183]. They used an ellipsometer to measure the thickness of the sample from temperature at 0°C to 120°C. The results showed that the thickness increases monotonically, with a thermal expansion coefficient turning point occurring at the glass transition temperature or so. In spite of their successful findings of the glass transition temperature, the thermal expansion coefficients found from their results showed a value of 1190 ppm and 2143 ppm below and above the glass transition temperature, respectively. Because of the contradiction between Wu and Huang, it is of interest to measure the parylene-C film thickness change in the usage thickness range.

In this section, the densification of 20-µm-thick parylene-C film is studied at 100°C. In addition, the parylene-C film's length change during thermal annealing at ramping rate of 3.33°C/min is measured as well.

5.3.1 Thickness-change measurement

To measure the thickness change of 20-µm-thick parylene-C film, a layer of parylene-C film of 20 µm thickness was first deposited on top of a clean glass plate. A parylene-C step was then created by stripping part of the parylene-C film for later thickness measurement. Parylene-C film was put in the convection oven which was preheated at 100°C for a targeted duration. When time was up, the parylene-C was taken out and cooled down to room temperature. A KLA-Tencor P-15 profiler was used to measure the parylene-C thickness. The measurement was performed before the thermal annealing and every time the parylene-C film was cooled down. 5 data points at different positions were obtained in each measurement corresponding to each annealing time.
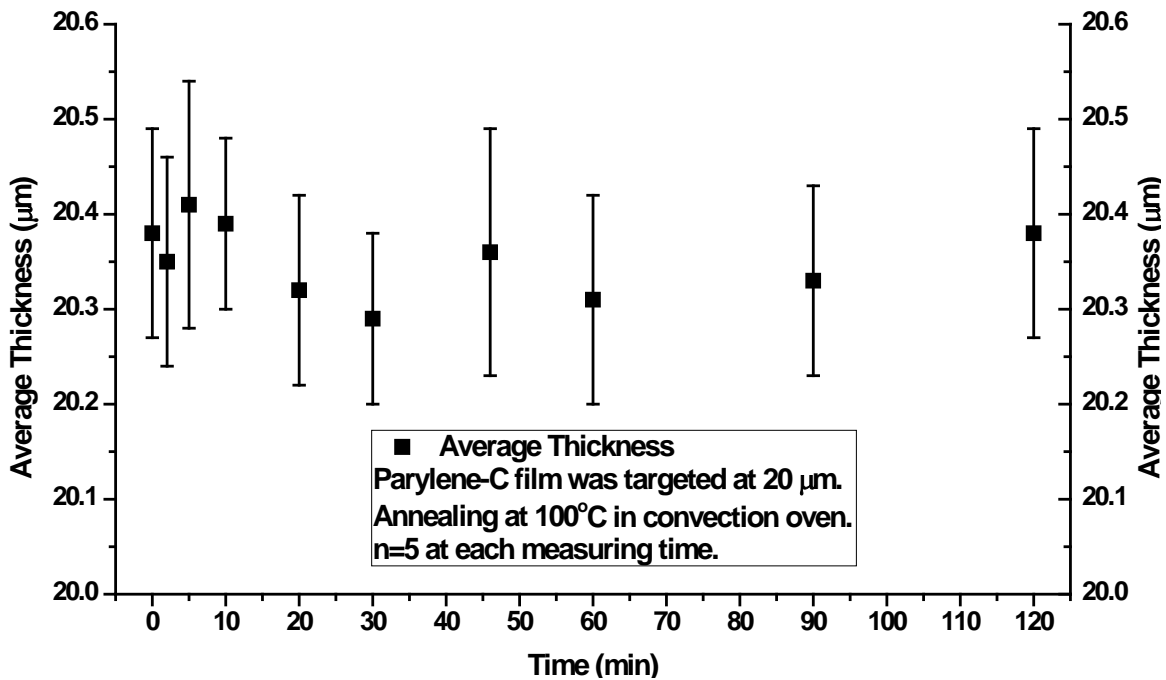
Figure 5-1: Measured thickness of 20 µm parylene-C film annealed at 100°C in the convection oven

The obtained thickness data versus annealing time is shown in Figure 5-1. Although there is some variation (error bar) at each measurement, the average thickness falls in a constant range without too much change during the thermal annealing. The changing of the average thickness versus time cannot show any correlation between the thickness and annealing time as the thickness always lies in the error range. The results demonstrate that the parylene-C film thickness change is not detectable within the 2 hours of annealing at 100°C in convection oven with our current measuring capabilities. Our measuring data agrees well with Wu's results. It might be due to the thickness effect that Huang's parylene-C film behaves differently.

5.3.2 In situ length-change measurement during thermal annealing

5.3.2.1 Length change under long-time thermal annealing process at 100°C

An experiment monitoring the length change of the parylene-C film during the thermal annealing was also conducted. With the same sample thickness prepared as above (as-deposited parylene-C film), the free standing parylene-C film was cut into 5.3 mm (W) by 10mm (L) in dimension and mounted onto the clamps of the DMAQ800 with a tiny little force (0.0027N). The chamber temperature was ramped up to 100°C in the machine's fastest way and the length of the sample was monitored at the same time. After the chamber was thermally stabilized, the sample was annealed in this environment for eight hours to observe its length change. Once the annealing is done, the chamber was then fast cooled down to room temperature by blowing cool nitrogen gas into the chamber. The whole system was kept in room temperature for another two hours to observe the parylene-C film length change.

The obtained length change of parylene-C film annealed at 100°C is shown in Figure 5-2. All system response is corrected and thus the data shown represents the true parylene-C film response. Figure 5-2 (a) shows the length change of the whole annealing and cooling period. Figure 5-2 (b) shows the closer view of the length response of the parylene-C film between 0–2.5 minutes. Figure 5-2 shows that the as-deposited parylene-C film length actually shrinks when the environmental temperature increases higher than ∼ 40°C. The rate of the length change reduces after the temperature reaches the target temperature, and slows down. In Figure 5-2 (b), it is observed that the sample length actually elongates before 0.25 minutes, which corresponds to 38.76°C in the raw data, and start to shrink afterward. It infers that the parylene-C starts to have some structural change at 38.76°C and thus the length shrinks. The hypothesis of this phenomenon is that the parylene-C is likely to start to crystallize at 38.76°C. As from the conventional wisdom of solid state thermodynamic transitions regarding the glass transition, no crystallization should be able to take place below the glass transition temperature [184, 185], plus the parylene polymer chain orientation is proved to lie in the plane of the film [186], Figure 5-2 could be treated as an evidence that the parylene-C film crystallization starts from temperature at 38.76°C, i.e., the onset of glass transition range. The concept and experiments regarding the glass transition temperature will be discussed more in detail in Section 5.6. It is postulated that the parylene polymer chain folds into several lamellae, constituting the spherulite of the parylene-C. Therefore, the parylene-C length reduces during this crystallization process. The slowly length shortening after thermally stabilized at 100°C is likely attributed to the slow isothermal crystallization behavior, which will be studied by XRD approach in Section 5.5.
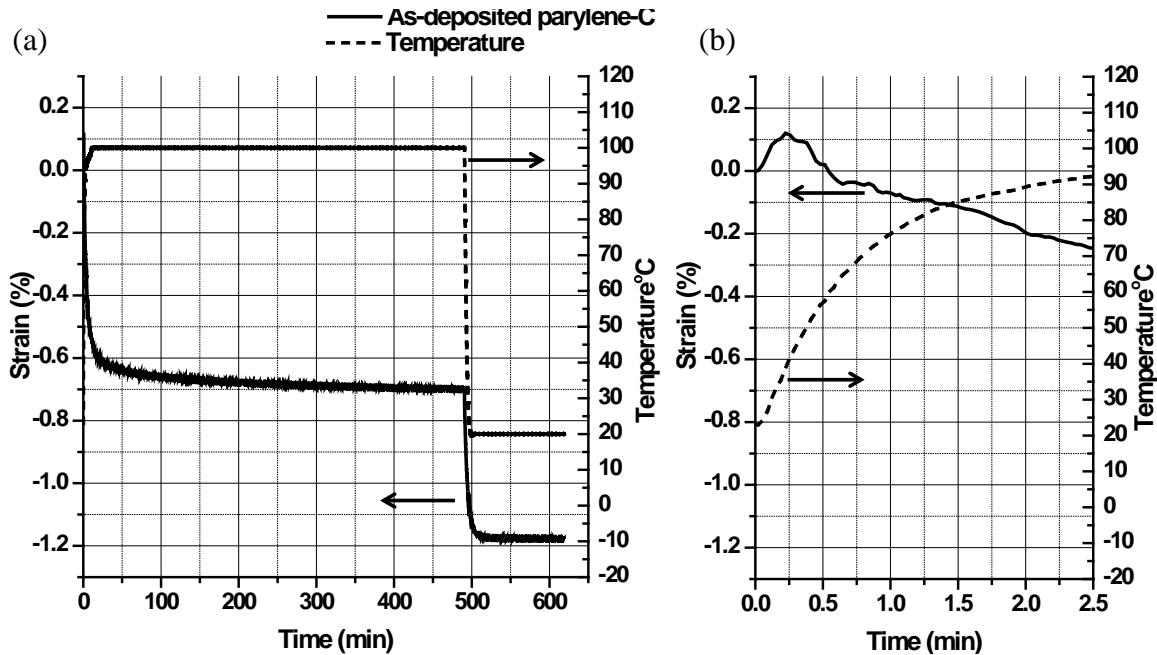
Figure 5-2: (a) Obtained length change of the parylene-C film annealed at 100°C in air for 8 hours, and (b) a closer view of the length change during the first 2.5 minutes

In order to further prove that the as-deposited parylene-C is crystallized during the annealing process, the parylene-C sample previously annealed at 100°C for eight hours was tested again in the same annealing condition for another two hours, and the testing results is shown in Figure 5-3. It can be clearly seen that, rather than length shrinkage, the parylene-C film expands during the early temperature ramping up period, which is totally opposite to the as-deposited parylene-C's results. Although the parylene-C is very likely still crystallizing during this period, the thermal expansion effect of the parylene spherulite dominates the length change. Thus the overall effect shows that the parylene-C film is expanding. After the chamber is thermally stabilized again, the parylene-C film has no (or very little) expansion and the crystallization mechanism dominates the length change again. The thermal coefficients of expansion (TCE) of as-deposited and annealed parylene-C film are also estimated from Figure 5-2 (a) and Figure 5-3. Three TCE

obtained from these two figures are shown in the first three columns of Table 5-1: TCE of the 8-hours-annealed sample cooled down, TCE of the annealed sample heated up, and TCE of the 10-hours-annealed sample cooled down.
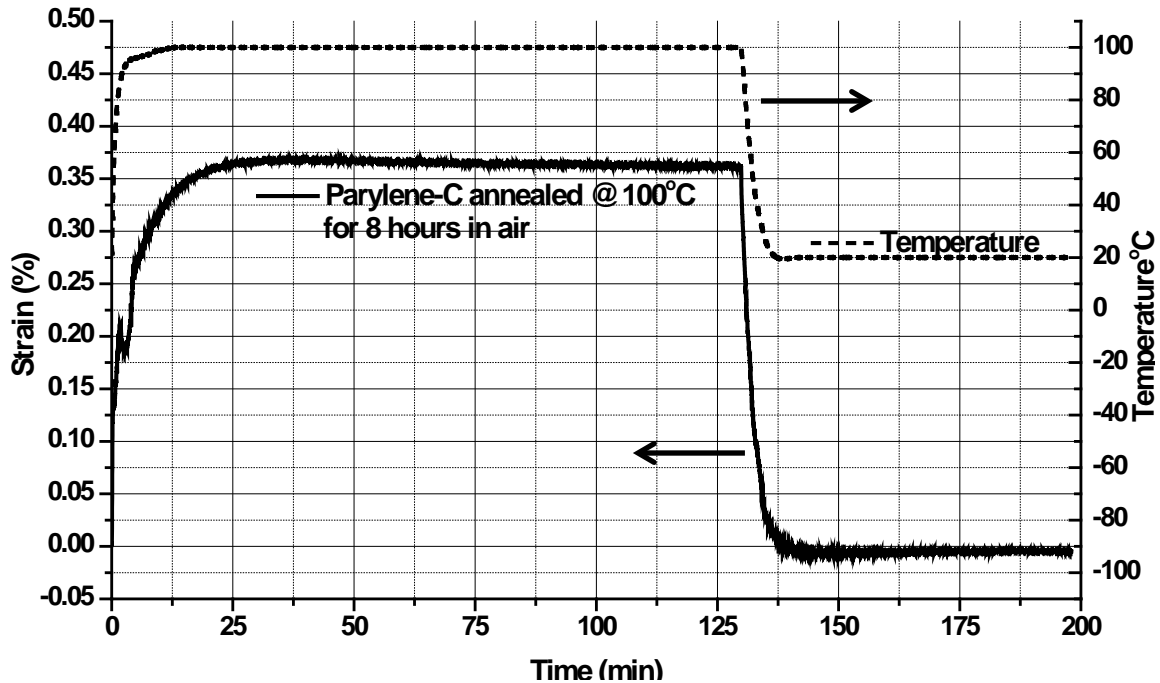
Figure 5-3: Length change of the parylene-C film which was annealed at 100°C in air for 8 hours in the previous test. The sample was annealed again at 100°C for another 2 hours.

Table 5-1: Table of thermal coefficients of expansions obtained in different states of the parylene-C film. The literature values are also listed for comparison.

	Annealed 8 hours at 100°C, cooled down to room temperature (Figure 5-2 (a))	Followed from the previous sample and heated up to 100°C (Figure 5-3)	Annealed another 2 hours and cooled down to room temperature (Figure 5-3)	As-deposited parylene-C heated up to transition (Figure 5-4)	Literature value by Beach [101]	Experimental value obtained by Dabral [110]
TCE (ppm)	60	56.3	58.8	35.5	35	50

5.3.2.2 One cycle thermal annealing treatment

Although the TCE below parylene-C's glass transition temperature can be obtained from the experiments described in Section 5.3.2.1, the temperature ramping, however, is extremely fast in that case. Therefore another test under a slower temperature ramping rate was performed to verify the expansion behavior below and above the glass transition temperature and the results are shown in Figure 5-4. It could be seen that in a slower temperature ramping profile, the sample expands until 53.75°C owing to the thermal expansion and starts to shrink afterward. The temperature, 53.75°C, actually agrees perfectly well with our glass transition found in Section 5.6 and therefore it is hypothesized that the parylene-C starts to crystallize at 53.75°C. The expansion phenomenon above 120°C is likely due to the dominating oxidation effect. The oxygen atoms are involved into the parylene-C structure and therefore expand the parylene-C sample again until it gets decomposed at 240°C.

The obtained TCE of each region is shown in Table 5-1. From Table 5-1, the TCE of annealed parylene-C usually lies in the range of 56.3–60 ppm. The TCE obtained before parylene-C's glass transition is 35.5 ppm, which agrees well with Beach's literature value measured at 25°C [101]. The difference of the TCE between annealed and as-deposited parylene-C can be explained on the basis of changes in the parylene-C's properties due to annealing which gives parylene-C higher crystallinity [110]. More discussion and study of crystallinity will be in Section 5.5. In addition, Dabral obtained TCE as 50 ppm from his annealing samples below 150°C. The difference between his result and our TCE result is about 11.2–16.7%. Apart from the measuring resolution errors, it is very likely that Dabral's parylene-C film has been annealed up to 250°C,

which could introduce another polymer structure transition from α form to β form. Thus the Dabral's TCE could represent the property of β-form parylene-C film while ours could represent α form as our sample annealed only up to 100°C.
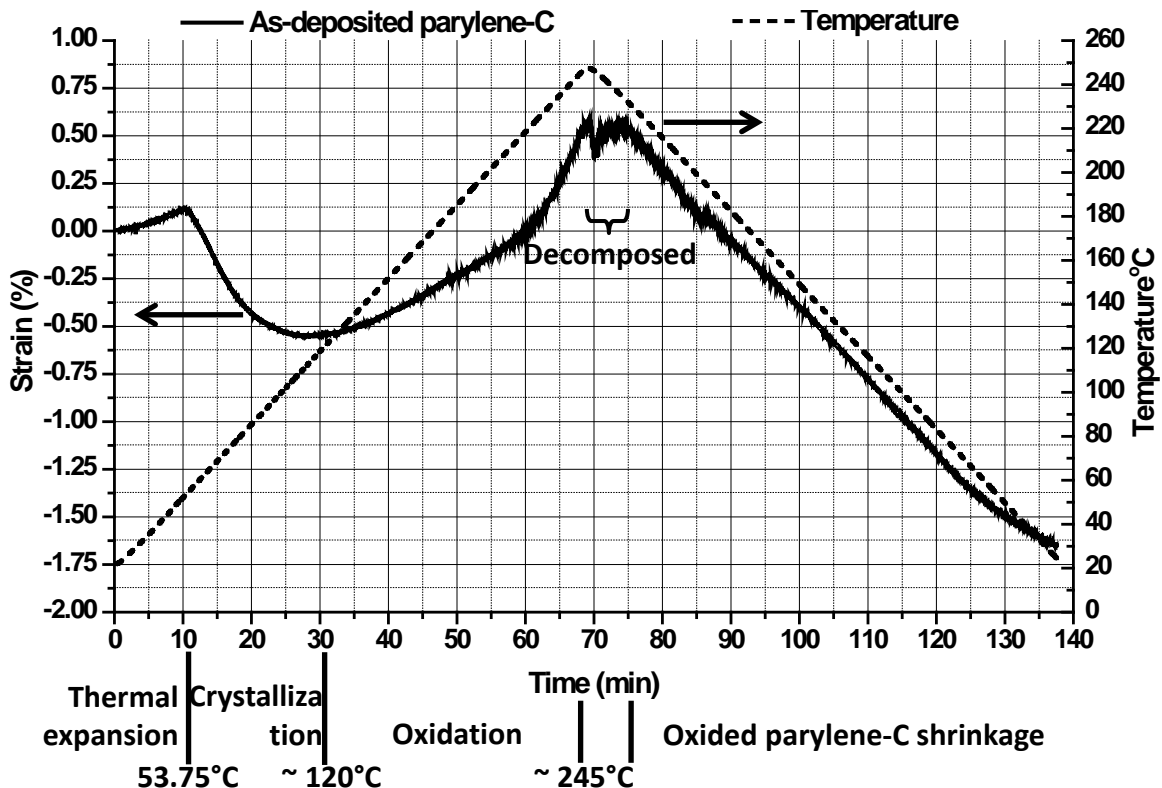
Figure 5-4: Length change of parylene-C film annealed under the temperature ramping rate at 3.33°C/min and its hypothesized phenomenon interpretation by dominant effect

5.3.2.3 Cyclic thermal annealing treatment up to 120°C

The experiment done in Section 5.3.2.2 shows only one cycle of parylene-C thermal annealing. The TCEs before and after the thermal annealing are found. Figure 5-4 also demonstrates that the parylene-C sample decomposed at ~ 240°C in the normal air environment. In this section, another experiment was designed to study the behavior of the parylene-C sample annealed under cyclic thermal conditions. As-deposited

parylene-C film was still used during the tests. The annealing temperature ramped from 20°C to 120°C at the ramping rate of 3.33°C/min. Right after the temperature reached 120°C, it cooled down to 20°C at the rate of -3.33°C/min. The chamber temperature was then maintained at 20°C for another 30 min. Six cycles were executed in this experiment and the temperature profile is demonstrated in Figure 5-5.

The measuring results are shown in Figure 5-5 and Figure 5-6. It can be seen that the parylene-C first expanded as expected until temperature reached 60°C, which can be identified as the glass transition temperature. The strain decreased dramtically to ~ -1.4% when the temperature reached 120°C, meaning the parylene-C sample was shrinking as annealing temperature increased over 60°C. The strain further decreased when the temperature decreased from 120°C to 20°C as well. However, the shrinkage showed more linear proportional to the temperature during this state than when the temperature-ramped from 60–120°C in the first state. The strain shrank to ~ -2% when the temperature reached 20°C. Furthermore, the film expanded pretty linearly proportionally to the temperature when the temperature either ramped up from 20°C to 120°C or cooled down to 20°C again in the second and later cycles. More detailed quantitative results are shown in Table 5-2. The TCE was found as 29.2 ppm in the first expansion state until 60°C and -249.6 ppm in average when parylene-C shrank to -1.41% afterward until 120°C. The TCE became 59.8 ppm during the first cooling process. The obtained TCEs of the second and later cycles were always higher than the literature value, 35 ppm. It is evident that the parylene-C experienced either transition, transformation, or crystallization, etc. during 60–120°C. Therefore, after the first-time annealing, the parylene-C possesses different thermal properties than the as-deposited one.
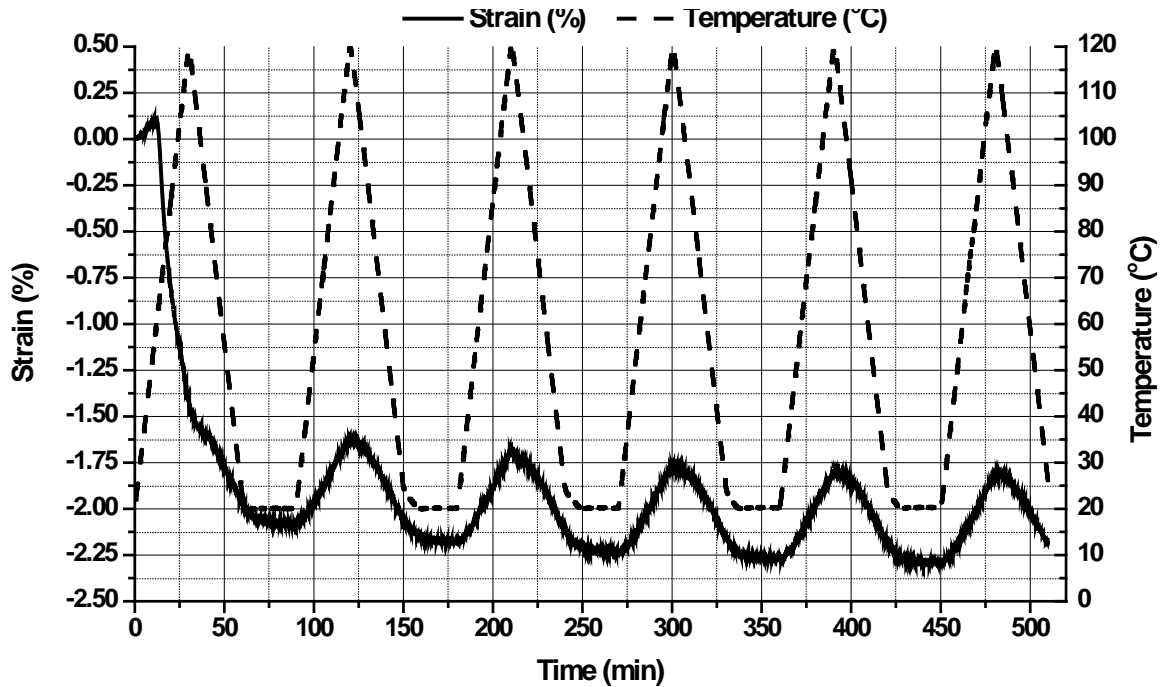
Figure 5-5: Six cycles of thermal annealing of parylene-C film up to 120°C: The length

of the film never goes back to its original length after the first-time thermal annealing.
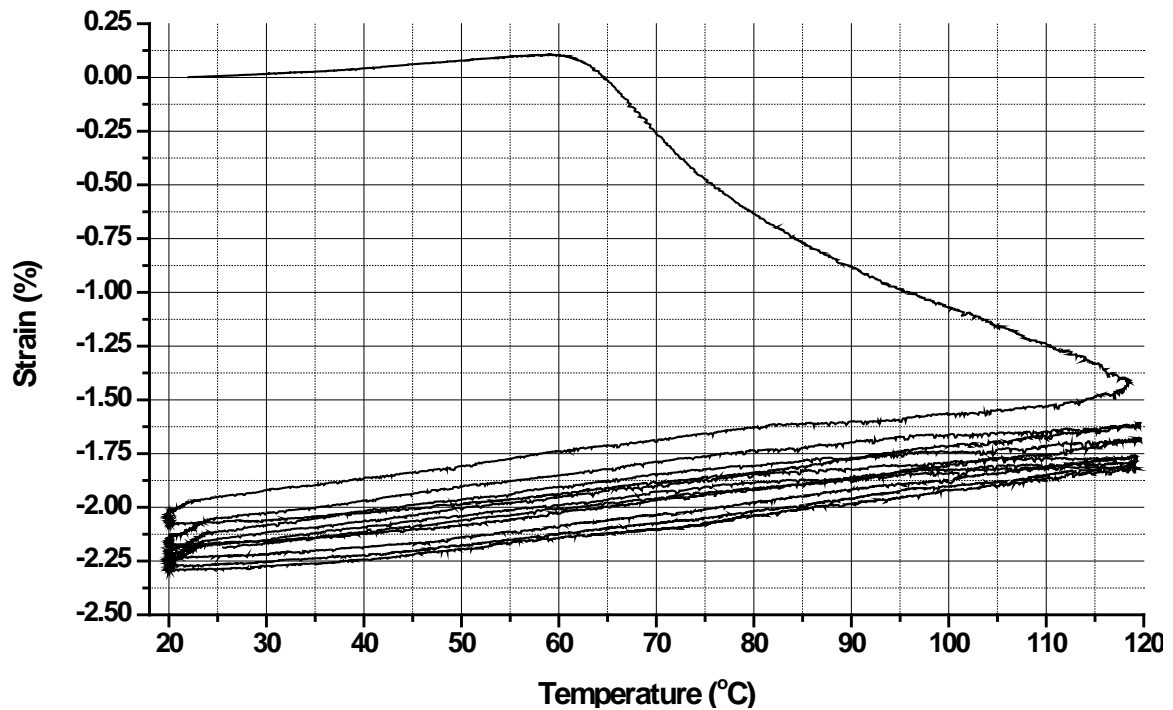
Figure 5-6: The parylene-C film behaves differently after the first-time thermal

annealing.

Table 5-2: Derived TCEs from six cycles shown in Figure 5-5 and Figure 5-6

n^{th} cycle		1			2		3		4		5		6	
Temperature range (°C)	From	22.0	57.9	118.6	20.0	119.7	20	119.7	20	119.3	20	119.3	20	119.4
	To	57.9	118.6	20.0	119.7	20	119.7	20	119.3	20	119.3	20	119.4	25.5
Strain variation (%)	From	0	0.105	-1.41	-2.08	-1.61	-2.18	-1.69	-2.23	-1.77	-2.27	-1.78	-2.29	-1.82
	To	0.11	-1.41	2.0	-1.61	-2.15	-1.69	-2.20	-1.77	-2.23	-1.78	-2.25	-1.82	-2.19
TCE (ppm)		29.2	249.6	59.8	47.4	53.9	49.1	51.2	46.3	46.3	49.3	47.3	47.3	39.4

5.3.3 Summary

Three experiments measuring the length change during the parylene-C thermal annealing were done. In the past, it was generally believed that the parylene-C film expands when it is heated up. In our tests, however, the as-deposited parylene-C film actually expands only up to the glass transition temperature and shrinks afterward until the temperature reaches 120°C. It is likely due to the crystallization effect above the glass transition temperature. The experimental results also show that the parylene-C sample expands again after 120°C, which is believed that the oxidation dominates this stage and oxygen atoms get involved into the parylene-C structure. The sample decomposed at temperature higher than 245°C. The thermal coefficients of expansion of as-deposited and annealed parylene-C film are found to be different. The thermal coefficient of expansion of as-deposited parylene-C is found pretty similar to the literature value, but it becomes higher after the thermal annealing. This is likely attributed to the higher crystallinity of annealed samples. Due to the miniature size of the MEMS devices, this thermal expansion effect and difference can be a critical issue when designing the parylene-C related MEMS devices and thus should be considered in the devices' design to avoid unwanted cracks or residual stress.

5.4 Oxidation

Like many other kinds of polymers, parylene-C can get oxidized by either thermally heating [187–189] or by UV light photoluminescence [190–194]. Because parylene-C is transparent, colorless, and conformal well to all irregularities, and has low permeability to air and moisture, and pin-hole free material structure, it has been used for conservation materials [187]. Therefore, research about parylene-C oxidation should focus more on predicting the lifetime of the as-deposited parylene-C film. Nowlin et al. published a paper studying the thermal oxidation of parylene-C film at temperatures between 125 to 200°C [189]. Nowlin used neutron activation (NA) oxygen analysis to quantitatively analyze the oxidative degradation of the parylene-C film's mechanical properties. Their result indicates that the amount of oxygen incorporated into the parylene-C before a significant degradation in mechanical properties is 5000 ppm. The activation energy for the parylene-C oxidation is found to be 27±3 kcal/mole. The temperature for 100,000 hour lifetime use of parylene-C is predicted as 72°C. In addition, they used IR spectrometer to conclude that the oxidation took place throughout the entire sample, not just on the surface. By IR spectrometry, Nowlin also claimed that the oxidized species produced during the oxidation process should be in the form shown in Figure 5-7, which contained the carbonyl bond, rather than the cleavage of the carbon-carbon bond. Baker founded in 1977 that no aging effects of yield stress and tensile modulus were noted in the parylenec-C annealed at 71°C [195]. Monk also suggested in 1997 that 105°C is the recommended maximum annealing temperature where parylene-C will not crack in their encapsulation coatings [188], which infers very little oxidation happens at those temperatures. In this section, the oxidative behavior will be first studied

by XPS (photoelectron spectroscopy) and FTIR (Fourier transform infrared spectroscopy). The corresponding mechanical properties will be discussed in later sections.
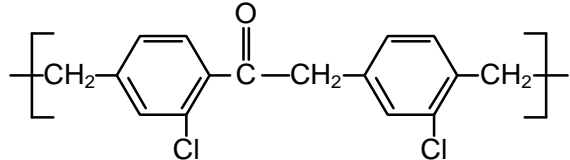
Figure 5-7: The oxidative species of parylene-C proposed by Nowlin [189]

5.4.1 XPS

XPS (X-ray photoelectron spectroscopy) is widely used by chemists in surface chemistry analysis. In XPS, the high-energy x-ray photons are emitted onto the material surface and the material's electrons are excited and come out due to the "photoelectron effect". The escaped electrons are collected by the detector and their corresponding electron energy (or binding energy) is analyzed. Because electrons' binding energy are different from molecule to molecule, the material's surface compound can be derived according to these obtained binding energy data. The XPS machine we used is M-Probe XPS by Surface Science Instruments. Argon sputter was always on to calibrate the peak which represents carbon at 285 eV.

To measure the level of the oxidation of the parylene-C film versus the annealing time, several as-deposited parylene-C films were annealed at 200°C in convection oven for different time durations. A figure of typical XPS scanning results representing four different oxidation treatments is shown in Figure 5-8: as-deposited, 200°C for two minutes, 200°C for one hour, and 200°C for two days, all in the convection oven. The XPS faithfully displays the chemical contents of parylene-C. The chlorine is shown by

two peaks of 199.9 eV (2p) and 270 eV (2s), respectively, and carbon is shown at the peak of 284.6 eV. If the oxygen exists on the parylene-C surface, the XPS can find it as a peak located at 531.6 eV. To clearly see the difference of oxygen peaks between parylene-C films of different treatment, a closer view around the oxygen peak at 531.6 eV is also magnified in the top left of Figure 5-8. The contents of the three atoms (oxygen, carbon and chlorine) can be calculated by integrating over every peak representing the corresponding atom, and the percentage is shown in Table 5-3. From the XPS results of as-deposited parylene-C film, it can be found that the ratio of contents of chlorine to carbon is about 1:8, which agrees well with the parylene-C's chemical compound structure. The correct XPS-measured ratio demonstrates the accuracy of the XPS equipment.
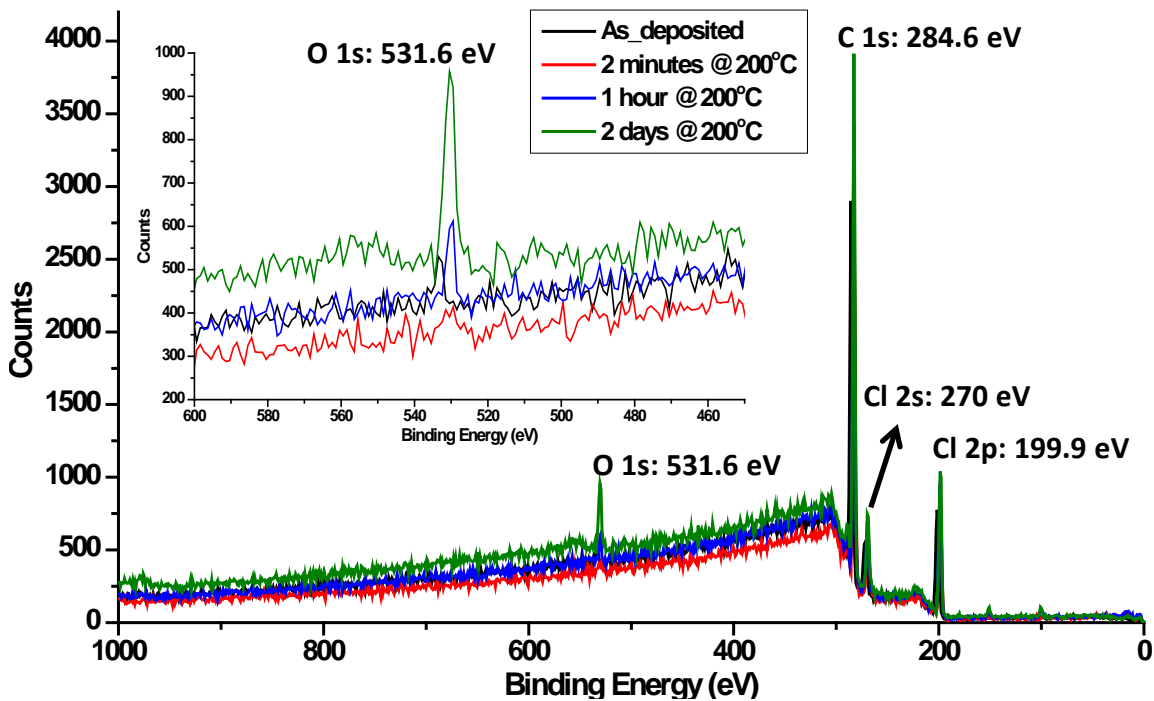
Figure 5-8: Typical XPS results of parylene-C samples. Top left: A closer view of the peak of 531.6 eV representing the content of oxygen

Table 5-3: Measured atom percentage of chlorine, carbon, and oxygen for different oxidative parylene-C films

	Atom Percentage		
Parylene-C treatment	Chlorine	Carbon	Oxygen
As-deposited	10.46	84.76	4.78
200°C 2 min. in air	13.00	87.00	Non-detectable
200°C 1 hour in air	12.57	84.44	2.99
200°C 2 days in air	11.41	82.03	6.56
200°C 2 days in vacuum	12.06	85.11	2.83

From Figure 5-8, and Table 5-3, it is observed that a small amount of oxygen signal can be originally found in the as-deposited parylene-C. After baking at 200°C in the air for the first 2 minutes, the oxygen peak becomes non-detectable by XPS. It infers that the oxygen found in the as-deposited parylene-C is likely from the moisture contamination, and it disappears after few minutes of baking. In terms of oxidation, the oxygen peak becomes detectable again after thirty minutes of annealing at 200°C in our experiments. The oxygen peaks shown in Figure 5-8 get higher when the annealing time gets longer, which means that parylene-C on the sample surface gets more oxidized during the annealing process.

Because oxidation can deteriorate the mechanical properties of the parylene-C [101], it is generally suggested to anneal the material in the vacuum system to avoid the oxidation. To verify that the vacuum environment can prevent oxidation, another parylene-C sample was annealed at 200°C for two days in vacuum and the result is shown in Figure 5-9. It clearly shows that the oxygen peak of the parylene-C annealed in

vacuum is much lower than in the air, meaning that the oxygen content in the annealed sample is much reduced by adopting this vacuum approach. The improvement can also be found in Table 5-3, the oxygen content is improved from 6.56% in air to 2.83% in vacuum. The little amount of oxygen detected can be explained by few oxygen residues remaining in the vacuum system.
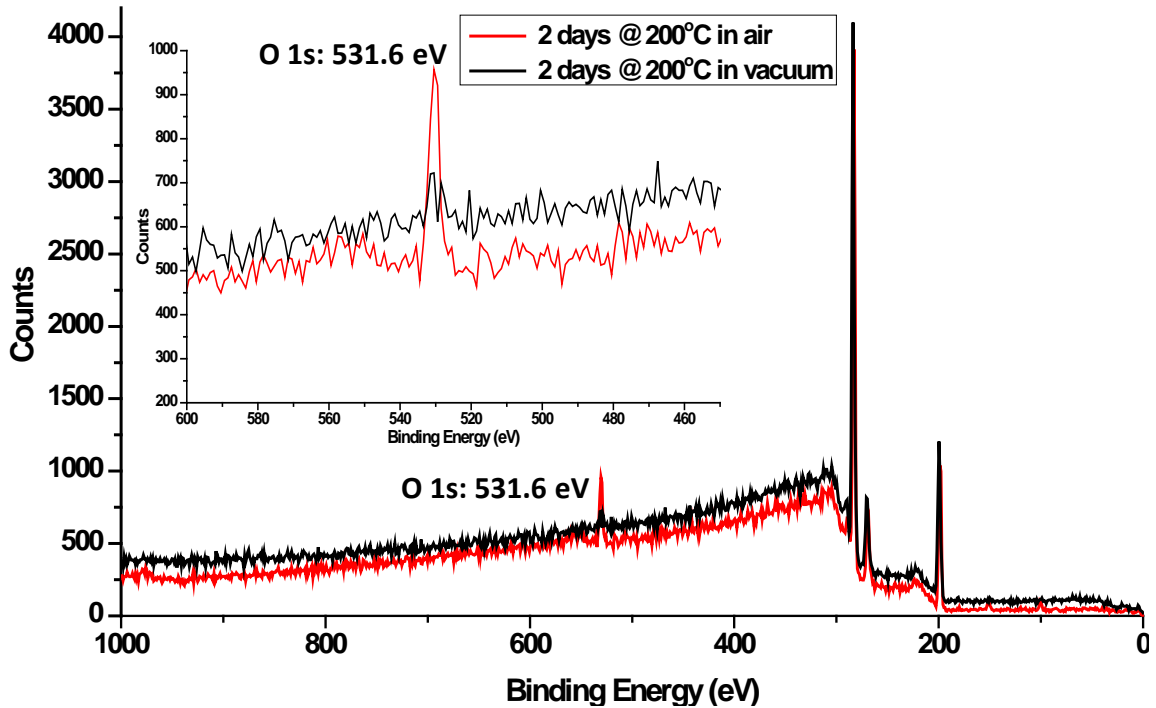
Figure 5-9: Comparison of two XPS results of parylene-C annealed at 200°C for two days in air and in vacuum

5.4.2 FTIR

Although XPS can provide us with the content of atoms involved in the oxidative parylene-C film surface, it is generally believed that XPS can only measure the surface chemical compounds of the material. In addition, XPS cannot provide us with a correct prediction of the chemical bonding of the oxidative species. Therefore, another

experiment using FTIR (Fourier transform infrared spectroscopy) is performed here to study whether the oxidation happens throughout the samples, and also what the chemical bonding after the oxidation is.

FTIR uses a broad band of infrared light to obtain material's IR absorption (or transmission) spectrum. As different chemical functional groups absorb different wavenumbers of infrared, the IR spectrum tells the specific chemical bond and functional group inside the material, which can be used to analyze the intermediate oxidative species of the material.

The FTIR scanning results of the parylene-C annealed in different situations are shown in Figure 5-10 to Figure 5-12. In Figure 5-10, all parylene-C were annealed at 100°C in the convection oven, but for different time durations. Two curves representing as-deposited parylene-C and parylene-C annealed at 100°C in the vacuum are shown for comparison. It is more interesting to look at the wavenumbers of carbon-oxygen single bond located at 1100–1300cm^{-1}, and also carbonyl bond located at 1695 cm^{-1} which show the clue of the oxidation. From Figure 5-10, it can be seen that no observable difference could be found among the five results within these two interested wavenumber ranges. No difference between the results of 100°C both in air and in vacuum means that the parylene-C gets oxidized very slowly at 100°C, which has also been pointed out by Monk in their real device parylene-C coating tests [188]. Same conclusion can also be obtained from Figure 5-10 that the annealing time of 4 days in the air makes no big difference to the as-deposited parylene-C film. The wave form variations between 1750–2750cm^{-1} and also among above 3250 cm^{-1} is likely due to the thickness variations of different samples.
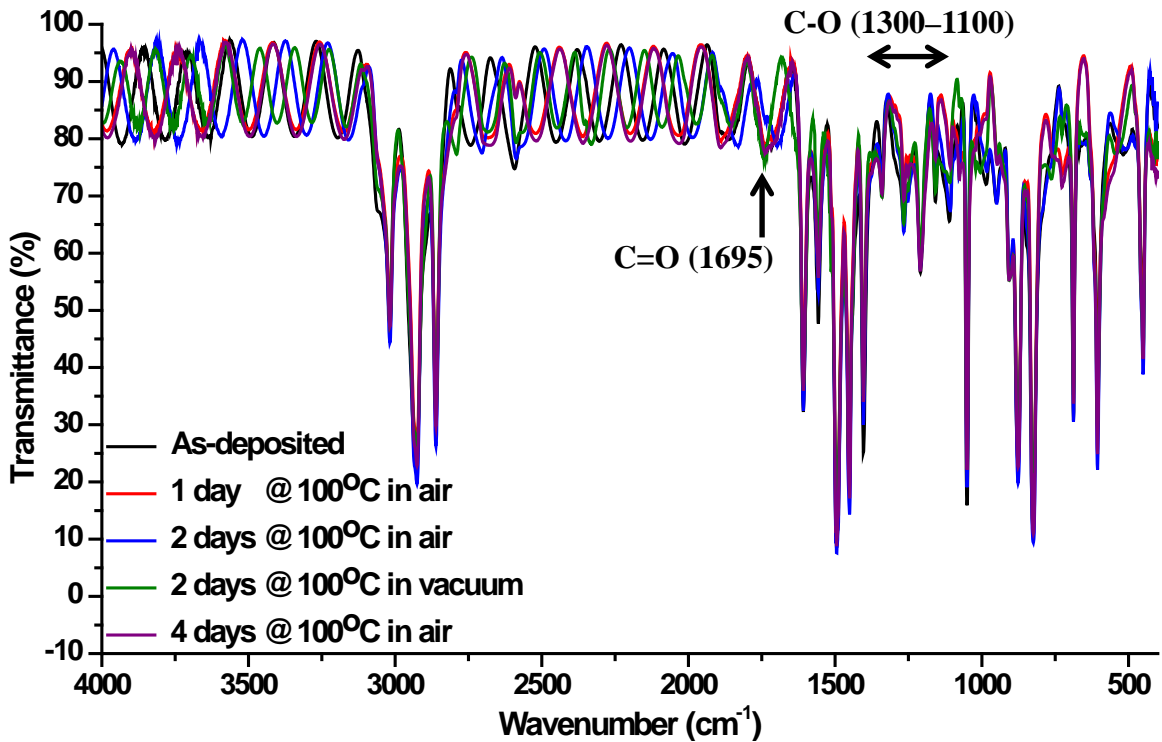
Figure 5-10: Typical FTIR results of parylene-C film. The black curve represents the as-deposited parylene-C film, while the others represent the results of annealing at 100°C.

Figure 5-11 shows the results of parylene-C annealed at 200°C in the convection oven. It can be clearly seen that the curves shift down more and more as the annealing time gets longer and longer. Both peaks representing carbon-oxygen single bond and carbonyl bond get deeper with the increasing annealing time, implying that more amount of parylene-C gets oxidized during the annealing. The peak growing at 1695 cm^{-1} means that the intermediate oxidative species have carbonyl functional group, which was also found by Nowlin [189]. Except for the three sharp peaks representing the C-H stretching, it is also found that the curve between 2500–3550 cm^{-1} gradually gets deeper as the annealing time gets longer. The regular FTIR database tells us that this range represents the OH functional group [196]. Therefore, the broader and deeper curve from 2500 cm^{-1}

166

to 3550 cm^{-1} might infer that the parylene-C has started to decompose into some chemical

compound after 1 day of annealing at 200°C, which has incorporated moisture to form

the OH functional group.
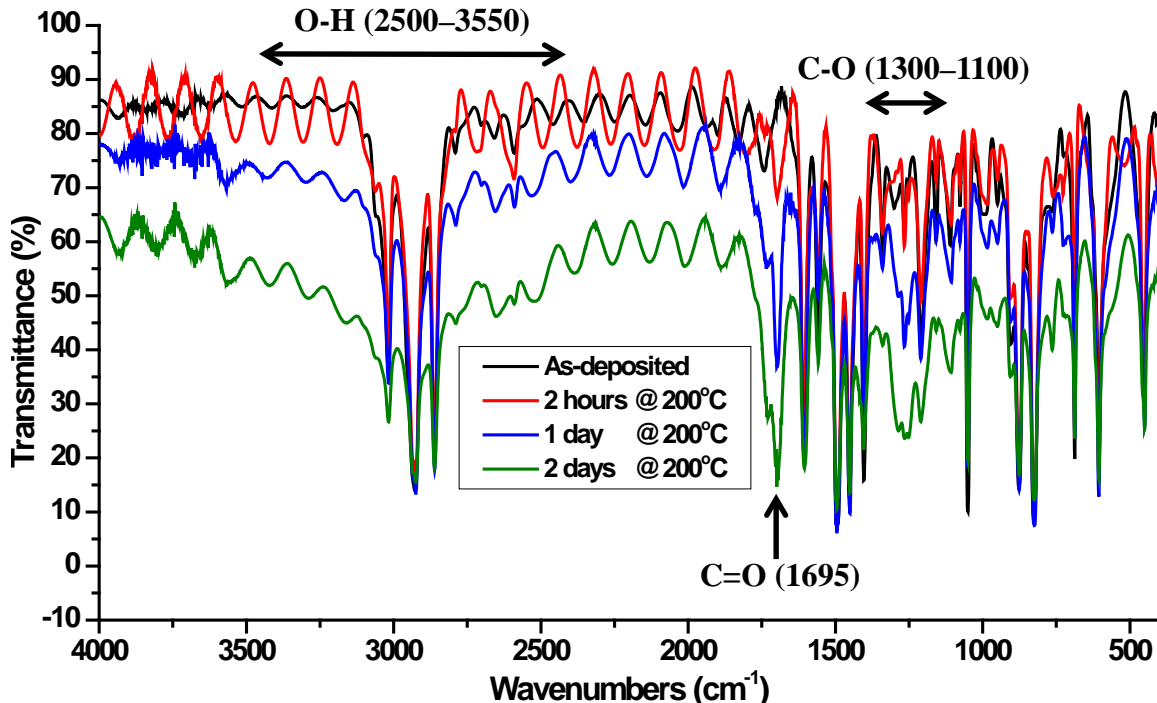
Figure 5-11: FTIR results of parylene-C annealed at 200°C in air for different times

To verify the vacuum improvement to the annealing, two results of praylene-C

annealed at 200°C with one in the air and one in the vacuum are shown in Figure 5-12. It

clearly shows that parylene-C annealed even at the temperature as high as 200°C in

vacuum has no observable curve difference from the as-deposited parylene-C.   It

concludes that annealing in vacuum can preserve the parylene-C material and agrees well

with what we found in Figure 5-9.
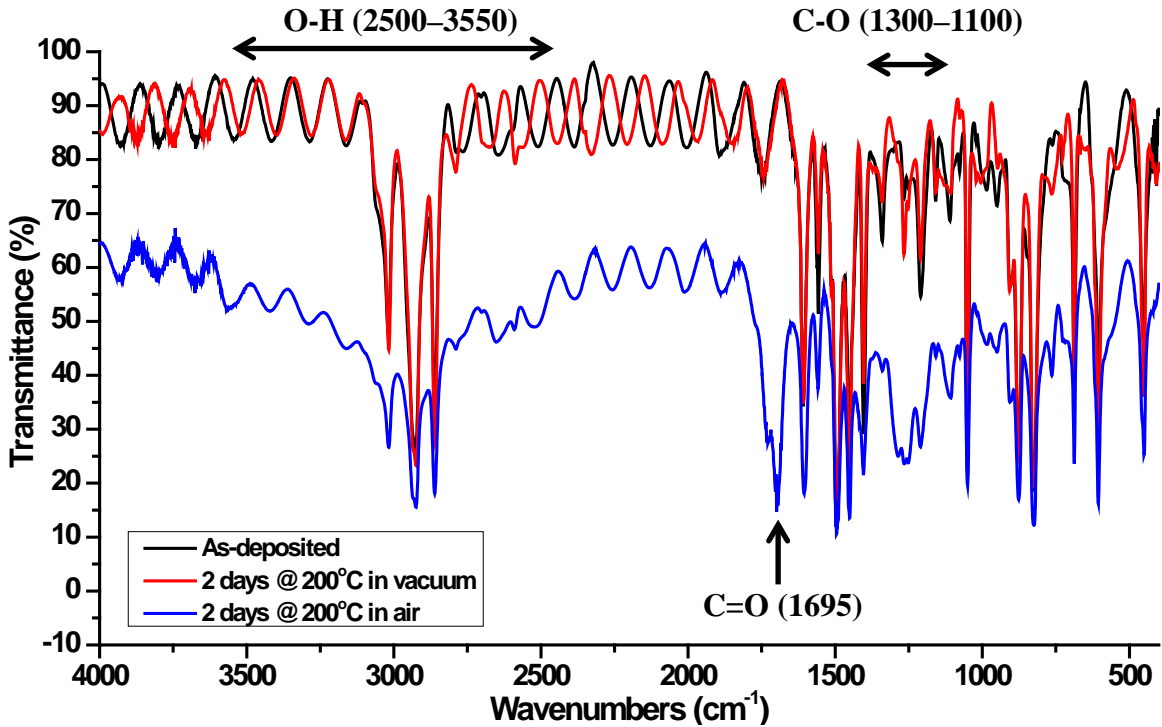
Figure 5-12: Comparison of the FTIR results of parylene-C annealed at 200°C in air and vacuum, all for two days

5.4.3 Summary and discussion

In this section, XPS and FTIR techniques have been used to study the oxidation behavior of the parylene-C film. Both techniques show that the parylene-C film has very little oxidation happening at 100°C. The results agree well with Nowlin and Monk's study, which is shown in Table 5-4. In Table 5-4, the oxidation rate is only found at the temperature higher than 125°C. If the oxidation rate at 125°C, i.e., 16 ppm [O]/hr, is taken for calculation, it can be estimated that it takes about 13 days for parylene-C to have a significant tensile strength degradation (5000 ppm). This demonstrates that parylene-C is still a very inert material at 100°C in the air.

Table 5-4: Measured initial (after 1 hour oxidation) oxygen uptake rate for parylene-C by Nowlin [189]

Temperature (°C) (ppm [O]/hr)			
125	**152**	**175**	**200**
16	290	1500	6600

Although XPS only qualitatively demonstrates the oxygen atom percentage of the paryelen-C film, the oxygen found on parylene-C surface could either come from the real oxidation during the annealing or the moisture contamination. This measuring insufficiency of the machines is compensated by using FTIR in our experiments. FTIR tells the present bonds throughout the parylene-C thickness. Therefore, it can be used to determine whether the oxygen atom comes from the moisture or the oxidative species. It is found that the oxidative species of parylene-C have a lot of carbonyl functional group, which has been predicted by Nowlin. The carbon-oxygen single bond found at 1100–1300 cm^{-1}, however, needs more studies to figure out its origin. By FTIR, it shows that the parylene-C might have already started to decompose after one day annealing at 200°C in the air. Both XPS and FTIR results provide strong evidence that annealing parylene-C at 200°C in vacuum does prevent serious parylene-C oxidation.

5.5 Crystallization

Crystallization is a process of phase transformation [197]. Like most of other polymers, parylene-C also has a certain degree of crystallization. It is reported that the crystallinity of the as-deposited parylene-C is about 60% [198–200], and is found to increase after post-fabrication thermal annealing [104, 184, 201]. On the other hand, however, parylene-C shares different paths of crystallization from other conventional polymers: it takes place during its chemical vapor deposition. Conventional polymers' crystallization is carried out by cooling the material from liquid type at higher temperature, T_m, to crystallization temperature, T_c, and hold at T_c until the crystallization is completed, which is called "isothermal crystallization". The mechanism, model, and theory of the crystallization of conventional polymers such as polyethylene, poly(phenylene sulfide), nylon-11, etc., have been extensively described and discussed [197, 202]. In contrast, the mechanism of polymer crystallization occurring during the chemical vapor deposition in which the polymerization happens is relatively less studied and discussed. In the 70s, Wunderlich's group had done some researches on the crystallization of poly-para-xylylene (parylene or parylene-N) during its polymerization process [198, 199, 203, 204]. Their results qualitatively reveal that the parylene deposited at room temperature starts to crystallize subsequent to polymerization but before the molecule is complete. Although it was parylene-N that Wunderlich worked on, it is generally believed that the parylene-C shares the same crystallization mechanism as well.

Researchers used to focus more on parylene-N's crystal structures. In 1953, Brown and Farthing found two types of crystal structures of the parylene-N, α form and β

form, and transition from α to β is achieved by thermal annealing (e.g., 220°C for parylene-N) [205, 206]. Iwamoto found that the parylene-N deposited at 80°C shows a mixture of α and β forms, while parylene-N deposited between 0–60°C only shows α form. Niegisch showed that the unit length of parylene-N is 6.58 Å and the orientation of parylene-N's polymer chains are aligned with lattice ac plane, which is parallel to the film plane [186, 207]. Iwamoto used x-ray diffraction technique to completely determine the structure of parylene-N's α form, finding that the parylene's benzene ring is parallel to the b axis, which is preferentially oriented along the direction perpendicular to the substrate surface [208]. The parylene-N is also found to have a monoclinic unit cell with a=5.92 Å, b=10.64 Å, c (fiber axis)=6.55 Å, and β=134.7°. L. You used x-ray pole figure technique to quantify the crystalline portion of the parylene-N film [200]. It was not until 1984 that, for the first time, Murthy used x-ray diffraction technique to figure out α form structure of alkylated and chlorinated poly-p-xylylene, i.e., parlene-C [209]. Murthy claimed that the dimensions of lattice constants in the plane, which was a and c, did not change with the substituents, but lattice constant b changed from 10.64 Å for parylene-N to 12.8Å for parylene-C.

The crystallinity and crystalline structure of parylene-C and parylene-N deposited at different temperatures have been studied by Surendran in 1987 [174, 210]. For parylene-C, several interesting findings are shown in Surendran's study:

1. The crystallinity of parylene-C increases as the dimer sublimation rate increases during the deposition process.

2. No polymorphism is observed either by decreasing the deposition temperature of by increasing the sublimation rate of the dimer.

3. Isothermal annealing increase brings the crystallization without any structural transformation.

4. At low temperature ($< -60°C$), all parylene-C depositions are all amorphous.

In this section, the parylene-C's crystallization was studied in more detail at 100°C in Helium to understand its crystallization kinetics. An in-situ temperature ramping annealing test was also performed to study its crystallization behavior at various temperatures. Several parameters of parylene-C's crystallite structure, e.g., d-spacing and crystallite size, are calculated and discussed. The time constant of the crystallization is evaluated in the last part of the section.

5.5.1 X-ray diffraction method

X-ray diffraction technique (XRD) has been widely used to study materials' crystallinity, crystal orientation, fiber structures, and even the stress inside the materials. The technique is executed by emitting x-ray onto the sample's surface *via* different incident angles. The x-ray is scattered by materials atoms and the reflected light is collected by a light sensor. The structure of the tested material can then be figured out by the observed light information. The machine used in our study is X'Pert PRO MRD made by Philips. The x-ray anode source is copper and its wavelength is 1.5406 Å.

5.5.1.1 **In situ** *consecutive XRD scanning at 100°C*

Our first XRD experiment was performed to measure the crystallinity and crystallite size of the parylene-C annealed at 100°C consecutively for four hours. The parylene-C sample was held on the sample holder and the x-ray was scanning the sample with the angle from 10° to 40° continuously, which took 5.3 minutes to finish one scanning. The temperature was ramped from room temperature to 100°C at the rate of

3°C/min. An inert gas of helium was flushed into the chamber all the time during the scanning to eliminate any possible oxidation effect.

A typical XRD scanning results showing the curve from $10°$–$30°$is shown in Figure 5-13. It can be seen that a clear peak happens at $2\theta = \sim 14°$, which represents the (020) surface of the monoclinic unit cell. Lots of information can be obtained from the XRD results and they are introduced and defined as follows.
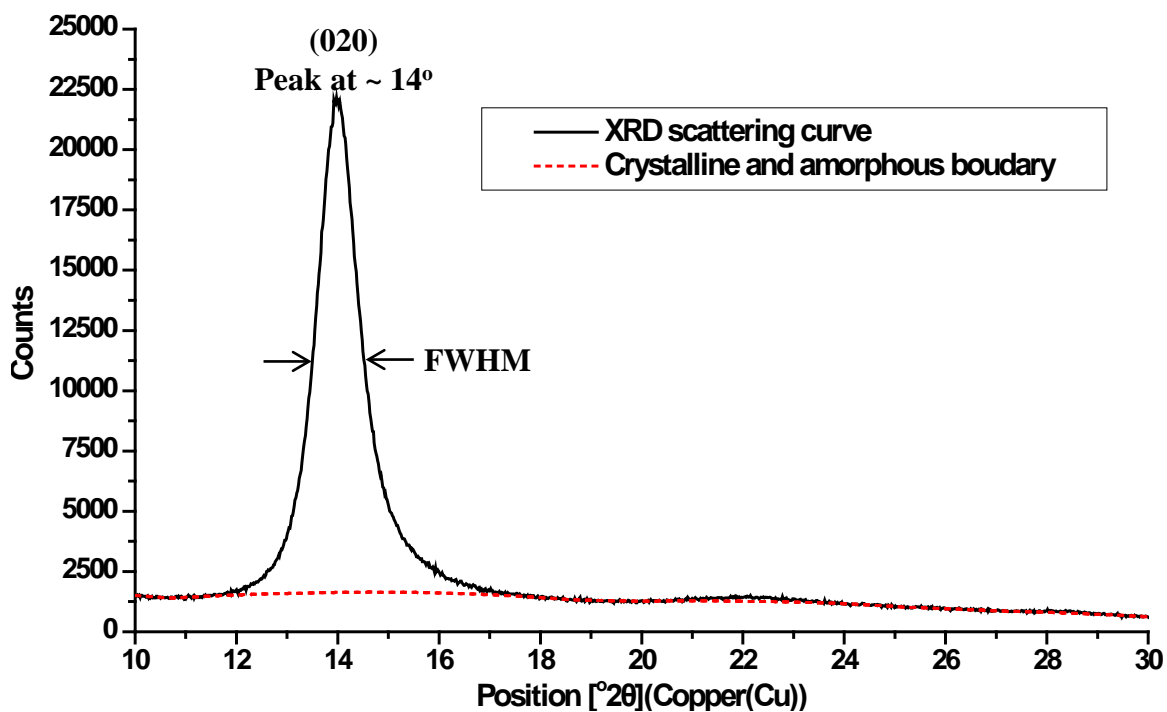
Figure 5-13: Typical XRD scanning results showing curve from $10°$–$30°$C

5.5.1.1.1 Crystallinity

Two fundamental approaches are usually utilized to calculate the material's crystallinity through the XRD scanning results. If either completely amorphous or crystallized state of the polymer under scanning exists, the XRD results can be calibrated according to them and the crystallinity at any state could be found [211–214]. Another

way to determine the crystallinity is using Hermans method [215–218], which resolves the curve into amorphous and crystallized portions, as shown in Figure 5-13. The crystallinity is then defined as the ratio of the crystallized portions, i.e., area bounded by the back and red lines in Figure 5-13, to the whole area under the black line.

Because the parylene-C shows as neither a completely amorphous nor completely crystallized polymer right after the deposition, Hermans method is adopted here to estimate the parylene-C's crystallinity [174, 210]. However, even though the boundary in Figure 5-13 can be determined by the commercial software, the estimated crystallinity still varies based on the algorithm of the boundary determinations. Since the crystallinity of the as-deposited parylene-C has been published as 60%, all our XRD results were calibrated to this crystallinity of the as-deposited parylene-C and then the crystallinity at any state was estimated based on this assumption. It is obvious that the crystallinity obtained in our experiments is not absolute, but only for comparison purposes.

5.5.1.1.2 d-spacing

d-spacing represents the interplanar spacing of two crystallite planes. d-spacing, d, can be calculated by Bragg's diffraction law as

$$2d sin\theta_B = n\lambda, \tag{5-1}$$

where θ_B is the Bragg angle, which can obtained from the location of the peak in Figure 5-13. λ is the wavelength of the emitting x-ray, which is 1.5406 Å. For the peak at $2\theta_B = \sim 14°$, n = 1.

5.5.1.1.3 Crystallite size

The crystallite size, D, can be obtained using Scherrer's formula:

$$D = \frac{0.9\lambda}{B cos\theta_B}, \qquad\qquad (5\text{-}2)$$

where λ and θ_B are the same as in eqn. (5-1). B is the full width at half maximum (FWHM), which can be found from the XRD results by commercial software.

Figure 5-14 shows the in situ XRD measurement results of the parylene-C consecutively annealed at 100°C in Helium. The first obtained curve was at the temperature of 30°C due to the machine's limitation. After the temperature reached 100°C, the machine scanned the sample every 5.3 minutes. It can be seen from Figure 5-14 that the height of the curve grows fast between 30° and 100°C. Once the temperature stabilizes at 100°C, the height keeps growing, but grows at a much slower rate. As the temperature ramp rate here is 3°C/min, the time constant of the parylene-C crystallization will be evaluated in Section 5.5.2 by individually annealing every sample.
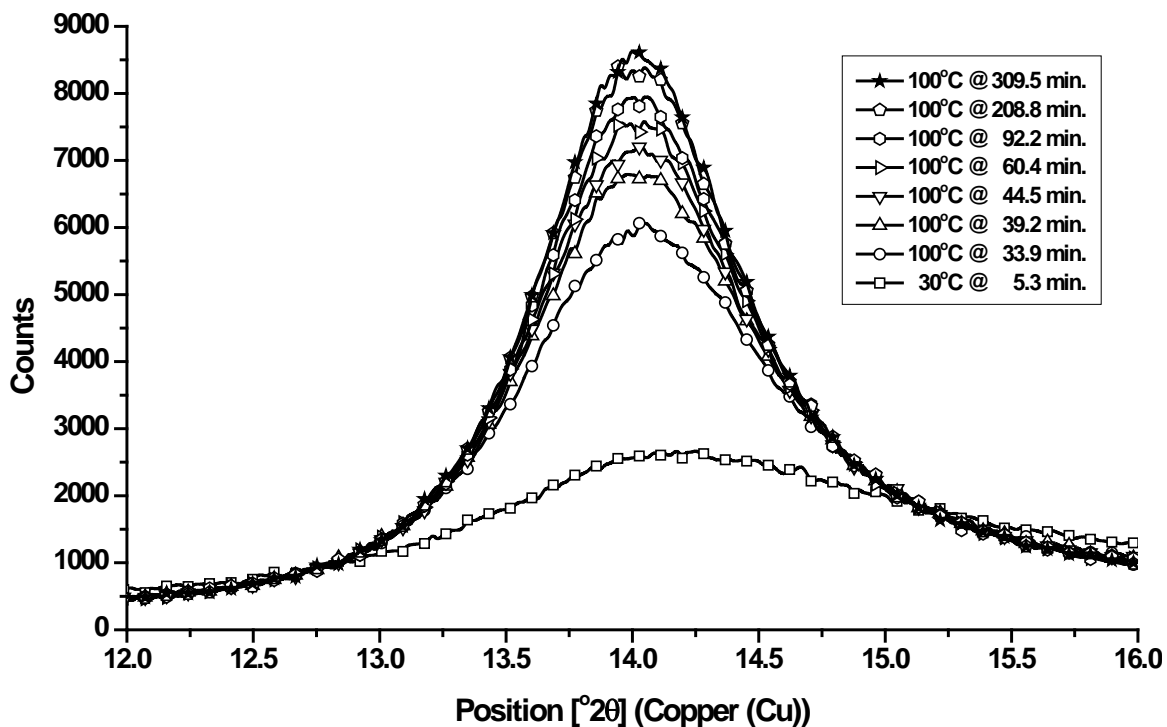
Figure 5-14: XRD results of in situ XRD measurement of parylene-C consecutively annealed at 100°C in helium

Table 5-5 is the list of the calculated parameters using the in-situ XRD measuring results of the parylene-C consecutively annealed at 100°C in helium. It can be seen that the crystallinity is growing up with the annealing time. The crystallinity does not go back after the parylene-C cools down to 30°C, meaning that the parylene-C structure has gone through crystallization and is irreversible. The position of the peak of 2θ is found to be at around 14°. The angle decreases to a bit less than 14.0194 during the annealing, but goes back to 14.1330. The varying 2θ position implies that d-spacing is changing during annealing. It can be found that the d-spacing increases more during 30–100°C than staying at 100°C. The d-spacing increase, therefore, could be explained by the thermal expansion of the parylene-C. Although the height is found to increase during the annealing, the FWHM, however, is also found to be narrower at the same time. The decreasing of the FWHM results in the increasing of the parylene-C crystallite size. As aforementioned, the crystallinity obtained through Hermans method for parylene-C is not absolute, it is more reasonable to use parylene-C crystallite size to analyze the level of the parylene-C crystallization behavior. The crystallite size of parylene-C annealed consecutively at 100°C versus annealing time is shown in Figure 5-15. It is found that the crystallite size saturates quickly once the temperature reaches 100°C, meaning that the crystallization of parylene-C responds spontaneously to the environmental temperature increase. The results show that the crystallite size saturates within 10 minutes. As the temperature ramping rate is slow, the time constant will be studied in Section 5.5.2 by annealing the samples in a pre-heated convection oven with different annealing time to mimic the step temperature change.

Table 5-5: A list of calculated parameters using the in situ XRD measurement results of parylene-C consecutively annealed at 100°C in helium

Time	Temperature	Crystallinity	Position	Height	FWHM	d-spacing	Crystallite size
min	°C	%	2θ	Counts	2θ	Å	Å
5.3	30	60.34	14.1755	2645.00	1.3382	6.2480	59.8226
33.93	100	86.39	14.0408	5985.00	0.9368	6.3076	85.4430
39.23	100	89.06	14.0277	6792.00	0.9368	6.3135	85.4418
44.53	100	89.81	14.0260	7146.00	0.8029	6.3143	99.6908
60.43	100	89.70	14.0261	7565.00	0.8029	6.3142	99.6908
92.23	100	90.45	14.0215	7944.00	0.8029	6.3163	99.6903
208.8	100	91.71	14.0199	8349.00	0.8029	6.3170	99.6901
309.5	100	90.45	14.0194	8476.00	0.6691	6.3172	119.6251
320.7	30	90.27	14.1330	8407.00	0.8029	6.2667	99.7023
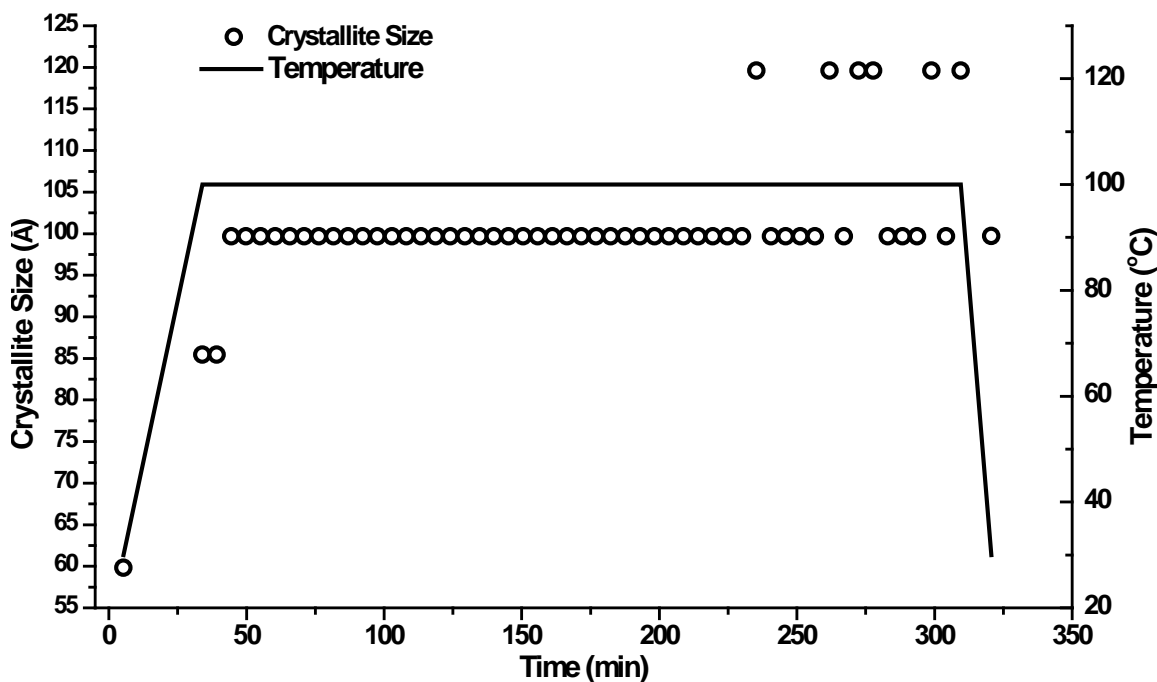
Figure 5-15: Crystallite size growing history of parylene-C annealed at 100°C in helium

5.5.1.2 **In situ** *temperature ramping annealing study*

Another experiment was performed to study the crystallization effect at different temperatures. In this experiment, the environmental temperature of the parylene-C sample was ramped up at the rate of 3°C/min up to 300°C. Each scanning also took 5.3 minutes, and the machine kept scanning the sample 6 times after the machine reached the targeted temperature; hence the parylene-C sample would experience each annealing temperature for about 31.8 minutes. Helium was also used during the experiment to prevent the oxidation especially in the high temperature.

The XRD results of the annealing temperatures from 30° to 50°C are shown in Figure 5-16. For temperature from 80°–250°C, the results are shown in Figure 5-17 in comparison with the result for 30°C. For Figure 5-16 and Figure 5-17, only the sixth scanning results for each temperature was selected and drawn, which is believed to be closely enough to reflect the crystallization saturation at each temperature. The derived crystallization parameters are listed in Table 5-6, and the crystallite growing history is shown in Figure 5-18. It is found from Figure 5-16 that parylene-C show very little crystallization when the temperature is below (including) 50°C. Although the curve of 50°C in Figure 5-16 is higher than that of the lower temperatures, the calculated crystallite size at 50°C still does not show any clue of growing up, which would imply that the crystallization does not happen yet, but have a more organized structure at 50°C. This phenomenon agrees well with the measured length change in 5.3.2. The result again proves that the parylene-C does not crystallize (or crystallize very little) below 50°C, i.e., the glass transition temperature, which can be explained well by thermodynamics. After the temperature is over 50°C, the height of the XRD curve starts to grow up dramatically,

and also shifts to the left as the temperature increases. This shift results in the increase of the d-spacing, which can be explained as the thermal expansion. The crystallite size also starts to increase when the temperature ramps up higher than 50°C and keeps growing as the temperature increases until 250°C. When the temperature reaches 300°C, the crystallize size suddenly drops, because it is believed that the parylene-C has been decomposed or melted, as shown in Figure 5-18. The obtained parylene-C decomposing (or melting) temperature agrees well with the literature value of 290°C [100, 101]. Although the XRD curves of each temperature is always getting higher in the first scanning, the crystallite size shown Figure 5-18 demonstrates a flat line at most of the temperatures, except at 80° and 100°C. It reveals that the crystallization of parylene-C is very likely to have been done within the first 5.3 minutes scanning. The non-flat results at 80° and 100°C implies that the higher the annealing temperature, the shorter the crystallization time constant.
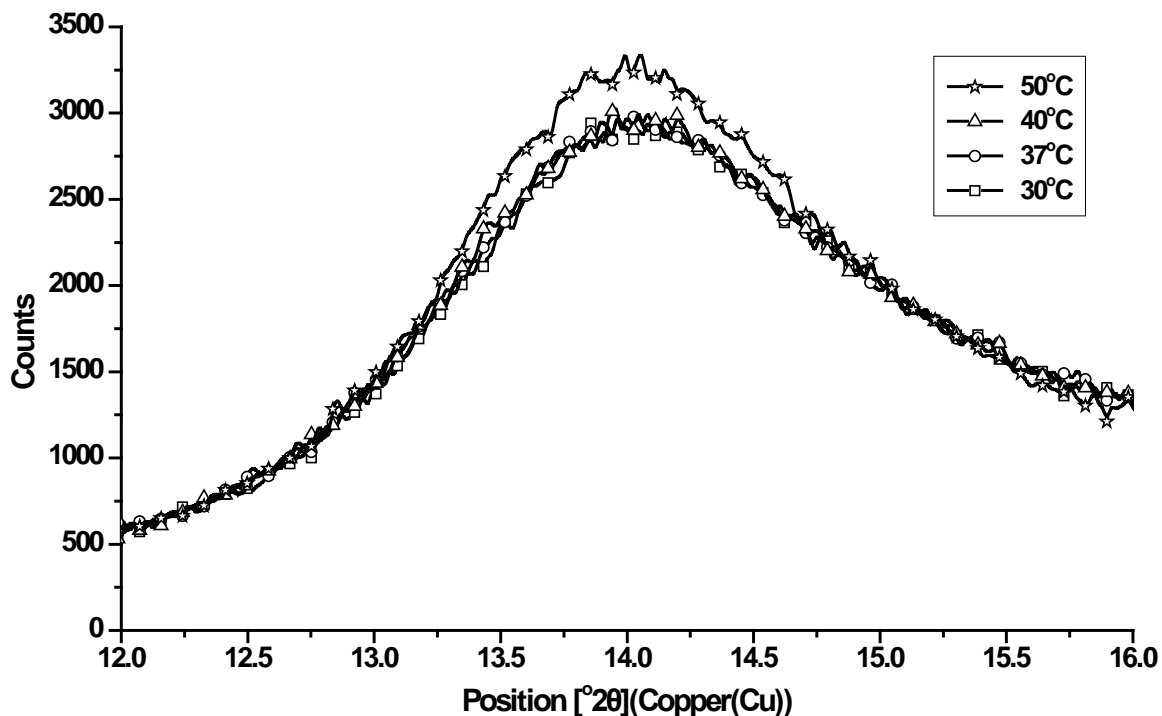
Figure 5-16: XRD results of parylene-C annealed at 30°, 37°, 40°, and 50°C
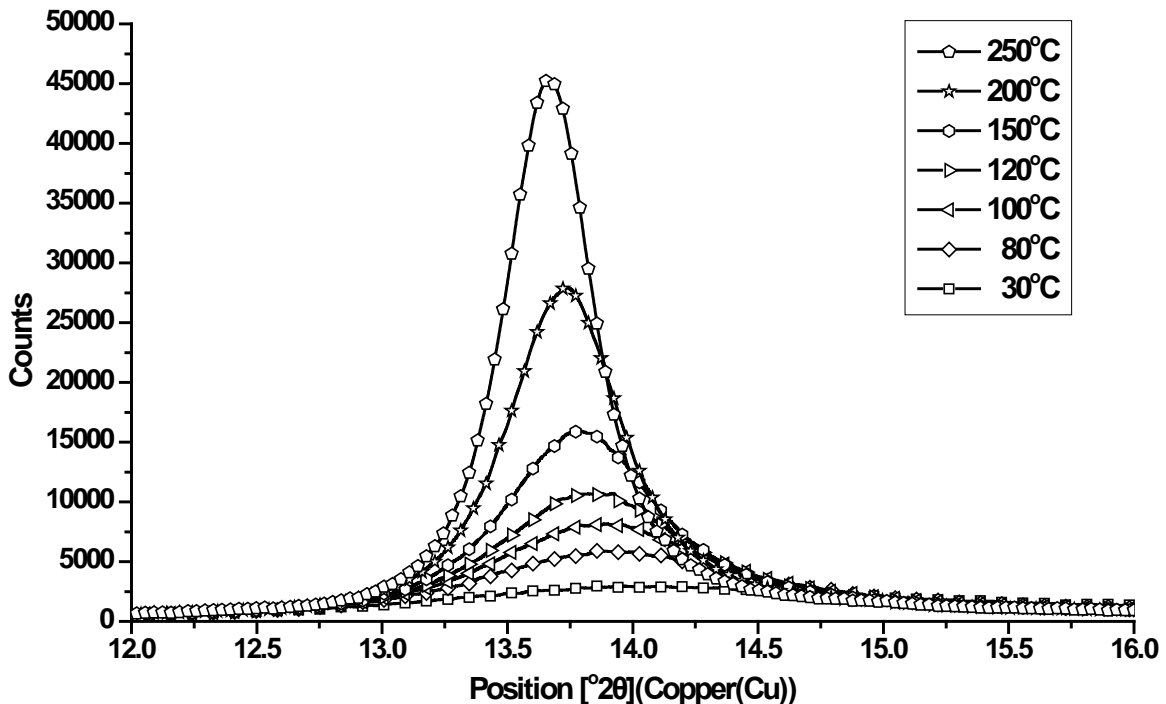
Figure 5-17: XRD results of in situ XRD measurement of parylene-C consecutively annealed at different temperatures in helium. Temperature ramping rate = 3°C/min.

Table 5-6: A list of calculated parameters based on the in situ XRD measurement of parylene-C consecutively annealed at different temperatures in helium

Time	Temperature	Crystallinity	Position	Height	FWHM	d-spacing	Crystallite size
min	°C	%	2θ	Counts	2θ	Å	Å
31.8	30	62.20	14.0482	2914.00	1.3382	6.3044	59.8144
65.7	37	60.74	14.0285	2935.00	1.3382	6.3132	59.8131
98.1	40	59.65	14.0473	2981.00	1.3382	6.3047	59.8143
133.0	50	58.11	14.0055	3273.00	1.3382	6.3235	59.8117
174.7	80	69.65	13.9203	5865.00	0.9368	6.3620	85.4320
213.1	100	75.04	13.8757	8117.00	0.8029	6.3823	99.6748
251.2	120	79.86	13.8393	10725.00	0.8029	6.3990	99.6709
292.6	150	81.64	13.7948	15898.00	0.6691	6.4196	119.5965
340.7	200	85.73	13.7270	27791.00	0.5353	6.4511	149.4794
388.8	250	86.21	13.6667	45185.00	0.5353	6.4795	149.4699
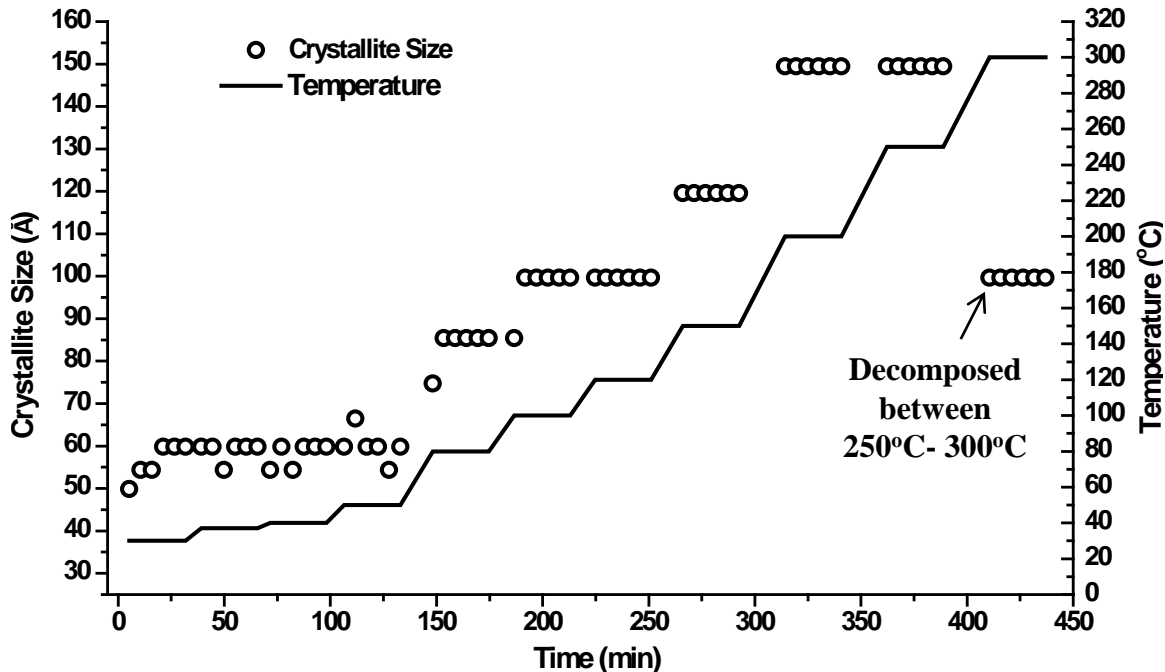
Figure 5-18: Crystallite size growing history of parylene-C annealed at different temperatures in helium

5.5.2 Time constant of parylene-C annealed at 100°C

Hsu has suggested in 2008 that the crystallization reaction is likely to be completed during the brief 20 min of annealing [201]. To find the time constant of the crystallization of the parylene-C at 100°C, several parylene-C samples were annealed at 100°C but for different annealing durations. To mimic a step-function temperature increasing profile, a convection oven was first pre-heated to 100°C before the samples were put in. The samples were taken out when the desired annealing time was up and then scanned separately by XRD machine.

The list of the XRD results of all parylene-C samples with different thermal treatment is shown in Table 5-7. It can be found that the crystallite size grows very fast in the early annealing process and saturates at 99.7 Å in two minutes. The crystallite size

as a function of the annealing time is drawn in Figure 5-19. The data points are curve fitted to the exponential equation as follows:

$$\text{crystallite size} = A + Bexp\left(-\frac{t}{\tau}\right), \tag{5-3}$$

where A and B are constants and τ is the time constant. The curve fitting result shows that A is 99.98 Å, B is -40.50 Å and the time constant is 0.845 min. The short time constant means that parylene-C is very sensitive to heat and crystallization happens very fast at the annealing temperature. It is attributed to that the polymer chain motion is restricted during the vapor deposition polymerization (VDP), hence the as-deposited parylene-C is generally in a metastable state, which means parylene-C is not fully crystallized right after the VDP [101, 219]. It is postulated that the parylene-C's polymer chain tends to move immediately once the temperature reaches the temperature higher than the glass transition temperature and the crystallization takes place easily afterward.
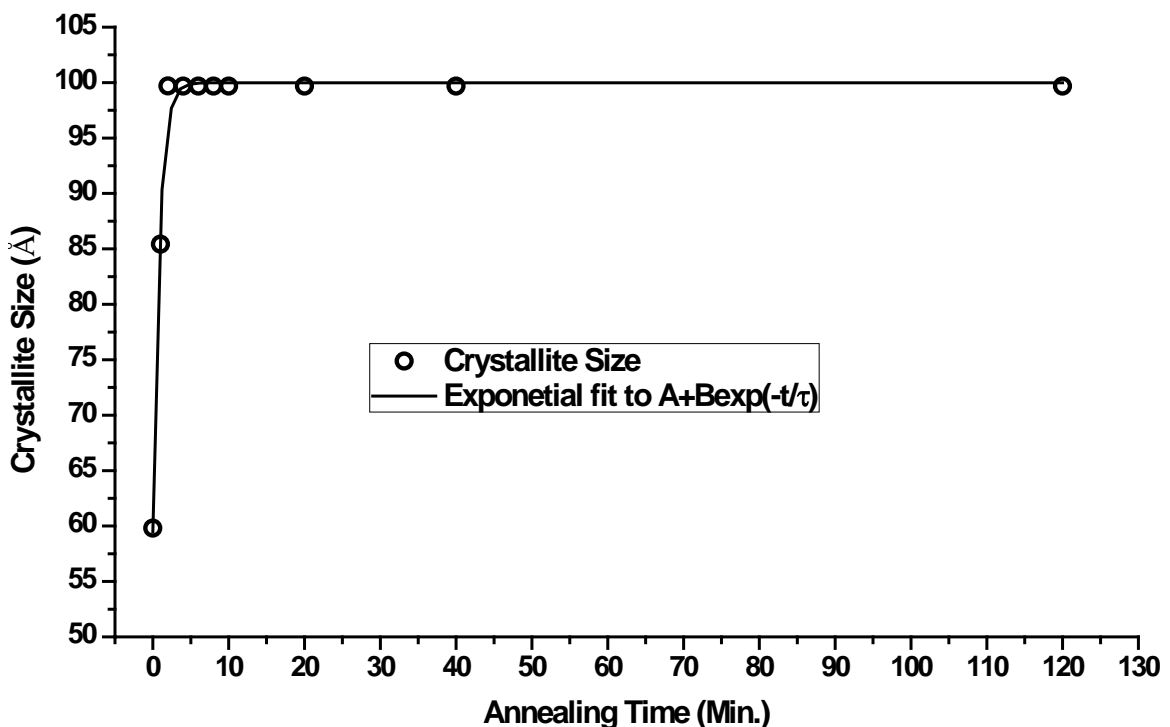
Figure 5-19: The crystallite size versus the annealing time

Table 5-7: The lists of the parameters of the crystallization of parylene-C individually annealed at 100°C for different annealing times

Time	Temperature	Crystallinity	Position	FWHM	d-spacing	Crystallite size
min	°C	%	2θ	2θ	Å	Å
0	Room Temperature	60.11	13.9535	1.3382	6.3469	59.8083
1	100	70.12	13.9141	0.9368	6.3648	85.4314
2	100	67.65	14.1324	0.8029	6.2670	99.7022
4	100	73.41	13.9785	0.8029	6.3356	99.6857
6	100	75.79	13.9886	0.8029	6.3311	99.6868
8	100	73.89	13.9729	0.8029	6.3382	99.6851
10	100	73.72	13.9776	0.8029	6.3360	99.6856
20	100	78.67	13.9615	0.8029	6.3433	99.6839
40	100	77.99	13.9894	0.8029	6.3307	99.6869
120	100	75.05	13.9910	0.8029	6.3300	99.6870

5.5.3 Effect of deposition pressure difference

In the previous research, it is found that increasing the deposition pressure will also increase the deposition rate [201] but decrease the crystallinity [104, 220]. When previous researchers were doing the parylene-C crystallization study, many of them usually used the height (or counts) signal of the XRD scanning results to represent parylene-C crystallinity [104, 201]. However, as has been discussed before, the FWHM

also narrows when the curve height increases, therefore the height might not be an adequate indicator to describe parylene-C's crystallization behavior.

Rather than using the height of the XRD results, the parylene-C's crystallite size is used to study the parylene-C's crystallization behavior in this section. Another as-deposited parylene-C film deposited at 35 mTorr was also prepared and scanned by the XRD machine. The calculated crystallization parameters are shown in Table 5-8 and the scanning results are shown in Figure 5-17 with the curve of 22 mTorr shown together for comparison. It is found that the peak of 35 mTorr curve is lower than 22 mTorr as expected. On the other hand, the obtained 2θ position, d-spacing, and the crystallite size are all very similar between the two parylene-C deposited at different pressures. Therefore it could be concluded that the crystallite structures of the two parylene-C films with different deposition conditions should be similar. The lower height (or intensity), and hence the lower crystallinity, of the parylene-C deposited at 35 mTorr is likely attributed to the fact that the percentage of amorphous phase is higher in parylene-C deposited at 35 mTorr than 22 mTorr. The corresponding mechanical properties will be discussed in detail in Sections 5.7–5.9.

Table 5-8: XRD results of two as-deposited parylene-C films deposited at 22 mTorr and 35 mTorr, respectively

Deposition pressure	Crystallinity	Position	Height	FWHM	d-spacing	Crystallite size
mTorr	%	2θ	Counts	2θ	Å	Å
22	60.27	14.0241	3979.00	1.3382	6.3151	59.8129
35	21.95	14.0507	1824.00	1.2044	6.3032	66.4595
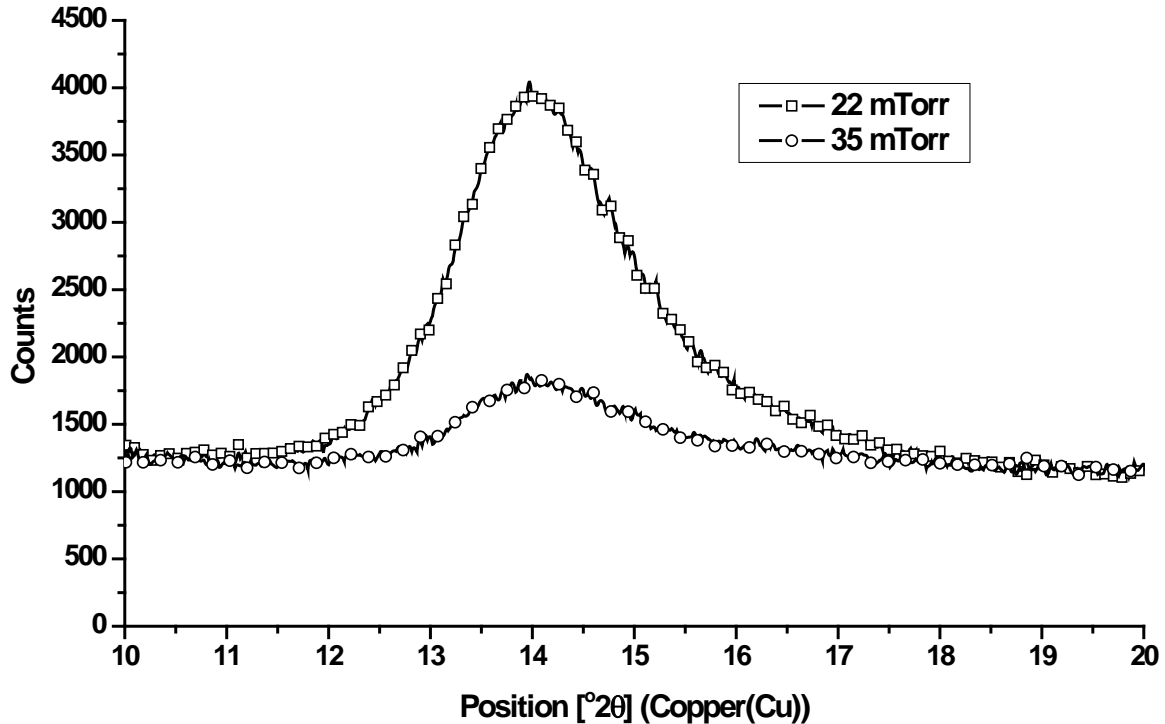
Figure 5-20: Comparison of the results of XRD measurement of parylene-C deposited at 22 mT and 35 mT

5.5.4 Summary and discussion

In this section, the crystallinity of parylene-C annealed at various temperatures or deposited at different pressures is studied. The time constant of parylene-C annealed at 100°C is found to be around 0.845 minutes. It infers that as-deposited parylene-C is at a metastable state and is very sensitive to heat. The crystallization at 100°C could be done within only less than one minute. The in situ ramping temperature experiments show that the parylene-C starts to crystallize above the glass transition temperature, which is found to be 50°C in this section *via* XRD approach. In addition, the crystallinity, or crystallite size increases as the annealing temperature increases.

In our experiments, the crystallite size of as-deposited parylene-C is found to be ~ 59.8 Å and increases to ~ 149.5 Å at 250°C and parylene-C decomposes at 300°C. It is

pointed out in Section 5.2 that the molecular length of the parylene-N is about 2000–4000 units per chain. If the unit length of 6.58Å is used, the chain length could be about 13160–26320 Å, or 1.32–2.63 µm. Based on the crystallite size shown in this section, it can be concluded that the one parylene-C polymer chain is very likely to contribute to more than one single parylene-C crystallite. The hypothesis is that parts of the long parylene-C polymer chain are folded to form multiple ordered crystalline structures, or called lamella, which might happen irregularly in between single polymer chain [221]. The rest of the polymer chain remains in amorphous type. When the parylene-C is heated up, the parylene-C polymer gets enough energy to move, therefore more polymer chains become well-organized, and therefore results in the length shortening shown in Section 5.3. It has been reported that another XRD peak happens at 28.2º when the parylene-C is annealed at 200ºC. The same phenomenon is also found in our XRD scanning results. It is very likely that another structure transformation takes place at this temperature. However, to our best knowledge, not too many papers have been working on the effect of the generation of this peak. The future work would focus on the cause of this peak and its corresponding crystallite structure. In addition, the future work would also focus on an another interesting claim which was made by Shaw in 1970 [222]. They claimed that the free radicals buried in the parylene film would react with other radicals at other polymer chain ends when annealing directly after the film deposition. Therefore the annealing process would terminate the as-deposited parylene film radicals and the radicals would not react with the available oxygen. It might imply that the annealing of as-deposited parylene-C film could hinder the oxidation of the material, which is very worthwhile to look into.

5.6 Glass Transition Temperature

It is well known that viscoelastic behaviors of polymers differ below and above the glass transition temperature. To understand the mechanism of polymer transition, the concept of free volume is first introduced in the first part of this section. The free volume of the polymer is defined as the space a molecule has for internal movement [223]. The polymer chain cannot move freely if there is not enough space for a single C-C bond to rotate. It is believed that the typical free volume of the polymer is 2.5 Vol.-% and it requires free volume to be greater than 2.5 Vol.-% for macromolecules to start to move [185].
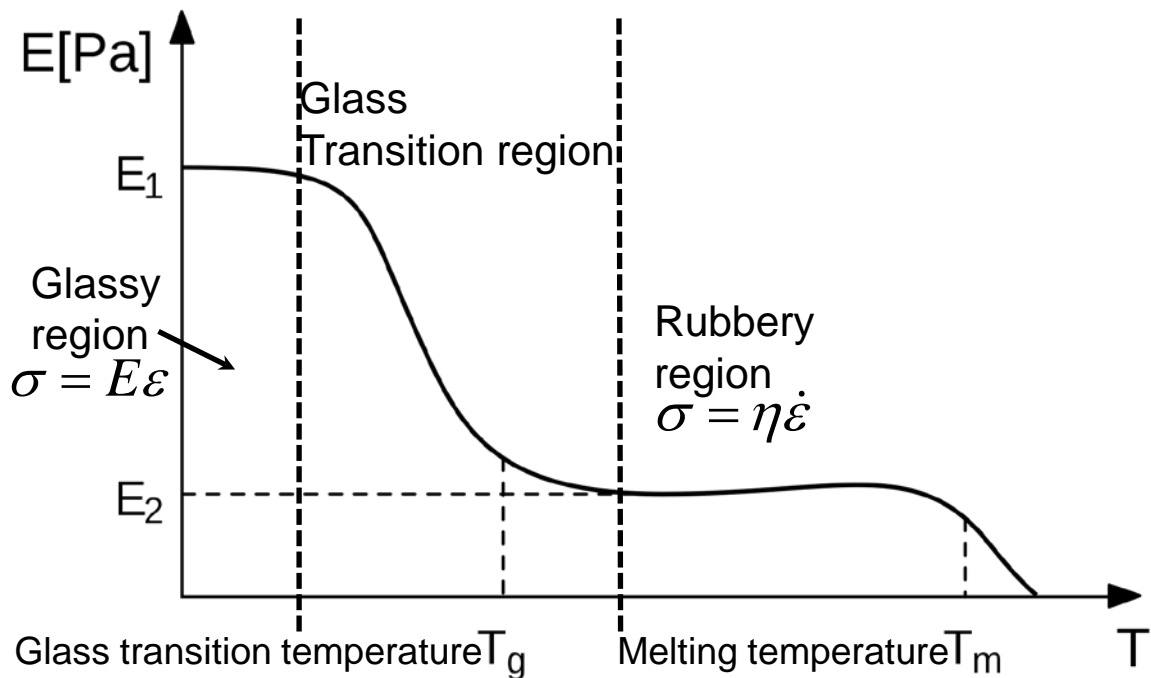
Figure 5-21: Elastic modulus response versus temperature change

As shown in Figure 5-21, the leftmost region is called glassy region. In this region, the material has relatively higher and flatter elastic modulus than others. The macromolecule is ceased in the glassy region and hence the polymer behaves like a

perfect elastic material at low temperature. It has been demonstrated that the free volume increases as the temperature increases [185, 223]. Therefore, as the temperature goes over a critical temperature, i.e., glass transition (or second transition) temperature, T_g, the free volume increases to be higher than 2.5 Vol.-%, permitting different kind of chain movements as well as moving in various directions [185, 223]. In addition, higher temperature also provides the polymer chain more energy and makes the chain movement even easier. Therefore, the elastic modulus decreases gradually due to this higher polymer chain mobility.

Glass transition temperature denotes a plastic material's onset of the transition of the reduced Young's modulus. The transition usually appears as a temperature range rather than just a deep-dropping step. This transition range is called the glass transition range. When the temperature passes the glass transition region, the elastic modulus enters another region called rubbery region. The plastic in this region has rubber-like response and its behavior can be predicted by viscous materials' model. The glass transition temperature usually defines one end of the materials' usage temperature, depending on what value the strength and stiffness is needed. The material can be used in the glassy region with a higher elastic modulus, or in the rubbery region with a lower elastic modulus. In any case, however, the operating range of the material should not fall within the glass transition region to avoid unpredictable material behaviors. Therefore, knowing the elastic modulus with a broad temperature spectrum and the temperature range of each region helps us select the right materials and also use it in the right operating temperature range. Furthermore, understanding the mechanism of the polymer elastic modulus transition can even help us tailor the materials' glass transition

temperature to fit our needs. This section would focus on the measurement of the glass transition temperature range of parylene-C and also several possible ways to modify it.

5.6.1 Identification of glass transition temperature

5.6.1.1 Reported glass transition temperature of parylene-C

Gorham did the first experiment to measure the glass transition temperature of parylene-C [172] in 1966 using secant modulus-temperature curve, and characterized parylene-C's glass transition temperature to be 80ºC. Many researchers have attempted to study parylene-C's T_g after Gorham. A table listing some T_g measuring results is shown in Table 5-9. Although most the T_g values lie in the range of 13-150ºC, the result demonstrate a sporadically spread numbers, indicating that the complexity of measuring paylene-C's glass transition temperature. As this second transition is attributed to the polymer movement as described before, it is postulated that the variation might be due to the parylene-C property difference (structure or crystallinity) of the samples obtained by different research groups, which might be influenced by different deposition conditions or post-deposition treatments. In this section, not only as-deposited parylene-C's T_g is characterized, but T_g of parylene-C annealed in different temperatures and environments is also studied to understand the T_g change with respect to the temperature, i.e., crystallinity.

As shown in Table 5-9, multiple approaches can be applied to measure parylene-C's glass transition temperature. From engineering point of view, measuring the relationship of the elastic modulus with respect to the temperature is most useful as it provides the information of not only elastic modulus at different temperature, but also the material thermodynamic properties including glass transition temperature. In this section,

the elastic modulus was measured by two methods: ramping-temperature-dependent modulus experiment and dynamic mechanical analysis (DMA).

Table 5-9: Some of the previous published parylene-C T_g characterizing results

Study	T_g (ºC)	Approach	Post script
Gorham, 1966 [172]	80	Secant modulus	
Gilch, 1966 [224]	70	NA	
Kubo, 1972 [199]	50–80	NA	
Alpaugh, 1974 [225]	50	DSC	
Iwamoto, 1975 [198]	65	DSC	As-deposited parylene-N, Heating rate: 10°C/min, Nitrogen atmosphere, Measured T_g varies with respect to the polymerization temperature (T_g=63–78)
Beach, 1989 [101]	13	NA	T_g is expected to have similar T_g as parylene-N's.
Dabral, 1991[110]	150	Stress-temperature curve	Likely to be 50ºC, according to the presented data.
Gratten, 1991 [187]	110	NA	
Senkevich, 1999 and 2000 [184, 226]	35–36, 44	DSC	Different testing rate corresponds to different T_g results. Quoted by Kamezawa, Suzuki and Kasagi as 50°C [227].
Noh, 2004 [228, 229]	< 90	DSC	
Huang, 2005 [183]	42.5–62.5	Thermal coefficient of thickness expansion	T_g is 10°C higher when thickness is < 50 nm.
Youn, 2007 [220]	90	NA	
Tewari, 2009 [230]	70	Current density peak	1-µm-thick sample

5.6.1.2 Ramping-temperature-dependent modulus experiment

The concept of this ramping-temperature-dependent modulus experiment is shown in Figure 5-22. The test was done with samples under a temperature ramping

from -20°C to 150°C. During the temperature ramping, a series of short and quick tensile tests were performed under 0.3N as the applied static force. In Figure 5-22, every peak represents one uniaxial tensile test. The stress-strain curve of every uniaxial tensile test is obtained and the elastic modulus is calculated.
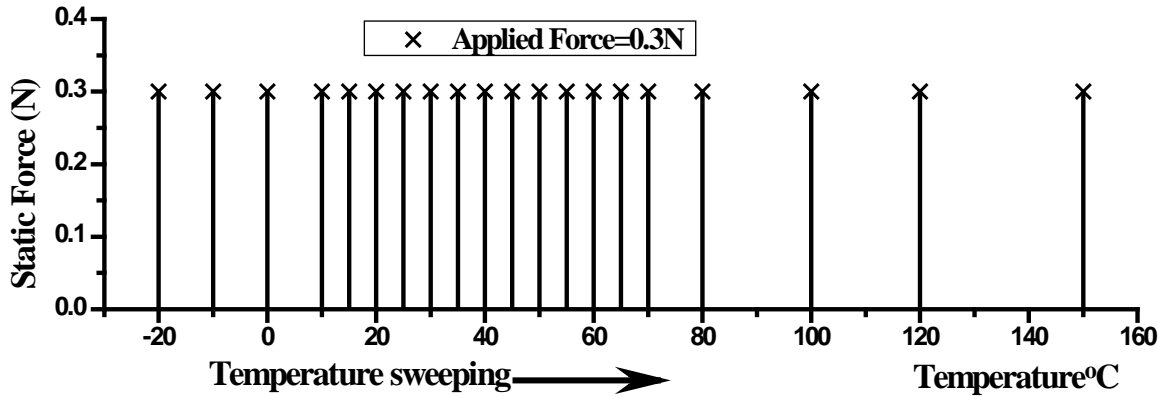
Figure 5-22: Concept of the ramping-temperature-dependent modulus experiment. Every peak represents one uniaxial tensile test.

Figure 5-23 shows four typical elastic modulus (Young's modulus) versus temperature curves, which are characterized by the ramping-temperature-dependent modulus experiments. Each curve in the Figure 5-23 can be identified into three regions: the glassy region, the transition region and the rubbery region. The measured elastic modulus and temperature range of each range of four differently-treated parylene-C are shown in Table 5-10. The first region (glassy region) shows the glassy state of the testing sample. The measured elastic modulus of parylene-C at this region varies mildly before the temperature reaches the onset of the next region. The range of the glass transition region was found between 30–60°C for as-deposited paryleneC and 80–120°C for parylene-C annealed at 100°C. When the temperature reaches the glass transition region,

the elastic modulus starts to drop quickly until the temperature reaches the onset of the third region, which is 60°C for as-deposited parylene-C and 120°C for parylene-C annealed at 100°C.
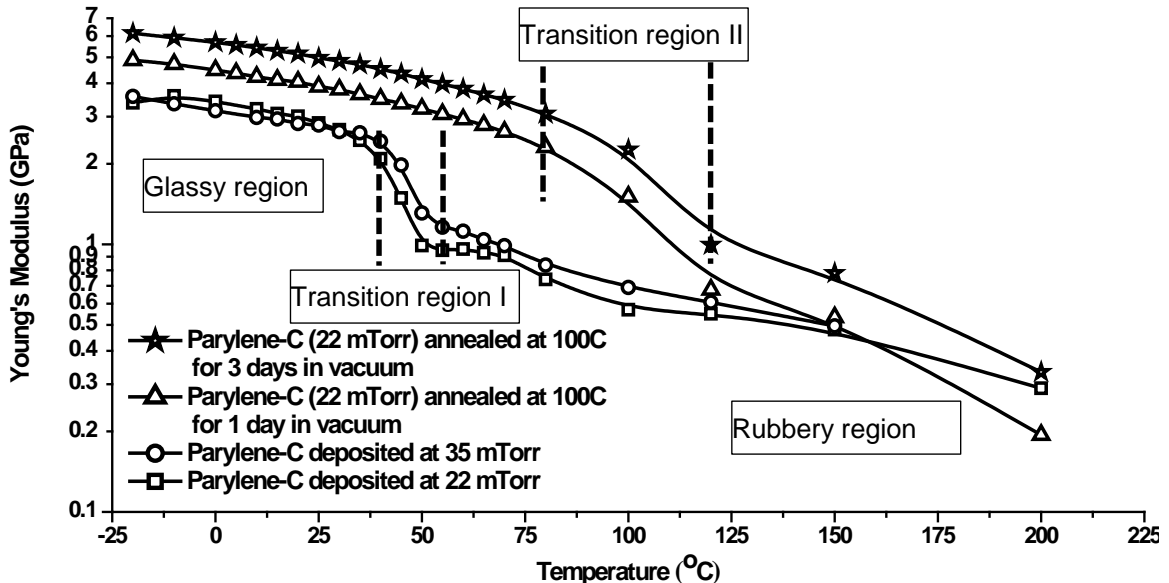
Figure 5-23: Elastic (Young's) modulus versus temperature curve. The transition region I represents the general glass transition region for as-deposited parylene-C, while transition region II represents the general glass transition region for parylene-C annealed at 100°C.

The four glass transition temperatures, T_g, which is normally defined as the maximum turndown point in the curve, i.e., maximum d^2E/dT^2 [231], are found and shown all in Table 5-10. The obtained T_g of as-deposited parylene-C are both 50°C for samples deposited at 22 mTorr and 35 mTorr. The T_g of parylene-C annealed at 100°C is between 100–120°C, which will be identified more clearly in the next section. The elastic modulus of the parylene-C obtained in the rubbery region was approximately one

order smaller than in the glassy region, implying that parylene-C can be stretched much easier than in its glassy state.

Table 5-10: Measured elastic modulus and temperature range of glassy, transition, and rubbery regions

Parylene-C treatment	Glassy region range		Transition region range			Rubbery region range	
	GPa	(°C)	GPa	(°C)	Glass transition temperature, T_g (°C)	GPa	(°C)
As-deposited (22 mT)	3.38–2.68	-20–30	2.68–0.96	30–60	50	0.96–0.29	60–200
As-deposited (35 mT)	3.57–2.64	-20–30	2.64–1.12	30–60	50	1.12–0.50	60–150
As-deposited annealed at 100°C for 1 day	4.88–2.31	-20–80	2.31–0.68	80–120	100	0.68–0.19	120–200
As-deposited annealed at 100°C for 3 days	6.15–3.08	-20–80	3.08–1.00	80–120	100	1.00–0.33	120–200

Although the ramping-temperature-dependent modulus experiment has shown its success characterizing T_g of the parylene-C samples, the uniaxial tensile test performed in this method is not continuous. If the temperature increment is too large, the T_g cannot be clearly resolved and only a rough T_g range can be identified. The T_g of parylene-C annealed at 100°C in Figure 5-23 demonstrates the problem. Another approach called dynamic mechanical analysis is commonly adopted to solve this problem and is introduced in the next section.

5.6.1.3 Dynamic mechanical analysis

Dynamic Mechanical Analysis (DMA) is a technique used to study material's viscoelastic/viscoplastic properties. As show in Figure 5-24 (a), the machine applied a continuous sinusoidal oscillatory stress, which is within material's linear elastic region, either by torsion, compression or tension to the specimen. The responded sinusoidal strain is recorded with respect to the time and the phase delay, δ, between the applied stress and the responded strain can be found as well. For a perfectly elastic material, δ equals to 0°; for a viscous material, δ equals to 90°. If δ falls in between 0° and 90°, the material is called viscoelastic material [223]. If the amplitude of the measured strain, ε, is denoted as ε_0, the frequency of the applied stress is ω, the measured strain can be represented as

$$\varepsilon = \varepsilon_0 \sin(\omega t + \delta) = \varepsilon_0 cos\delta \sin(\omega t) + \varepsilon_0 sin\delta \cos(\omega t)$$
$$= \varepsilon' \sin(\omega t) + \varepsilon'' \cos(\omega t), \tag{5-4}$$

or

$$\varepsilon^* = \varepsilon' + i\varepsilon'', \tag{5-5}$$

where ε^* is called the complex strain, ε' is the strain which is in-phase with the applied stress and the ε'' is the out-of-phase strain. If the amplitude of applied stress is σ_0, the modulus of the material can also be considered and represented as:

$$E = \left(\frac{\sigma_0}{\varepsilon_0}\right) cos\delta + \left(\frac{\sigma_0}{\varepsilon_0}\right) sin\delta = E' + iE'', \tag{5-6}$$

or

$$E^* = E' + iE'', \tag{5-7}$$

where E^* is called the complex modulus and the E' is called the storage modulus and the E'' is called the loss modulus. The relationships of E^*, E', and E'' can be shown in

Figure 5-24 (b). Physically, E'' represents the energy dissipation of the materials during the oscillatory excitation. E' represents how elastic the material is and ideally it is equivalent to Young's modulus [223]. Tan δ is the parameter representing the damping properties of the materials. Tan δ is an indicator of how efficiently the materials loses energy to molecular rearrangements and internal friction [223].
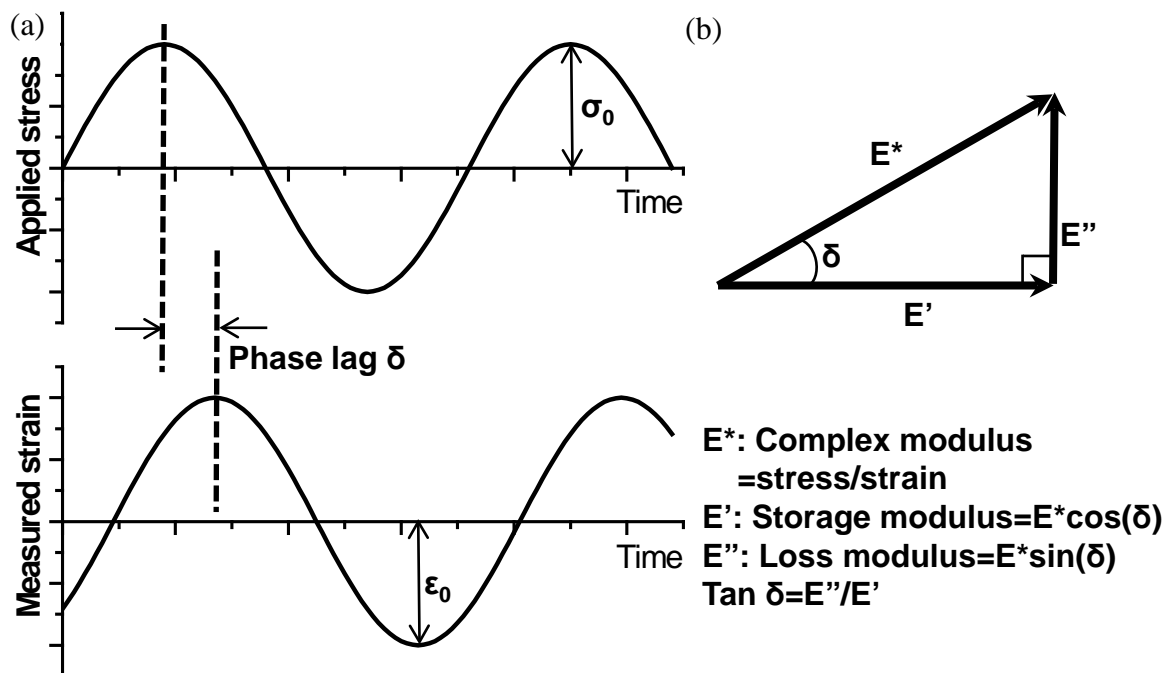
Figure 5-24: The concept of dynamic analytical analysis. (a) A sinusoidal oscillatory stress is applied and the material's sinusoidal strain response with a phase delay (viscoelastic materials) is measured. (b) The relationship of complex modulus (E*), the storage modulus (E'), and the loss modulus (E")

This sinusoidal oscillatory experiment can be performed under different temperatures and the corresponding mechanical parameters are then measured and calculated. A typical DMA result is shown in Figure 5-25. The solid line represents the

storage modulus of the specimen. For the rest of the two lines, one is the loss modulus and the other one is tan δ. It can be seen that the tan δ increases as the storage modulus decreases and the loss modulus increases. The tan δ reaches its maximum at the maximum ratio of the loss modulus to the storage modulus.
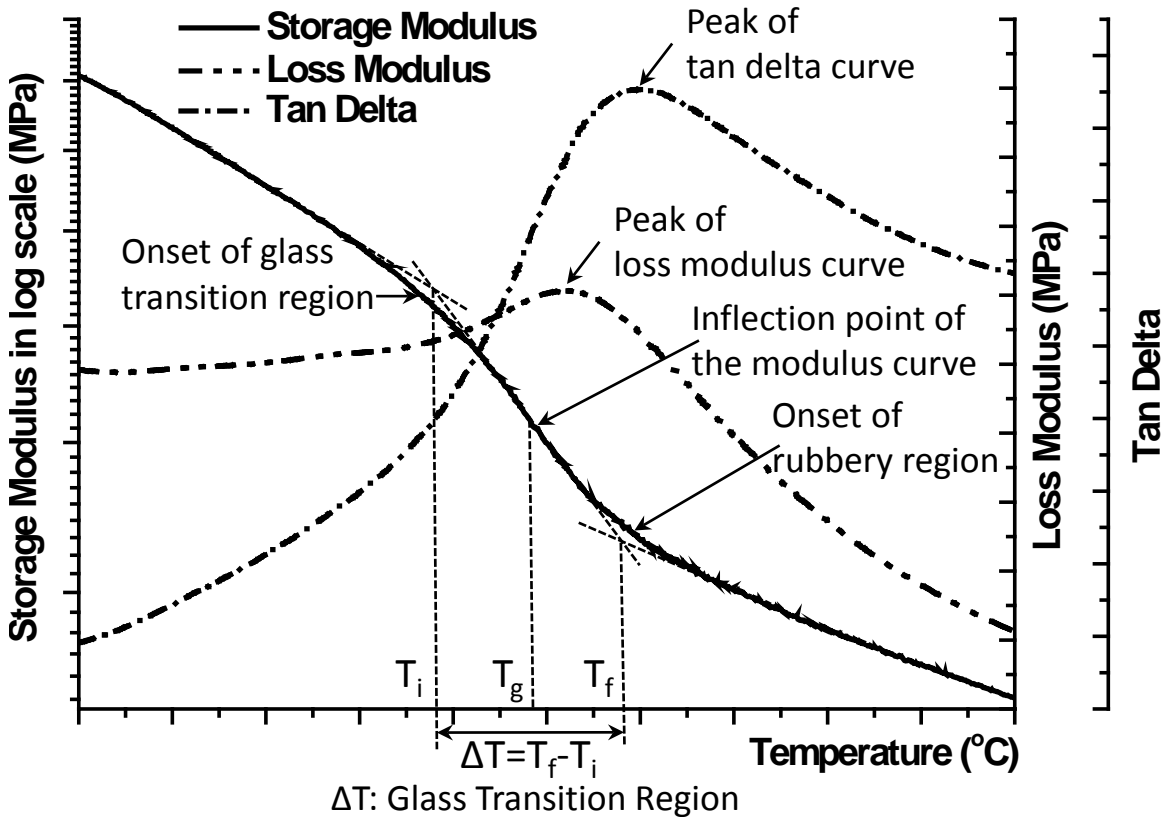
Figure 5-25: A typical DMA testing curve showing the results of storage modulus, loss modulus, and tan delta. Every curve has its corresponding definition to identify T_g.

Three different ways corresponding to the three curves in Figure 5-25 are commonly used to identify T_g of the testing samples from the DMA results [185]. For the storage modulus curve, the glass transition temperature, T_g, is defined at the inflection point of the glass transition region. The onset temperature of the glass transition region,

T_i, is defined as the intersection of the two tangents of the storage modulus curve in the glassy region and the glass transition region. The onset temperature of the rubbery region, or the end of the glass transition region, T_f, is defined as the intersection of the two tangents of the storage modulus curve in the glass transition region and the rubbery region. The glass transition temperature of the loss modulus curve and the tan δ curve are both defined as the peak of the curves. As the storage modulus represents the Young's modulus, it is more meaningful to use the storage modulus curve to study the glass transition region, and therefore will be used in our whole glass transition temperature study.

To compare the accuracy and the capability of the two approaches discussed above, a comparison of two typical results of the two approaches is shown in Figure 5-26. The sample tested is the parylene-C annealed at 100°C for one day in vacuum oven. The T_g provided by DMA is 113.1°C and the other method measures the T_g to be in the range between 100°C and 110°C. The comparison shows that two methods both provide results which are very close to each other. The discrepancy found between two curves might be attributed to the testing frequency difference, which is worth more studying. From the analytical point of view, however, the DMA approach provides a much smoother, non-interrupted curve so that T_g is able to be defined more accurately. Therefore, DMA measurement is generally used in most glass transition temperature study in the thesis unless otherwise specified.
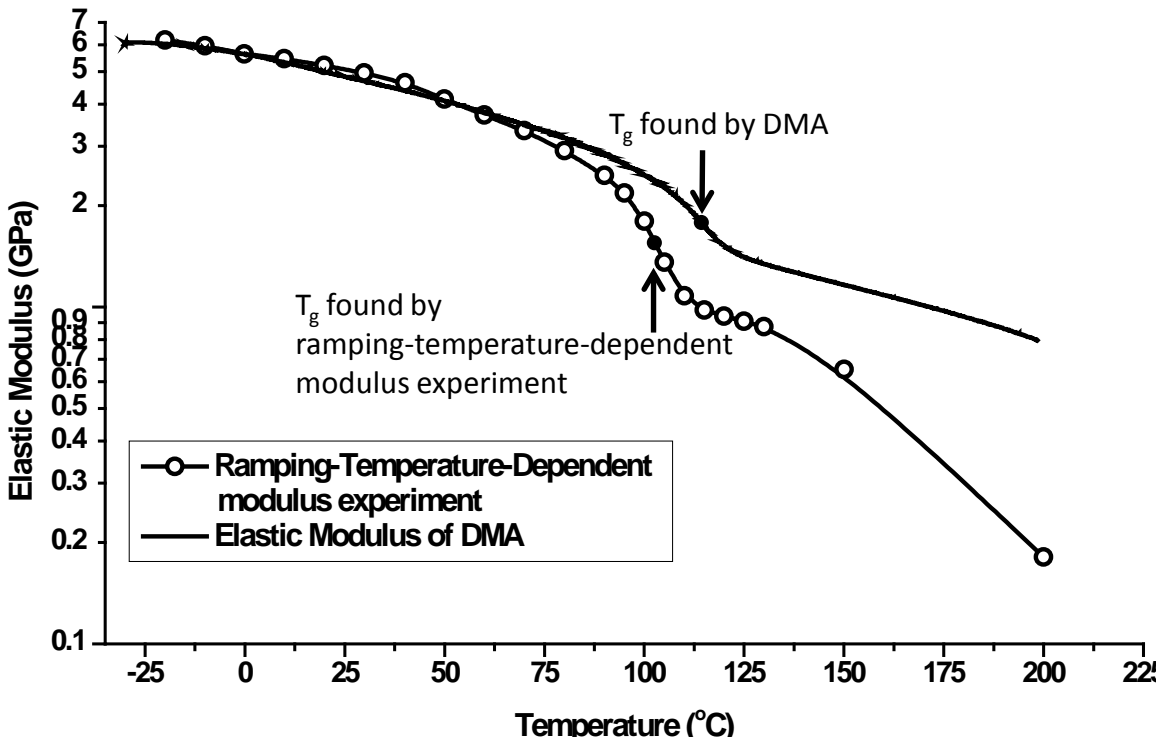
Figure 5-26: A comparison of the results of the ramping-temperature-dependent modulus experiment and the DMA test. Parylene-C sample was annealed at 100°C for one day in vacuum. T_g is found at the inflection point of each glass transition region.

5.6.2 Measuring results and discussion

Several selected measured storage modulus curves and their obtained corresponding T_g are shown in Figure 5-27, Figure 5-28, Figure 5-29, and Figure 5-30. The convection oven used in the T_g measurement experiment was always preheated to the target temperature before the parylene-C sample loading, and therefore samples always experienced step-function temperature profile during the annealing. In Figure 5-27, three samples were annealed at 100°C but for different annealing times with one curve representing the as-deposited parylene-C for comparison purposes. In Figure 5-28, four parylene-C samples were all annealed at 100°C, but for a different period of times shorter

than Figure 5-27, with one as-deposited parylene-C result for comparison. In Figure 5-29, two parylene-C samples were annealed at 200°C in vacuum for one and two days and one parylene-C annealed at 100°C for two days, with one as-deposited parylene-C result for comparison. In Figure 5-30, seven parylene-C samples were annealed at different temperatures as shown in the DMAQ800 chamber (no vacuum) for the first 30 minutes followed by the regular T_g measurement procedures. Several observations and conclusions can be found from those four figures:

1. It is clearly seen from Figure 5-27 to Figure 5-30 that the measured Tg increases as the annealing temperature increases. As shown in Figure 5-29, because all the parylene-C samples shown in the figure were all annealed in vacuum, the possibility of the oxidation effect could be eliminated. Therefore, the Tg increment is very likely attributed to the crystallinity increase after the parylene-C annealed at high temperature. Compared to the amorphous part of the polymer, the crystallite part is generally assumed to be much stronger and will remain intact under the applied force [185]. As it has been verified in Section 5.5 that the crystallinity increases when the annealing temperature increases, the deformable amorphous part of the annealed parylene-C reduces. Owing to the less amorphous part after higher temperature annealing, the molecular structure of parylene-C becomes more difficult to move, and hence the Tg is obtained to be higher after annealed. The result found agrees well with Senkevich's observation: "semicrystalline polymers exhibit an increase in their Tg, a larger Tg range and a decrease in ΔCp, making Tg determination more difficult as less amorphous material exists to contribute to the Tg" [184].

2. The measured Tg increases as the annealing time increases. The effect can be found in Figure 5-27 to Figure 5-29. This phenomenon could be explained by the same reason of parylene-C crystallinity increment. As described in Section 5.5 that the longer annealing time increases the crystallinity of the parylene-C, and therefore it can thus increase the Tg as well, as the amorphous part is the weaker part inside the polymer.

3. It is also found that the Tg increases extremely fast at the early stage of the annealing when it experiences the elevated temperature. As shown in Figure 5-28, it can be seen that Tg increases to 86.2°C after the first 30sec of annealing at 100°C and the Tg increasing rate slows down afterward. According to the previous conclusion that parylene-C's Tg increases due to its crystallization, the testing result is another strong evidence that parylene-C crystallizes fast when it experiences temperature higher than its Tg, i.e., ~ 50°C found from Section 5.6.1.2. It further confirms that the time constant of the parylene-C crystallization is shorter than one minute, which agrees well with our findings in Section 5.5.2.

4. From Figure 5-27 to Figure 5-30, it is found that the obtained Tg is usually close to, but a bit higher than, the annealing temperature. This can be explained that the free volume inside the annealed paryelne-C has been reduced to or lower than 2.5% [185] during the annealing. As it requires making the free volume go over 2.5% to make the parylene-C reach glass transition again, the temperature needs to go at least as high as or even a bit higher than the prior annealing temperature and therefore the re-measured Tg will be close to the prior annealing temperature.

5. The glass transition region of the storage modulus curve of parylene-C annealed at 200°C becomes very vague and hard to find a definite Tg. According to the trend of other Tg of the parylene-C annealed at lower temperature, this Tg might be higher than 200°C and cannot be defined from Figure 5-29 because of the insufficient testing data. Both curves of parylene-C annealed at 200°C for either one or two days shown in Figure 5-29 look like almost linear, which implies parylene-C would behave similar to the perfectly elastic material at temperatures lower than 200°C after annealed at 200°C. This will be verified again by the creep tests in Section 5.8.1.

6. It can be found from Figure 5-30 that there is no significant difference between the Tg measured at the temperature at 20°C and 40°C. As the Tg of the as-deposited parylene-C can been revealed to be around 50°C from Figure 5-27, it is hypothesized that the crystallization does not happen at temperatures less or equal to 40°C. Therefore, when the parylene-C is annealed at 20 or 40°C, there is not enough energy to cause the parylene-C polymer chains to move and crystallize. It could be concluded that Tg of parylene-C will not change as long as the prior annealing temperature is less than Tg.

7. The measured elastic modulus, i.e., Young's modulus, increases when either the annealing temperature or time increases. As it is generally believed that the crystallite has a much stronger modulus than amorphous part, it could also imply that more parylene-C is crystallized at higher annealing temperatures or longer annealing times. This finding agrees well with what has been found in Section 5.5. In addition, the descending slopes of the storage modulus are all very similar

before and after the glass transition region. In the same region, either glassy or rubbery region, the descending slopes of the storage modulus curve of every sample are also similar to each other no matter what kind of treatment the sample has experienced prior to the DMA test.

8. It is observed that the glass transition range tends to broaden as either the annealing temperature or annealing time increases. It is also likely due to that fact that the amorphous part of the annealed parylene-C is reduced, and therefore it takes more energy, i.e., higher temperature, to bring parylene-C into the rubbery region.
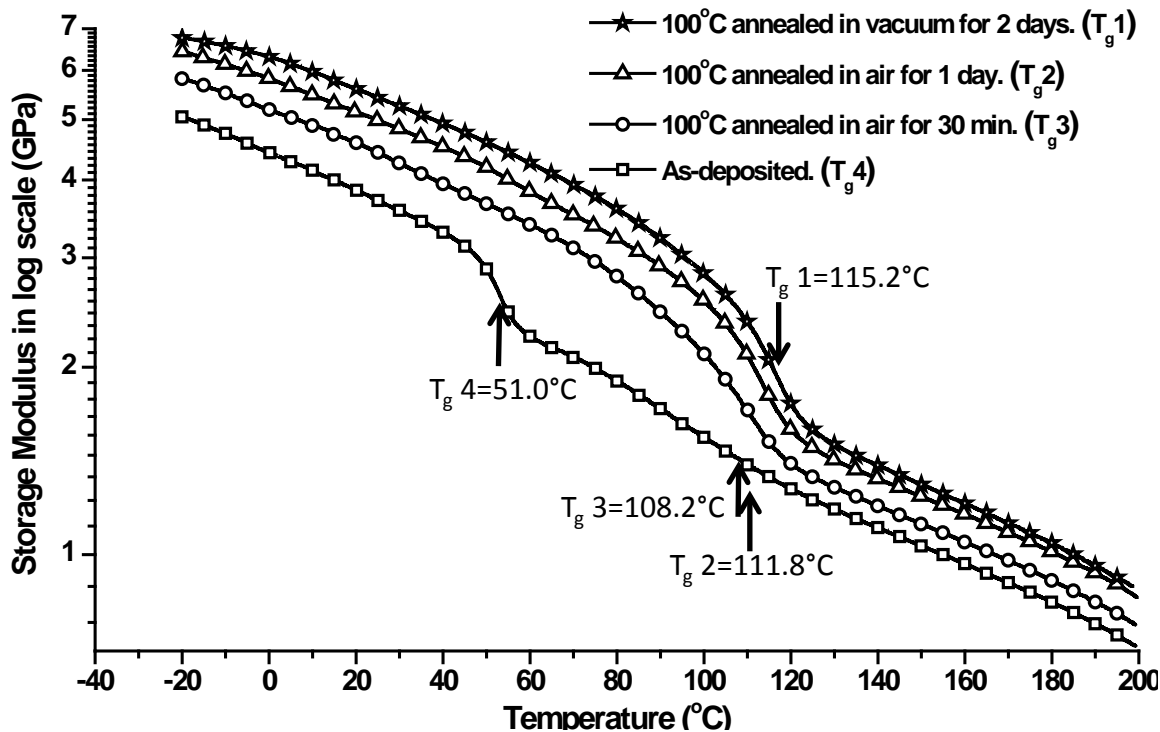
Figure 5-27: Measured T_g of four parylene-C annealed in different conditions: 3 samples at 100°C, with as-deposited parylene-C as a comparison
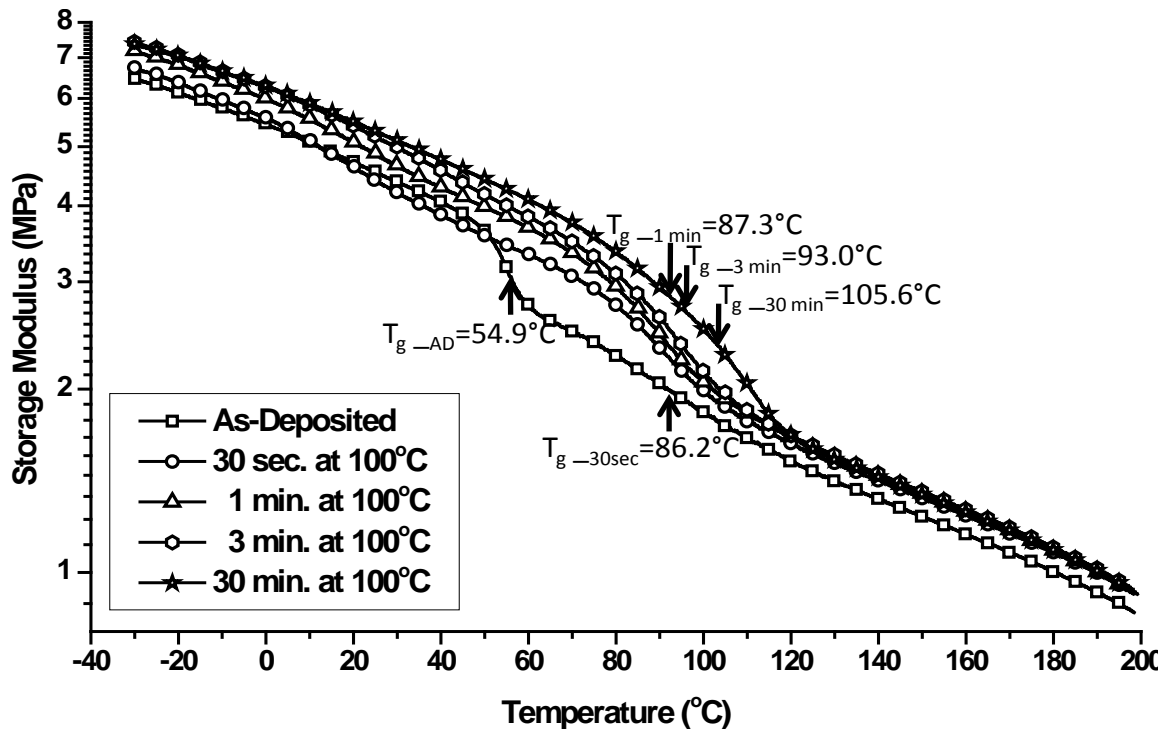
Figure 5-28: Measured T_g of parylene-C samples all annealed in 100°C but for different

times: 30 sec, 1 min, 3 min, and 30 min
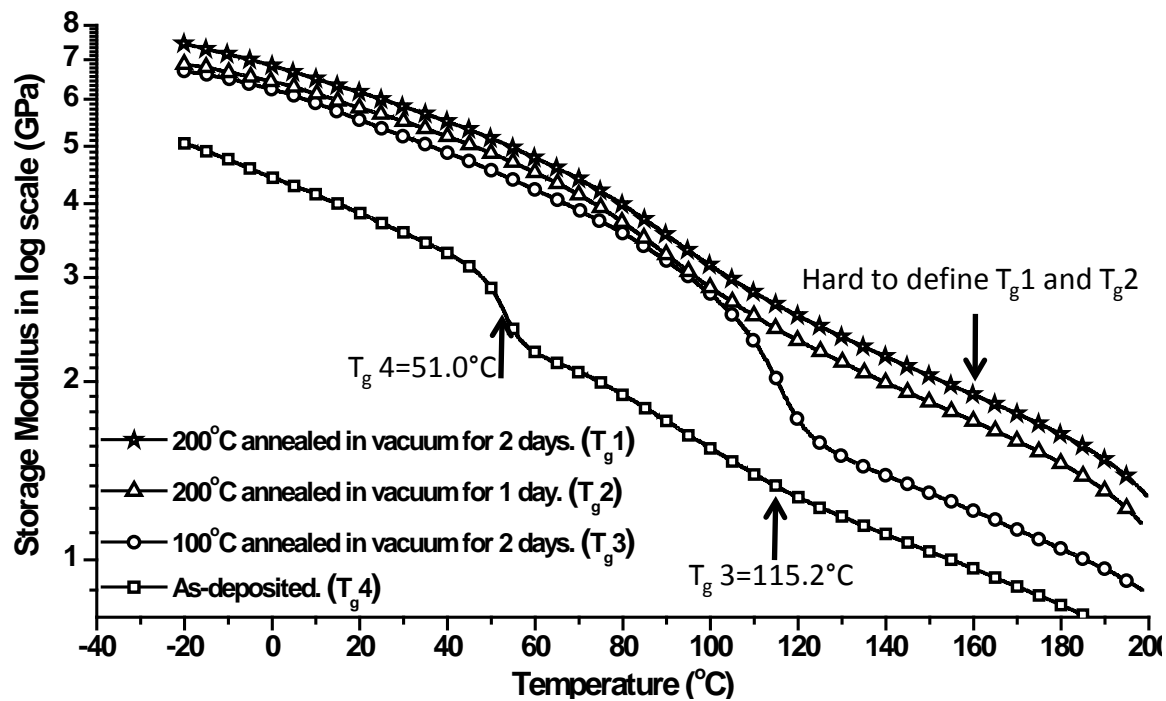
Figure 5-29: Measured T_g of four parylene-C samples annealed in different temperatures
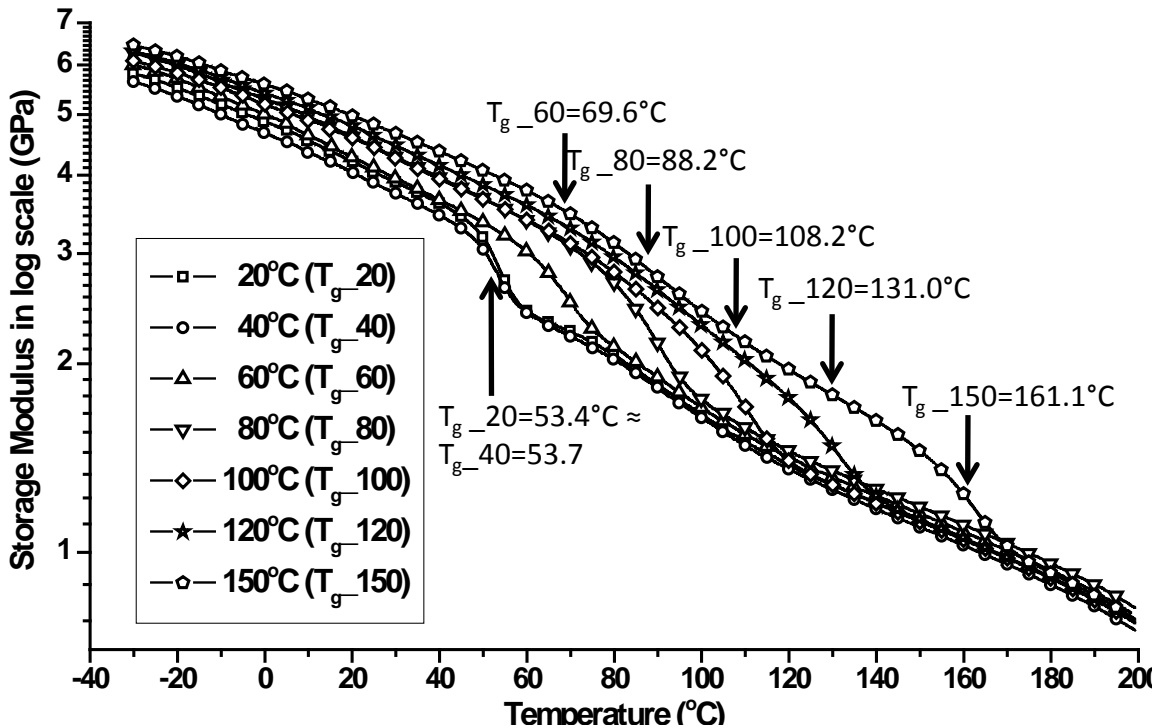
Figure 5-30: Measured T_g of seven parylene-C samples annealed in different temperatures. Samples were annealed in the DMA Q800 chamber for 30 min prior to the T_g test.

Table 5-11 systematically and quantitatively displays the measured T_g and the glass transition region of every testing sample shown in Figure 5-27 through Figure 5-30. In addition, the T_g obtained by the peak of loss modulus curve and the tan δ curve are also listed for comparison.

Table 5-11: Measured glass transition temperature *via* DMA approach

Parylene-C treatment	T_g obtained by storage modulus (°C)				T_g obtained by peak of loss modulus (°C)	T_g obtained by peak of tan δ
Sample treated in DMA chamber	T_i	T_g	T_f	ΔT	T_L	
As-deposited	50.2	53.4	57.0	6.8	68.4	94.1
40°C in air for 30 min	50.8	53.7	55.5	4.7	67.2	91.6
60°C in air for 30 min	65.3	69.6	73.3	8	78.15	93.84
80°C in air for 30 min	83.6	88.2	94.9	11.3	95.3	101.14
100°C in air for 30 min	105.6	108.2	115.6	10	113.9	119.1
120°C in air for 30 min	124.9	131.0	138.0	13.1	136.8	143.6
150°C in air for 30 min	155.3	161.1	169.1	13.8	168.9	-
Sample treated outside DMA chamber	T_i	T_g	T_f	ΔT	T_L	
As-deposited at 35 mT	52.5	55.1	58.8	6.3	71.6	92
As-deposited	50.2	53.4	57.0	6.8	68.4	94.1
100°C in air for 30 sec	78.4	87.3	98.4	20	95.3	101.8
100°C in air for 1 min	81.8	86.2	100.6	18.8	93.7	103.9
100°C in air for 3 min	82.7	93.0	103.2	20.5	98.9	107.0
100°C in air for 30 min.	96.7	105.6	115.8	19.1	111.2	120.6
100°C in air for 1 hour	95.1	103.0	109.6	14.5	106.7	115.9
100°C in air for 2 hour	96.2	101.5	109.6	13.4	109.6	114.4
100°C in air for 3 hour	96.4	101.8	111.2	14.8	108.3	115.9
100°C in air for 6 hour	97.8	106.3	115.9	18.1	112.2	118.9
100°C in air for 16 hour	103.1	110.3	118.9	15.8	116.8	122.9
100°C in air for 1 day	104.4	111.8	119.7	15.3	117.4	123.3
100°C in air for 2 days	106.9	114.7	122.3	15.4	120.2	125.3
100°C in air for 3 days	111.4	116.9	122.2	10.8	122.1	128.0
100°C in vacuum for 1 day	100.5	113.1	121.5	21.0	118.4	124.7
100°C in vacuum for 2 days	103.7	115.2	122.4	18.7	120.2	125.3
200°C in vacuum for 1 day	Hard to find a Tg					
200°C in vacuum for 2 days	Hard to find a Tg					

Apart from the findings aforementioned, more things can be observed from Table 5-11:

1. The Tg of as-deposited parylene-C is found at 53.4°C. On the contrast to the ramping-temperature-dependent modulus experiment which provides a rough Tg and the glass transition range, DMA measurement provides much more accurate Tg of the parylene-C and also its range. Even though, Tg provided by both methods are very close, meaning that they are both reliable approaches.

2. It is shown in Table 5-11 that Tg of the parylene-C deposited at 35 mTorr (55.1°C) similar to 22 mTorr (53.4°C). Although it has been shown in Section 5.5.3 that the parylene-C is likely have lower crystallinity when the deposition pressure increases, the crystallinity difference does not seem to influence the Tg results of these two parylene-C samples. On the other hand, however, it also shows in Section 5.5.3 that the crystallite size of these two parylene-C deposited at different pressure are very similar, which might explain the Tg-similarity result obtained in this section. More future work is required to figure out the cause of this observation.

3. As discussed in Section 5.4, it is assumed that the mechanical properties of parylene-C annealed at 100°C have no significant difference between in the air or in the vacuum. The hypothesis applies in Table 5-11 as well. For instance, there is no distinguishable difference found between the Tg of the parylene-C annealed at 100°C for one day in air (111.8°C) or vacuum (113.1°C). Therefore, sample oxidation is likely not to be the dominant issue in terms of the Tg measurement.

4. Although Tg increases as the annealing time increases, it is found that Tg actually increases fast from 53.4°C to 87.3°C during the first 30 sec when annealed at 100°C, and reaches 105.6°C after 30 min of annealing. As the parylene-C's Tg change within only one minute agrees well with result of Section 5.5.1 that the time constant of the crystallization of parylene-C annealed at 100°C is less than 1 minute, it can be concluded that the Tg is mainly influenced by the fast progress of the crystallization of the parylene-C.

5. It is also phenomenally observed that the Tg obtained using the peak of the loss modulus curve and the tan δ curve is usually higher than storage modulus curve. In spite of the discrepancies between Tg obtained from storage modulus, loss modulus and tan δ, researchers accept it as the glass transition represents a range of the behavior and people have agreed to accept a single temperature as the indicator for certain standards [232]. Scientists working on different aspects may pick up different values from the same set of data. In our experiments, the order of the three Tg can be generally shown as:

$$\text{Storage modulus } T_g < \text{Loss modulus } T_g < \text{Tan } \delta \ T_g$$

6. Dabral et al. predicted the parylene-C Tg as 150°C according to the their obtained stress-temperature curve [110]. The Tg was determined by them at the time when the stress started to show no large variations. However, it is also noted that the Tg could be found as different via a different approach and therefore a different value is obtained according our new observation. It is first found from Dabral's curve that the as-deposited parylene-C shows -6 MPa (i.e. compressive stress) after the deposition. The stress then decreases (i.e., becomes more compressive) as the

temperature increases until 50ºC. The stress keeps increasing until it balances with the silicon substrate. From Dabral's reported curve of stress versus temperature, a turning point is found at 50ºC. The most negative stress (i.e., the most compressive stress) is found at this turning point and then starts to increase as the temperature increases and then stabilizes after 100ºC. The assumption of this phenomenon is that the parylene-C expands until 50ºC due to thermal expansion of the sample, and starts to shrink after the temperature becomes higher than 50ºC due to the crystallization. This result actually agrees well with what has been found in Section 5.3. Therefore, according to our discussion in Sections 5.3, 5.5 and also Dabral's stress-temperature curve, the parylene-C starts to crystallize at around 50ºC, and therefore the Tg could be defined as 50ºC.

5.6.3 Summary

Although the study of parylene-C T_g started as early as in 1966 by Gorham, the past results indicated that there still exists inconsistency of the reported glass transition temperatures of parylene C, which widely ranged from 13 to 150ºC. It can be found from Table 5-9 that different measuring techniques can produce different T_g results. This is not surprising, though. Different researchers from research fields would adopt different approaches which is more relevant to their works. The different can be as much as 25 degree difference in data from a DSC to DMA data reported as peak of tan delta [232]. In two of our experiments, ramping-temperature-dependent modulus experiment and DMA analysis, the obtained T_g of as-deposited parylene-C show consistent results and all of them fall in the range of ~ 50–55°C. Our measured T_g agrees well with the numbers published by Alpaugh, Senkevich and Huang. Annealing temperature and time are

proved to be the main cause affecting the results of T_g and its range. High annealing temperature (higher than the T_g of as-deposited parylene-C) and long annealing time can make the parylene-C more crystallized and therefore increases its final T_g. Apart from the different measuring approaches, it could be concluded that unstandardized parylene-C sample preparation is likely one of the reasons causing the variation of the T_g's literature value. On the other hand, the deposition pressure does not seem to influence the measured T_g, in our tests, which need more data points to verify this observation. Future work would also focus on the influence of the deposition temperature and also the deposition rate.

With its superb biocompatibility and its compatibility with the CMOS fabrication process, parylene-C is widely used as a biocompatible material in MEMS technology. Since many cleanroom processes introduce high temperature during the process, parylene-C is very likely to be annealed during the device fabrication. These heat-generating processes could cause the T_g to shift during the fabrication and the parylene-C will not behave the same as the as-deposited one after the clean room fabrication process. In other words, knowing the temperature history of the parylene-C fabrication is crucial and can be very helpful in predicting its glass transition temperature and also mechanical properties, therefore the device properties after the manufacturing. If the device's parylene-C mechanical property is the main concern during its operation, the temperature history needs to be recorded in order to control its final functional behaviors.

5.7 Uniaxial Tensile Test

Uniaxial tensile test is one of the most fundamental and popular tests used to measure the mechanical properties of a material. Figure 5-31 shows a typical stress-

strain curve of an as-deposited parylene-C film obtained from our uniaxial tensile test at room temperature. The solid line shows the nominal stress-strain curve while the dashed line represents the modified true stress-strain one. From the regular engineering aspect, nominal curve is more conservative and therefore will be considered in this section unless otherwise specified. In most of the testing results, it is very common to see an artifact showing a toe region in the early stage of the testing curve as seen in the Figure 5-31. This is caused by a takeup of slack and needs to be corrected to obtain correct parameters following the ASTM standards D882-09 and D638-08 [233, 234]. In this section, five different parameters: elastic modulus (Young's modulus, E), nominal tensile strength (σ_T), yield strength (σ_Y), percent elongation (%El) and percent elongation at yield (ε_Y) were considered and calculated according to the definition of ASTM standards. In terms of the identification of the yield point, there are different ways to find out the point depending on the curve feature of the material. Provided by ASTM standard D638-08, the yield point is defined as the first point on the stress-strain curve at which an increase in strain occurs without an increase in stress. By this definition, it is very likely the nominal tensile strength shares the same value of the yield strength due to parylene-C's stress-strain curve characteristics.

A film of 20µm thick parylene-C was first deposited on a clean glass plate and then the film was cut into 5.3-µm-wide strips for testing. The gauge length was taken as 10 mm for uniaxial tensile test. The parylene-C strips were then treated at different temperatures to study the temperature effects. In addition, parylene-C film deposited at different pressure was also obtained to study the deposition pressure influence. As oxidation is recognized as a key control factor affecting final parylene-C's properties, it
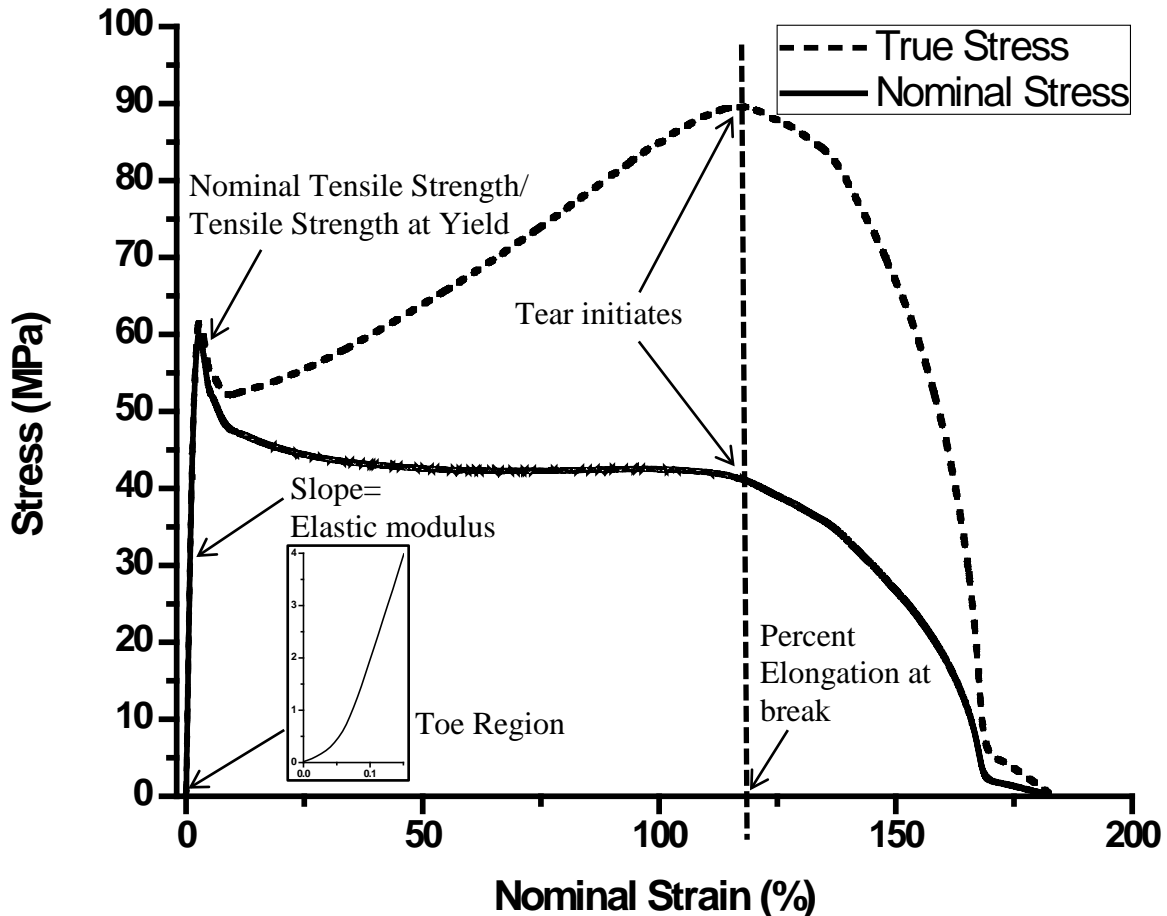
Figure 5-31: Typical as-deposited parylene-C film uniaxial tensile test results obtained by TA instrument DMA Q800 system. Toe region is compensated to give the final correct calculated parameters. All terminologies follow the definition of the ASTM standard D882-09 and D638-08 [233, 234].

was also explored in this section. The testing environmental temperature was 20°C unless otherwise specified. The strain loading rate was 1% / min. At least three samples treated in the same condition were tested to calculate the average number and standard deviation of the parameters. Table 5-12 shows the uniaxial tensile tests testing results of parylene-C film treated under different conditions. The literature numbers provided by SCS, and reported by Gorham [172], Spivack [235], Baker [195], and Beach [101, 102]

are also listed for comparison. The results of different post-deposition treatment and their different effects are discussed in the following sections.

5.7.1 As-deposited parylene-C film

The as-deposited parylene-C was deposited at 20°C and 22 mTorr. A typical uniaxial tensile curve of the as-deposited parylene-C is shown in Figure 5-31. Table 5-12 lists five different types of mechanical properties of the as-deposited parylene-C film obtained in our uniaxial tensile test. Due to a common toe region effect, elastic modulus can be calculated based on two different reference points. One is to take the tangent to a short section of the proportional region after toe region correction, denoted as E. The other is to take a slope from the measuring point with respect to 0 MPa in stress and 0 % in strain, denoted as E_0. The value shown in Table 5-12 is always higher than the literature values. Because the proportional region of parylene-C does not show a linear line but a gradually-changing curve, it is believed that the elastic modulus measured at different strain can be different and the value decreases with the increase of the strain.

Two values of tensile strength are provided here as well. One is the maximum nominal tensile stress, σ_T, according to ASTM standard D882-09, while the other one represents the modified maximum true stress, σ_T. For the tensile strength obtained from SCS, the value represents the maximum stress prior to plastic deformation. However, whether the value is calculated as nominal or true stress is not clearly stated from the parylene-C provider. Therefore both our measured numbers are listed to compare to the literature values.

Table 5-12: Measured mechanical properties of parylene-C film's uniaxial tensile test

Parameter / Parylene-C treatment	Elastic modulus	Elastic modulus from 0 MPa and 0%	Nominal tensile strength	Max true tensile stress	Yield strength	Percent elongation at yield	Percent elongation
Symbol	E	E_0	σ_T	σ_{TT}	σ_Y	ε_Y	%El
Unit	GPa	GPa	MPa	MPa	MPa	%	%
SCS	2.758		68.948[*]		55.158	2.9	Up to 200
Gorham [172]	3.172		73.08**		NA	NA	220
Spivack [235]*	2.354; 2.746 (1% strain)		61.302; 68.658		57.9; 54.9	4.2; 2.9	170; 200
Baker [195]	2.917		NA		56.904	NA	NA
Beach [101, 102]	3.2		70**		55	2.9	200
As-deposited (22 mTorr)	3.841	3.470	58.37	67.869	58.37	2.861	119.139
Standard deviation	0.315	0.285	5.718	7.290	5.718	0.472	17.611
As-deposited (35 mTorr)	2.999	2.452	49.189	50.45	49.189	2.506	66.325
Standard deviation	0.156	0.066	2.186	2.264	2.186	0.039	23.767
30 sec100°C in air	4.339	3.650	77.506	80.938	77.506	4.260	43.969
Standard deviation	0.125	0.355	1.307	1.274	1.307	0.271	4.250
1 min100°C in air	4.680	4.060	77.233	81.066	75.687	3.197	37.848
Standard deviation	0.094	0.197	6.660	6.016	9.188	0.873	11.224
3 min100°C in air	4.467	3.757	81.087	84.733	81.087	4.164	43.383
Standard deviation	0.234	0.517	2.520	2.460	2.520	0.374	5.896
30 min100°C in air	4.251	3.239	74.153	77.276	74.153	4.153	36.963
Standard deviation	0.057	0.052	4.273	4.147	4.273	0.598	6.037
1 day 100°C in air	4.547	4.070	83.921	86.834	83.921	3.367	8.526
Standard deviation	0.292	0.286	1.288	1.204	1.288	0.313	1.366
1 day 100°C in vacuum	4.312	4.058	72.700	75.166	72.700	2.200	6.897
Standard deviation	0.189	0.264	2.893	3.227	2.893	1.530	5.172
2 day 100°C in vacuum	5.298	4.835	92.185	95.135	92.185	3.157	6.313
Standard deviation	0.216	0.165	3.466	3.666	3.466	0.286	1.312
1 day 200°C in vacuum	4.961	4.472	81.659	84.636	81.659	3.399	6.515
Standard deviation	0.086	0.192	2.439	3.034	2.439	0.357	3.236
2 day 200°C in vacuum	6.058	5.629	102.933	106.591	102.933	3.449	4.512
Standard deviation	0.129	0.268	7.490	8.325	7.490	0.603	0.447

*The first number corresponds to 0.12–28.0 µm thick while the second one is 25 µm thick.

**It is not clearly specified what type of tensile strength— nominal or true tensile stress—is given in the SCS parylene-C data sheet and references [100–102].

The yield strength given by SCS is calculated with a 0.2% offset from the elastic strain. Because different elastic modulus could lead to different yield strength value, the tensile strength shown in Table 5-12 is calculated according to standard ASTM D882-09. The obtained value is higher than SCS's due to the offset, but the deviation is within 10%.

Percent of elongation is obtained as 119.14 %, which is much smaller than the literature value. It is believed that the testing specimen tore before the specimen really broke which is actually caused by a nicks or imperfect cutting edge. Cutting the parylene-C film specimen needs to be very careful to prevent nicks or tears at the edge. With the knowledge of the fracture mechanics, when the loading goes high, the nicks can induce stress concentration locally and suddenly propagate, becoming a crack causing the rupture earlier to happen and lead to anomalous results. Specimen with nicks at the edge will end up with a lower percent elongation at break. In practice, however, micro nicks are difficult to avoid and tears happen very often during the tests as shown in Figure 5-31. In addition, it is also found that the alignment of the specimen installed in the testing machine affects the percent of elongation. A proper installation of the specimen gets rid of unwanted bending stress and thus helpful in getting a more appropriate testing result.

5.7.2 Deposition pressure influence

To study the deposition pressure influence of parylene-C mechanical properties, another parylene-C film deposited with pressure at 35 mTorr was also prepared with the same geometry and then tested under the same testing conditions. The testing data is also shown in Table 5-12. It is found that all mechanical properties of parylene-C film

deposited at 35 mTorr have smaller values compared with parylene-C film deposited at 22 mTorr. It is likely because the parylene-C deposited at higher pressure has a higher deposition rate and thus more polymerization centers form. It then results in more micro voids of the parylene-C film deposited at 35 mTorr than 22 mTorr, and thus the mechanical properties show smaller values. Such kind of parylene-C has more and shorter polymer chains and therefore cannot organize in order as they can at low deposition pressures [104]. As aforementioned in Sections 5.5 and 5.6, because amorphous parylene-C is weaker than crystalline parylene-C, it is reasonable that the mechanical properties of parylene-C deposited at 35 mTorr are more amorphous and therefore generally smaller than 22 mTorr.

Figure 5-32 shows the comparison of typical stress-strain curves of parylene-C film deposited at the pressures with both 35 mTorr and 22 mTorr. It is observed that the elongation of parylene-C film deposited at 35 mTorr is smaller than at 22 mTorr. It can also be seen that there is no strain hardening for parylene-C deposited at 35 mTorr. It is probably because the looser structure or the likely short polymer chain of the parylene-C film which cause the material easy to be broken, which means less ductility. Although the parylene-C film deposited at 22 mTorr shows better ductility, the sporadic spread data points, however, make it still hard to exactly conclude the influence of the deposition pressure to the percent elongation. The same phenomenon, i.e., widely spread percent of elongation data points, was also observed by Hassler [104]. One interesting observation in Hassler's result shows: in spite of the widely spread data values, Hassler's parylene-C film deposited at 20 mTorr has only 20% elongation at break in average, which is much less than the literature value of 200%, and also our testing value of 119.139%. In

addition, it also has been found that a lower strain rate will favor higher elongations and somewhat lower stress values [235]. Therefore, although Hassler prepared parylene-C samples with the same thickness as ours, it is shown that Hassler's strain rate was much faster than ours (about 1%/sec versus our 1%/min), and thus Hassler had much less percent of elongation results than ours.
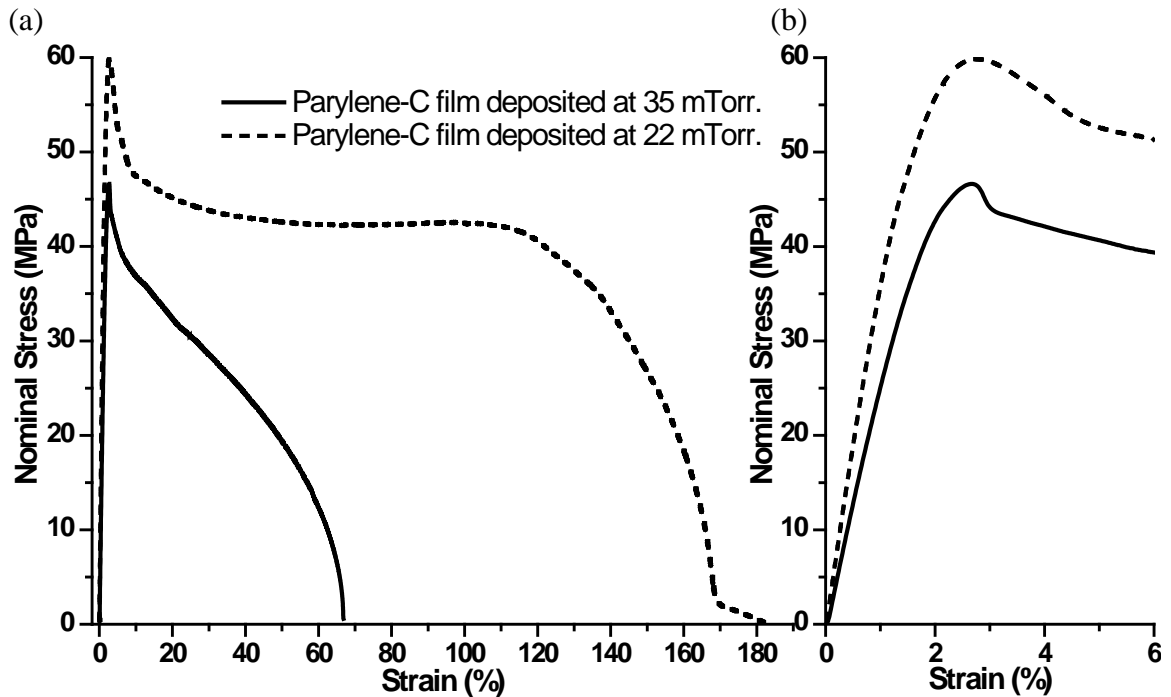
Figure 5-32: Comparison of parylene-C film deposited at different pressures. (a) Two stress-strain curves. (b) A closer view of elastic modulus and yield point

5.7.3 Oxidation effect

It has been discussed in Section 5.4 that parylene-C can be oxidized either by heat or ultraviolet (UV) light. To study the influence of the thermal oxidation effect on parylene-C's mechanical properties, two different parylene-C film samples are prepared: one is parylene-C film annealed at 100°C for 1 day in the convection oven, i.e., in the air, the other one is annealed at the same temperature for the same time but in vacuum. The

quantitative results are both shown in Table 5-12, and a closer view representing the strain less than 15% is shown in Figure 5-33.
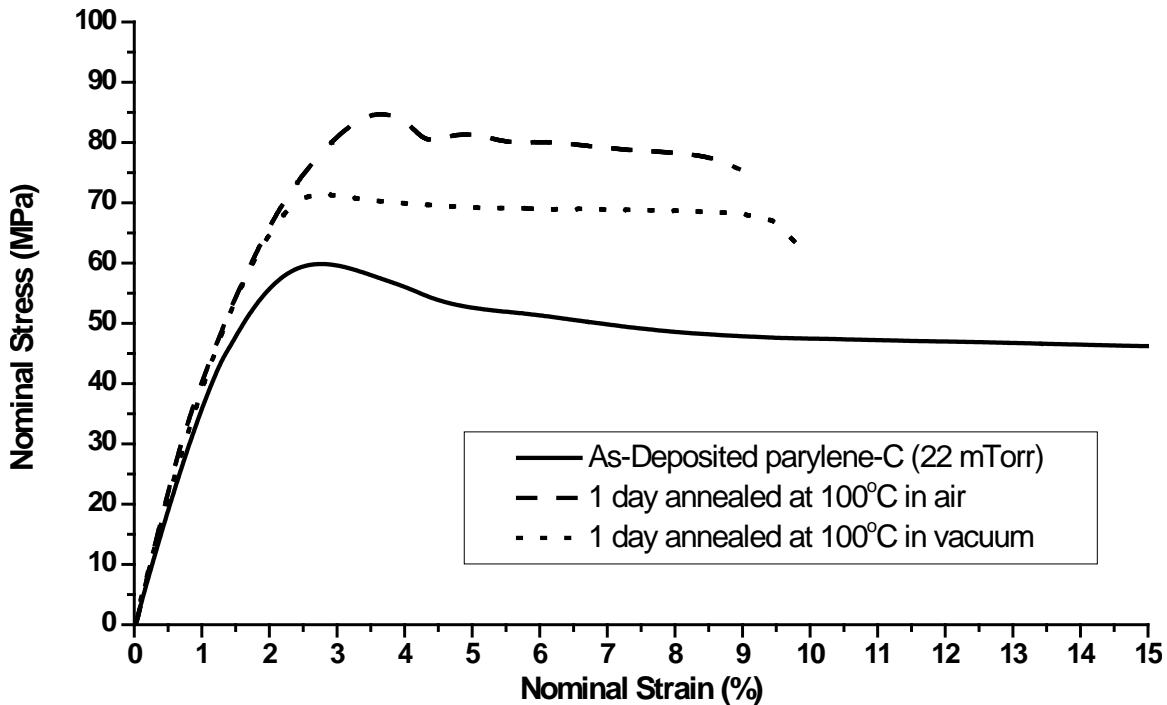
Figure 5-33: Comparison of uniaxial tensile test results of parylene-C film with three different treatments: as-deposited, 1 day annealed at 100°C in air, and 1 day annealed in vacuum

The Young's modulus of the sample annealed in the air is 4.547 GPa and 4.312 GPa in the vacuum, which are both higher than the as-deposited. This is attributed to the crystallization of the parylene-C film. Two Young's modulus do not show an significant difference as both average numbers fall in the other's standard deviation range. Two tensile strengths, or the yield strengths, are obtained as 83.9 MPa in the air and 72.7 MPa for in vacuum, which are both higher than the as-deposited parylene-C film. The tensile strength obtained for the samples annealed in the air seems to have consistantly higher values. It is likely implying that samples annealed in the vacuum system preserve the

parylene-C's mechanical properties. The tensile strength difference, however, is only within 13%. More tests need to be done to statistically isolate the two groups of results and confirm this hypothesis.

The percent of elongation of the two samples are both much lower than the as-deposited sample. Again, the difference between samples annealed in the air and in the vacuum still cannot be statistically distinguished. Lower percent of elongation infers that the parylene-C is more brittle. That is, the toughness decreases. This is attributed the crystallization that happens during the annealing at 100°C. Since two samples were both annealed at the same temperature for the same time, the crystallinity of the two samples should be similar and therefore it is reasonable that they had similar percent of elongations.

In summary, according to the uniaxial tensile test results of the two samples annealed at 100°C in the air and in vacuum, oxidation seems not to be mainly responsible for the mechanical properties change of parylene-C, which agrees well with the conclusion in Section 5.4. The main reason causing the mechanical properties to change should be the crystallization of the parylene-C, which happens quickly during the annealing.

5.7.4 Annealing temperature and time influence

The influence of the annealing temperature in terms of the mechanical properties of parylene-C will be discussed in the section. Five different parylene-C samples were annealed at five different conditions: 100°C for 30 min, one day and two days, and 200°C for one day and two days. To eliminate the possibility of the oxidation effect, all samples were annealed in vacuum with the exception of the sample annealed at 100°C for 30 min. The quantitative results are shown in Table 5-12 and graphical results of the full strain range are shown in Figure 5-34 with the result of as-deposited parylene-C for comparison. A closer view of the stress-strain curves within 5% strain is also shown in Figure 5-35.
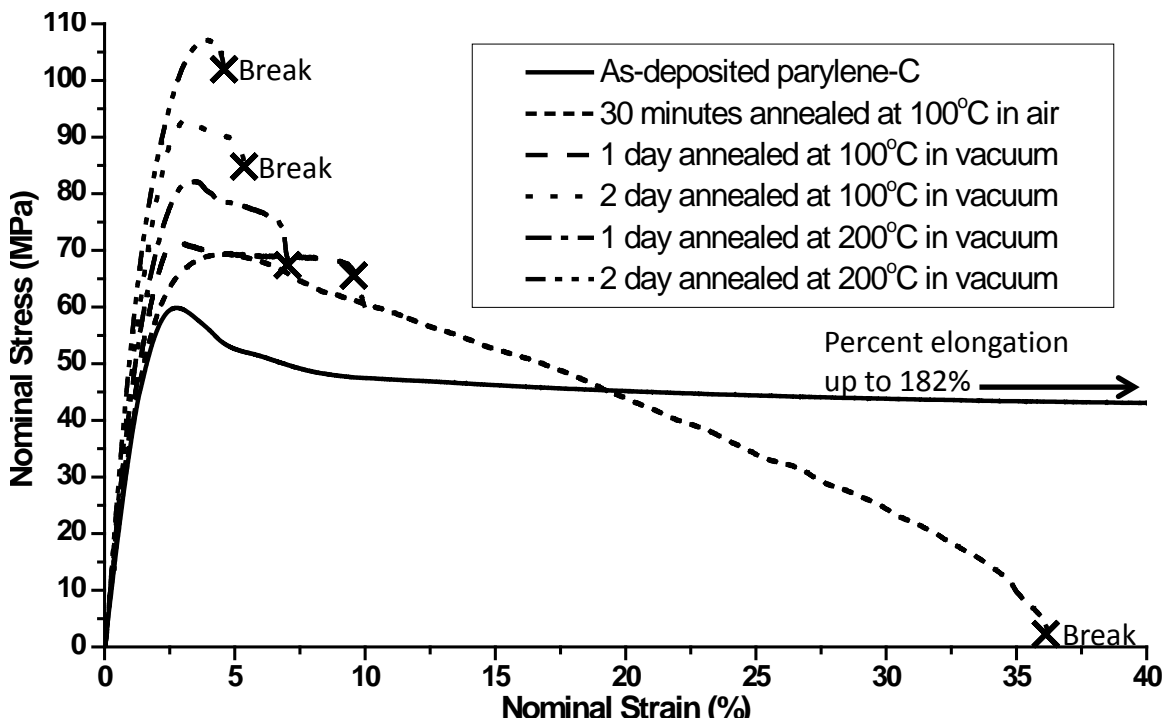
Figure 5-34: Comparison of uniaxial tensile test results of parylene-C film with six different treatments
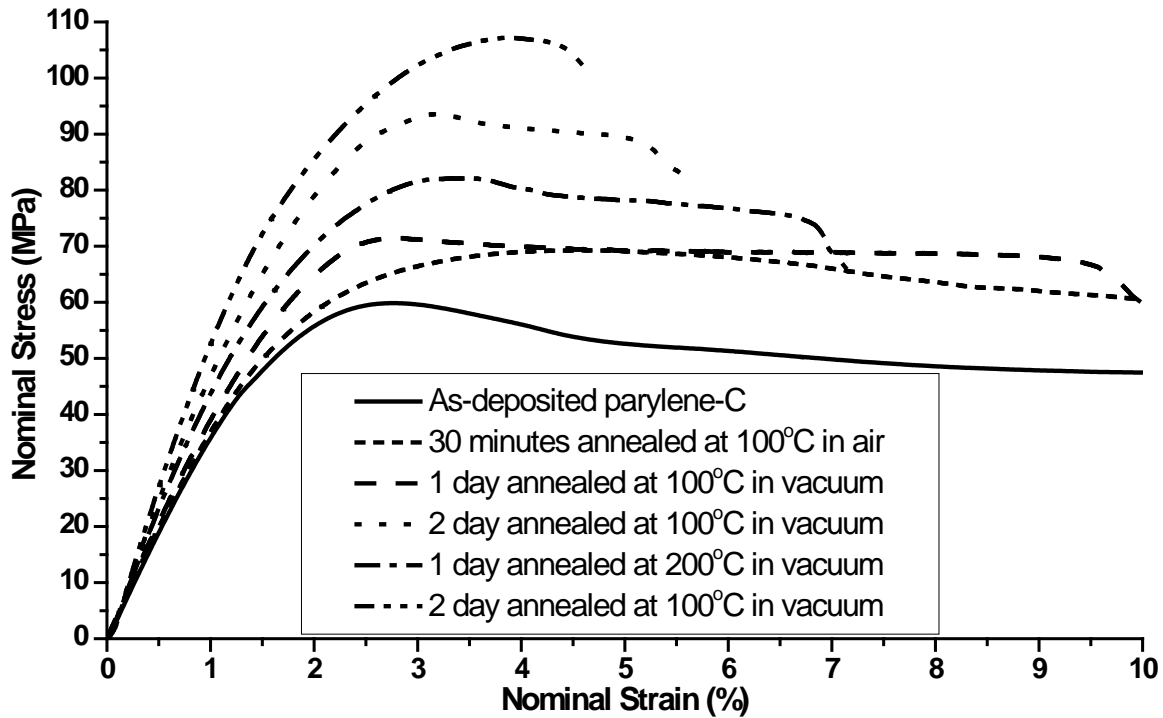
Figure 5-35: A closer view of Figure 5-34 (strain lower than 10%)

According to the testing results shown in Figure 5-35, the order of the Young's modulus of six parylene-C samples can be found as follows:

6.058 GPa (200°C, 2 days) > 5.298 GPa (100°C, 2 days) > 4.961 GPa (200°C, 1 day) >

4.321 GPa (100°C, 1 day) > 4.251 GPa (100°C, 30 min.) > 3.841 GPa (as-deposited).

It is therefore observed that the Young's modulus increases as the temperature increases. Similar effects are also found on tensile strength and the percent of elongation. The order of the tensile strength is found as:

102.933 MPa (200°C, 2 days) > 92.185 MPa (100°C, 2 days) > 81.659 MPa (200°C, 1 day)

>72.700 MPa (100°C, 1 day) > 74.153 MPa (100°C, 30 min.) > 58.370 MPa (as-deposited).

The order of the percent of elongation is found as:

4.512% (200°C, 2 days) < 6.313% (100°C, 2 days) < 6.515% (200°C, 1 day) <

6.897% (100°C, 1 day) < 36.963% (100°C, 30 min.) < 119.139% (as-deposited).

Therefore, the parylene-C stiffness, tensile strength and the toughness (brittleness) can be tailored by annealing the material at the necessary temperature to achieve the desired properties. According to what has been found in Section 5.5, it is not surprising that parylene-C becomes stiffer, stronger and more brittle as either the annealing temperature or time increase. This is attributed to the occurrence of the parylene-C crystallization during the thermal annealing which reduces the amorphous part that is in charge of the polymer chain movement. During the sample preparation, it is found that parylene-C annealed at 200°C in air became too brittle to handle and mount on to the testing equipment after the first hour annealing. Therefore there are no data points obtained to represent the condition of annealing at 200°C in the air. This is in contrast to the results of parylene-C samples annealed at 200C in the vacuum, which can still be handled easily and still maintain most mechanical properties. It can be concluded that the oxidation is a strong effect that can deteriorate the parylene-C film at 200°C. This agrees well with the conclusion in Section 5.4.

The time constant of the parylene-C crystallization at 100°C has been found to be less than one minute in Section 5.5.2. It infers that the parylene-C's mechanical properties should have experienced a big change during the first few minutes due to the crystallization. To further confirm this, another three samples were also prepared and tested to verify the assumption. Those three samples were all annealed at 100°C but for different times: 30 sec, 1 min and 3 min, which are all much shorter than 30 min. The

results are also shown in Table 5-12. It can be seen that the elastic modulus increases from 3.841 GPa (as-deposited) to 4.339 GPa (30 sec annealing) within only 30 seconds. The value has already reached the number which normally can be found for 30 minutes annealing or longer. The elastic modulus does not seem to show any significant increment for the parylene-C samples annealed at the time longer than 30 sec until 2 days of annealing. Similarly, the tensile strength increases from 58.37 MPa (as-deposited) to 77.506 MPa (30 sec annealing) after only 30 seconds annealing and shows saturation (or grows slowly) afterward. Combining what we have found in Section 5.5.2, it is evident that the parylene-C does crystallize extremely fast with a time constant less than one minute (0.845 min) and therefore the mechanical properties change fast in the first few minutes. In addition, from the discussion in Section 5.6, it is also evident that the crystallization can actually affect the glass transition temperature, and therefore would hugely change parylene-C's viscoelastic/viscoplastic properties, as will be discussed later in Sections 5.8 and 5.9.

5.7.5 Effect of testing environmental temperature

Most of the uniaxial tensile tests discussed in the previous few sections were performed at room temperature. Because parylene-C is often used in implantable biomedical devices, the mechanical properties of parylene-C at different temperatures (especially the human body temperature) needs to be understood as well. In this section, seven uniaxial tensile tests of the as-deposited parylene-C were performed at seven different temperatures: 20°C, 40°C, 60°C, 80°C, 100°C, 120°C, and 150°C. The parylene-C sample were first heated up to the targeted temperature and then annealed for 30 minutes to crystallize and stabilize the mechanical properties. After that, rather than

cooling down to room temperature, the sample was pulled at the strain rate of 1%/min while the temperature was kept unchanged during the whole uniaxial tensile test.

Table 5-13: Measured mechanical properties obtained at different testing temperatures

Parameter As-deposited parylene-C testing temperature	Elastic modulus	Elastic modulus from 0 MPa and 0%	Nominal tensile strength	Max true tensile stress	Yield strength	percent elongation at yield	Percent elongation
Symbol	E	E_0	σ_T	σ_{TT}	σ_Y	ε_Y	%El
Unit	GPa	GPa	MPa	MPa	MPa	%	%
SCS	2.758		68.948[*]		55.158	2.9	Up to 200
Spivack [235]*	2.354;2.746 (1% strain)		61.302; 68.658		57.9; 54.9	4.2; 2.9	170; 200
Baker [195]	2.917		---		56.904	---	---
Beach [101, 102]	3.2		70[**]		55	2.9	200
20°C	3.654	2.641	56.275	100.163	56.275	2.955	>166.03
40°C	3.166	2.677	37.089	81.187	37.089	1.894	>165.68
60°C	2.400	2.400	23.987	77.047	23.987	2.223	161.98
80°C	2.270	2.270	21.699	65.511	21.699	3.513	>164.77
100°C	1.771	1.771	18.473	78.775	18.473	2.872	>165.49
120°C	1.575	1.575	16.897	72.557	16.897	3.717	>164.81
150°C	1.123	1.123	14.021	51.775	14.021	3.211	136.77

*The first number corresponds to 0.12–28.0 µm thick while the second one is 25 µm thick.
**It is not clearly specified what type of tensile strength—nominal or true tensile stress—is given in the SCS parylene-C data sheet and references [100–102].

The measured mechanical properties are listed in Table 5-13 and also graphically shown in Figure 5-36. A closer view of Figure 5-36 with strain less than 5% is also zoomed in and shown in Figure 5-37. The measured Young's modulus shown in Table 5-13 has very good agreement with the curve shown in Figure 5-27, which is measured by DMA method. The comparison is shown in Figure 5-38.
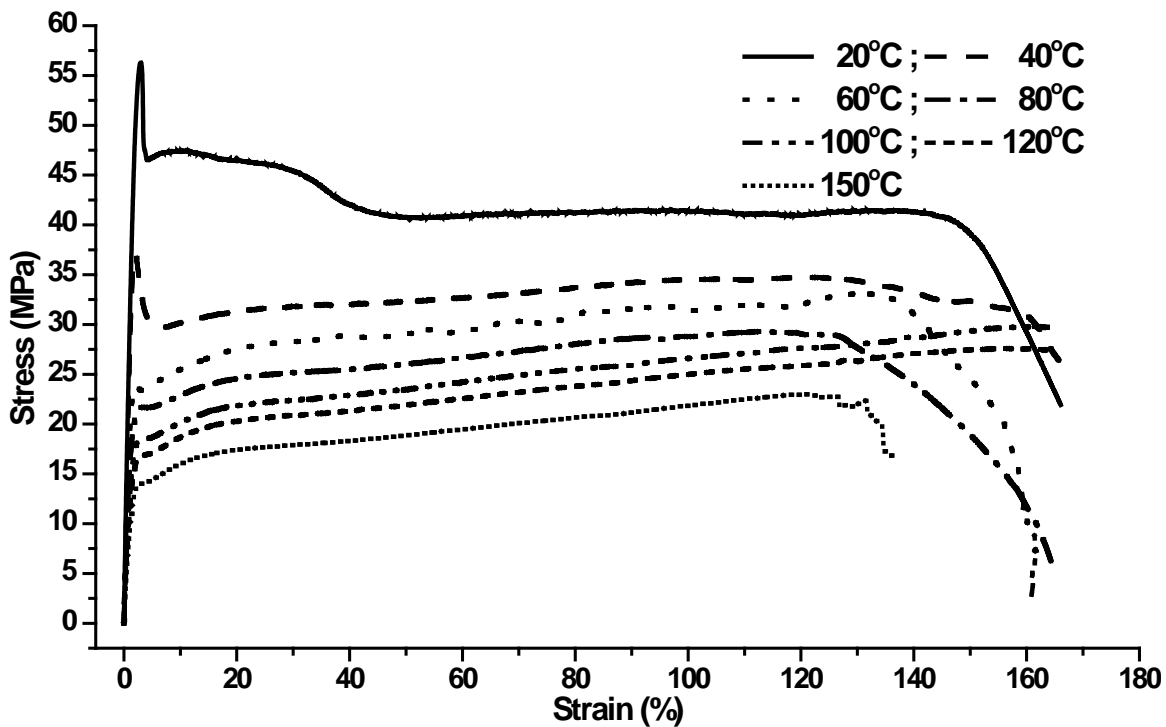
Figure 5-36: A series of uniaxial tensile tests of parylene-C performed at different environmental temperatures
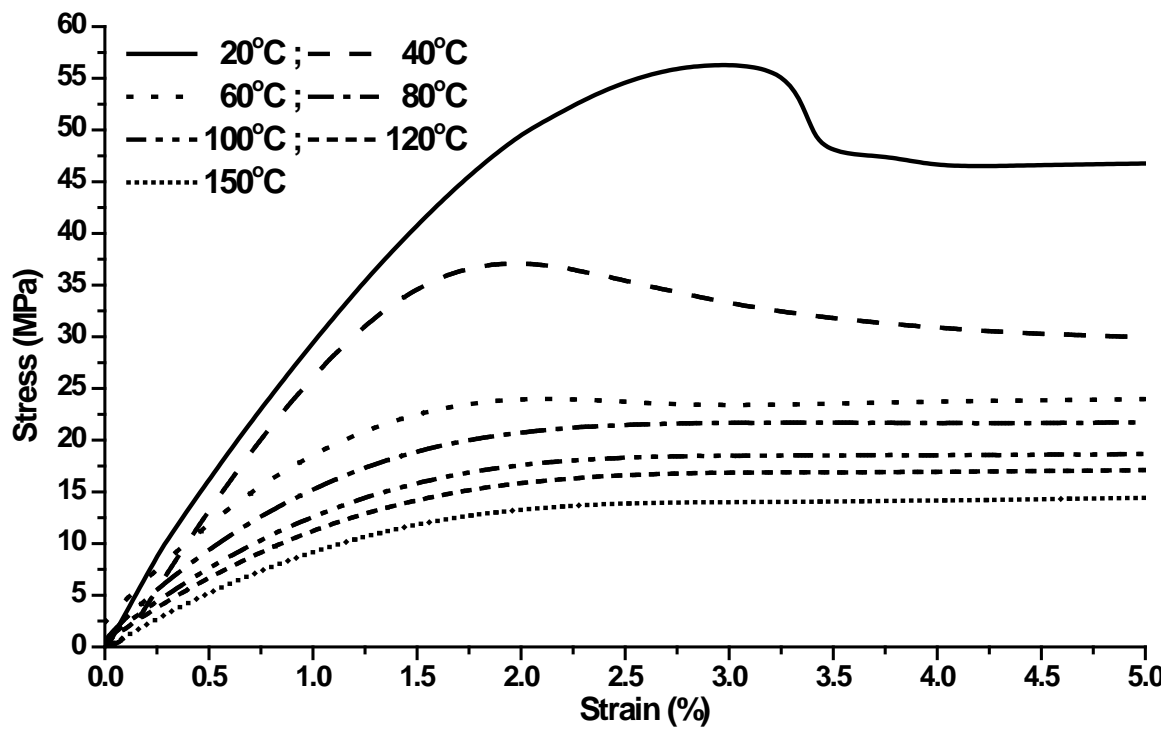
Figure 5-37: A closer view of Figure 5-36 (strain lower than 5%)
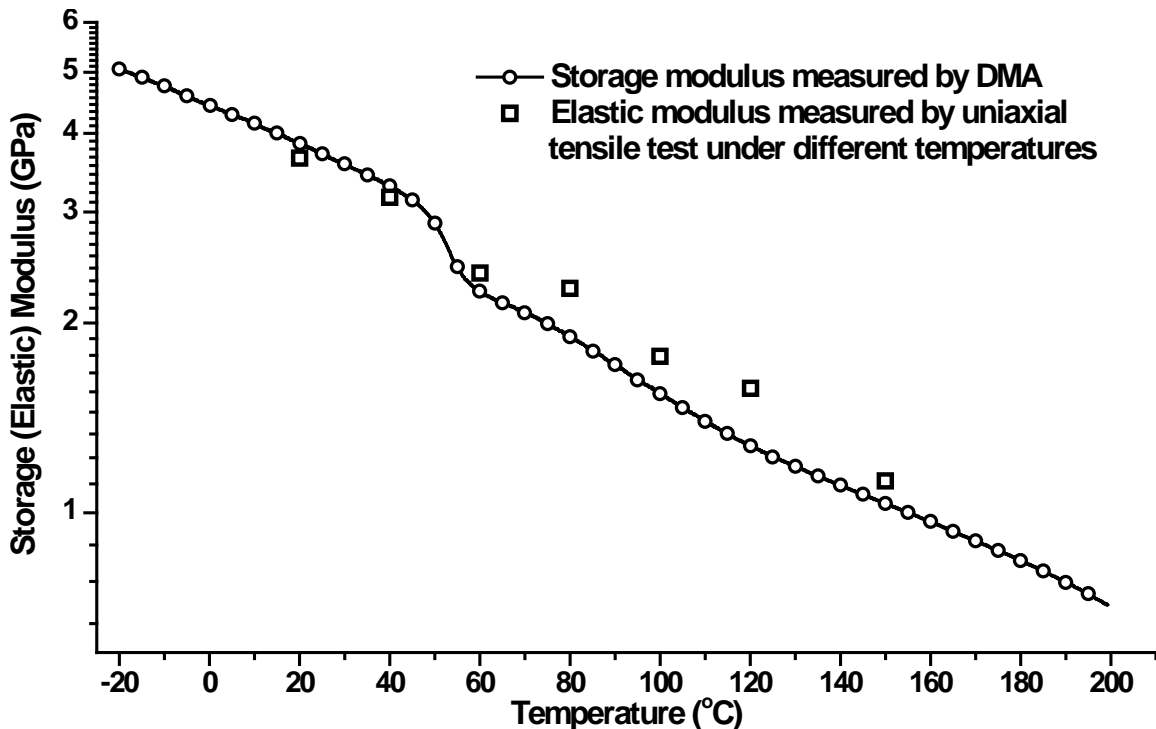
Figure 5-38: A comparison of elastic modulus measured by DMA (as-deposited curve in Figure 5-27 in 5.6) and obtained from Table 5-13

It is clearly found from Table 5-13 that the Young's modulus, tensile strength, and yield strength all decrease as the testing temperature increases. In addition, parylene-C tested at the elevated temperature normally shows elongation larger than 160%, except the one tested at 150°C. Many samples did not break when the machine reached its clamp displacement limit, meaning the parylene-C molecule can move easily without any interruption. Although the sample is crystallized, the results imply that the amorphous part of the material is softened at the elevated temperature. Therefore the parylene-C is weaker and more ductile when it is tested at the elevated temperatures.

One of the interesting results is found when the parylene-C was stretched at 150°C, which snapped earlier than most other lower temperatures. Although parylene-C might be expected even softer at 150°C than other temperatures, the phenomenon that

parylene-C snapped earlier at 150°C is likely due to sample at 150°C as described in the Section 5.4.

In terms of the yield strength determination, the numbers shown in Table 5-13 still follow the definition in ASTM standard D638-08. However, whether the sample can restore to its original length under a stress state lower than the yield strength shown in Table 5-13 is still questionable. A more accurate loading-unloading experiment, which will be introduced in Section 5.6, needs to be executed to figure out the yield point by definition: the point that material starts not to behave elastically.

5.7.6 Summary

It is generally believed that parylene-C with higher crystallinity increases the Young's modulus and the tensile strength, and lowers the percent of elongation [101]. However, there is still lack of quantitative representation of the statements. In this section, the uniaxial tensile results quantitatively provide more information about the relationship between the crystallinity and the mechanical properties. Before every uniaxial tensile test, the crystallinity is tailored by systematically annealing the parylene-C samples at different temperatures and time. It is found that the first minute contributes to most of the change in mechanical. This implies that most sample crystallization has completed in this short period of annealing time. Higher crystallinity introduces larger Young's modulus, larger tensile strength, and less percent of elongation, which correspond to produce stiffer, stronger and more brittle (less tough) parylene-C. In addition, it is also found that the oxidation effect is not very obvious when parylene-C is annealed at 100°C. However, the early snapping of the parylene-C stretched at 150°C implies the oxidation plays an important role at this temperature.

As the annealing temperature influence the crystallinity of the parylene-C and thus the mechanical properties, Hsu suggested thermal anneal the device at a higher temperature than the device's designed operation temperature [201]. This would generate and maintain stable parylene-C crystallinity throughout the device operation period and thus the mechanical properties.

Thickness effect has never been discussed in the section. It has been pointed out by Spivack in 1972 that the uniaxial mechanical properties show very little variation with thickness [235]. Future work would focus on the time constants of the mechanical properties change. In addition, the degree of crystallinity may affect the electrical properties (dielectric loss) and the optical properties (birefringence) [201], which all needs more studies and attentions before the implantable devices are designed and fabricated.

5.8 Rheological Properties of Parylene-C Film

It is well know that parylene-C is a thermoplastic material. Like many other thermoplastic materials such as polypropylene and polycarbonate, it shows viscoelastic/viscoplastic behaviors, i.e., characteristics with combined elastic and viscous properties especially beyond glass transition temperature, T_g [236, 237]. In addition, with its biocompatibility, parylene-C has been widely used for many biomedical implantable devices [238]. It is then important to study its viscoelasticity/viscoplasticity especially at human body temperature.

Unfortunately, although many properties, such as Young's modulus and tensile strength of parylene-C have been studied [100, 101, 172, 195, 235], there is still a lack of study of viscoelasticity/viscoplasticity of parylene-C. On the other hand, viscoelastic and

vsicoplastic behaviors of a material depend upon many parameters such as temperatures, loading frequencies, and stress/strain rates. Among various viscoelastic tests, creep and stress relaxation are two of the most fundamental studies. Creep test, i.e., the tendency of a solid material to slowly move or deform under the influence of constant stress, is done as a tensile test that the applied stress is maintained constant while the strain is measured during the loading. On the other hand, stress relaxation, i.e., the tendency of a solid material to slowly release the built-in stress under the influence of a constant strain, is done as a tensile test that the applied strain is maintained constant while the stress is measured during the strain loading. Creep and stress relaxation tests characterize the time dependent behavior of a polymer [239].

In this section, a series of creep and stress relaxation tests are performed. Following previous sections, parylene-C samples annealed at different conditions are prepared for creep and stress-relaxation experiments.

As aforementioned, parylene-C annealed at different temperatures results in different crystallinity. Therefore, the creep and stress relaxation tests of parylene-C annealed at different temperature reveal the rheological response of the parylene-C at different crystallinity. However, to study the creep behavior of the as-deposited parylene-C, i.e., creep test without first 30 minutes thermal stabilization to avoid the crystallization as much as possible, the current DMA Q800 machine will not do the job due to its inherent limitations of the sample loading design and the temperature ramping rate. To overcome the problem, another creep experiment was also performed in the pre-heated convection oven with a transparent observing window.

5.8.1 Creep of parylene-C

5.8.1.1 Creep overview

A typical creep test curve measures the total strain (under a constant stress, Figure 5-39 (a)) versus time at a fixed temperature as shown in Figure 5-39 (b). As shown, the creep curve is traditionally divided into 3 different regions [240]. The primary creep, also called transient creep, represents the first instantaneous elastic strain and also the early stage of the creep behavior. In this stage, the main feature is that the strain rate of the polymer tends to decrease gradually from a very high initial rate. The secondary creep region, also called steady state region, shows a constant or little changing strain rate at a fixed temperature. The tertiary creep region shows an expedited or fast growing strain rate and ends at the material's rupture. In addition, the creep test is usually accompanied with a recovery test, i.e., strain recovery after the loading is removed, as shown in Figures 5-39 (c) and (d). For an ideal thermoset polymer, the total strain recovers to zero after a certain amount of time, whereas for a thermoplastic polymer, the strain never goes back to zero and a permanent deformation exists [239]. Creep is of great interest to us since parylene-C MEMS has to go through various fabrication processes with elevated temperatures and stresses, although mostly in the primary creep region. In addition, as the implantable parylene-C bioMEMS devices are being widely developed, creep behavior is more important to understand than ever. This section presents the study of the primary and secondary creep of parylene-C film. Burger's model is used to analyze the measured data points. Furthermore, the recovery behavior after the creep test is also performed and analyzed. For the viscoplastic behavior part will be discussed more in detail in Section 5.9.
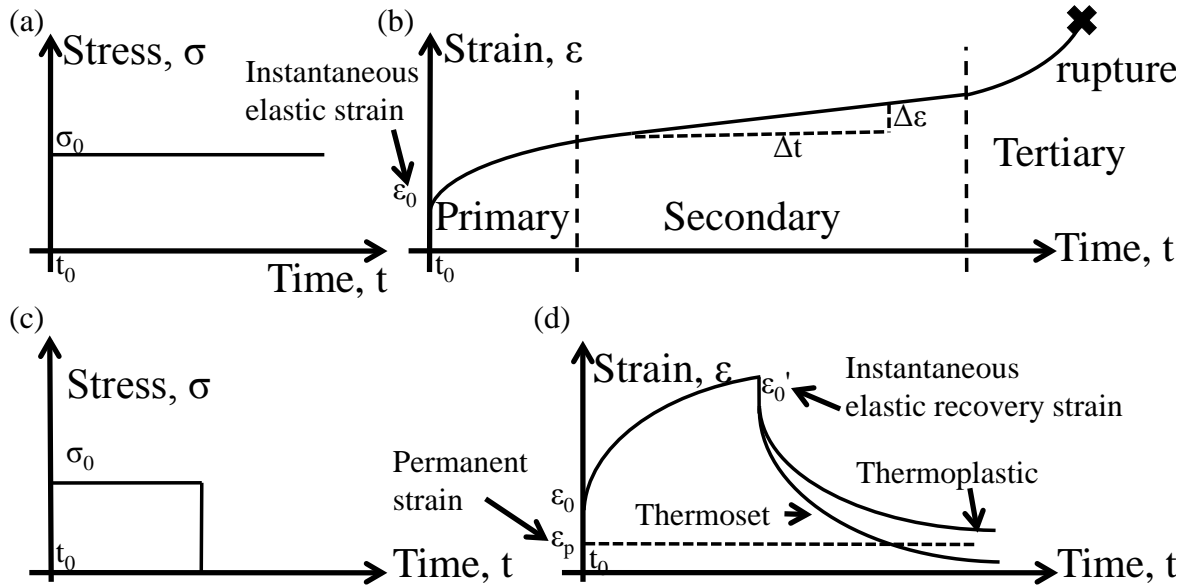
Figure 5-39: Creep behavior of polymers: (a) constant applied stress during creep test at a constant temperature; (b) total strain versus time; (c) removal of the stress at the beginning of the creep recovery test; (d) recovery strain curve

5.8.1.2 Introduction of the Burger's model

Many physical models have been developed and utilized to quantitatively analyze and represent the rheological behavior. The Maxwell model and the Kelvin model are two of the most fundamental ones. A single Maxwell model consists of one linear spring in series with a dashpot, while a single Kelvin model is composed of one spring in parallel with a dashpot, as shown as the inserts in Figure 5-40. Both Maxwell element and Kelvin element are often combined either in parallel or in series to model material's rheological behavior. Among all the possible combinations, one Maxwell element with multiple Kelvin elements in series is widely used for creep modeling due to its simple form of the differential equations and ease of solution [239]. In this section, it is found that 4-element Burger's model, i.e., a Kelvin element in series with a Maxwell element

(hence a single retardation time constant) is adequate to describe our data. Figure 5-40 shows the schematic diagram of the Burgers' model.
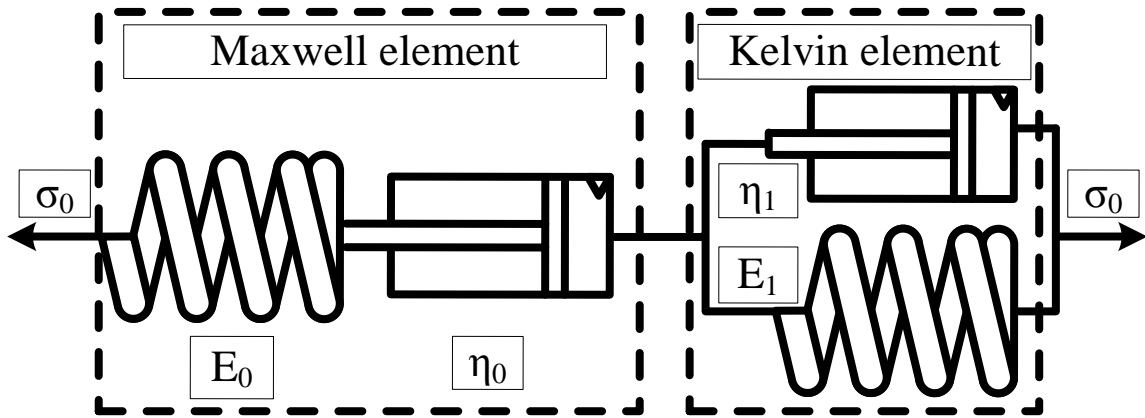
Figure 5-40: Schematic diagram of the Burger's model

5.8.1.2.1 General Burger's model constitutive equation

As the Burger's model shown in Figure 5-40, the spring of the Maxwell element represents the instantaneous strain and the dashpot simulates the steady strain rate of the creep behavior in the long time. The equilibrium equation of the Burger's model is:

$$\sigma_0 = \sigma_M = \sigma_K, \tag{5-8}$$

where σ_M and σ_K are the stress applied to Maxwell and Kelvin element, respectively. The kinematic equation is:

$$\varepsilon = \varepsilon_s + \varepsilon_d + \varepsilon_K, \tag{5-9}$$

where ε_s, ε_d, and ε_K are the strain of the spring, the dashpot and the Kelvin element, respectively. The fundamental constitutive equation of one spring can be represented as:

$$\sigma_s = E_0 \varepsilon_s, \tag{5-10}$$

In addition, the fundamental constitutive equation of one dashpot can be represented as:

$$\sigma_d = \eta_0 \frac{d}{dt} \varepsilon_d, \tag{5-11}$$

where η_0 is called the viscosity of the dashpot. Combining eqns. (5-8), (5-9), (5-10), and (5-11), the constitutive equations of the Burger's model can be represented as:

$$\sigma_0 + \left(\frac{\eta_0}{E_0} + \frac{\eta_0}{E_1} + \frac{\eta_1}{E_1} \right) \dot{\sigma}_0 + \frac{\eta_0 \eta_1}{E_0 E_1} \ddot{\sigma}_0 = \eta_0 \dot{\varepsilon} + \frac{\eta_0 \eta_1}{E_1} \ddot{\varepsilon}. \tag{5-12}$$

5.8.1.2.2 Solution for creep behavior

The Burger's model can be fit to different rheological situation. To fit the creep results, given the initial condition as $\sigma = \sigma_0 H(t)$, where $H(t)$ is the Heavyside function defined as:

$$H(t) = \begin{cases} 1, & \text{for } t \geq 0 \\ 0, & \text{for } t < 0 \end{cases} \tag{5-13}$$

the solution of the strain of the model can be derived as

$$\varepsilon(t) = \sigma_0 \left[\frac{1}{E_0} + \frac{1}{E_1} \left(1 - e^{-t/\tau_1} \right) + \frac{t}{\eta_0} \right]. \tag{5-14}$$

where $\tau_1 = \eta_1/E_1$ is called the retardation time constant. The creep compliance is obtained as

$$D(t) = \frac{1}{E_0} + \frac{1}{E_1} \left(1 - e^{-t/\tau_1} \right) + \frac{t}{\eta_0}. \tag{5-15}$$

5.8.1.2.3 Solution for creep recovery behavior

To model the strain behavior of creep recovery after the applied stress is unloaded, the initial strain $\varepsilon(t_0)$ is set to be $\varepsilon(t_0) = \varepsilon(t_0)H(t_0 - t)$ in eqn. (5-12), where t_0 is the starting point of the removal of the stress. The stress then can be derived as

$$\varepsilon(t) = P_1 + P_2 \exp\left(-\frac{(t - t_0)}{\tau_r} \right). \tag{5-16}$$

where the time constant $\tau_r = \frac{E_1}{\eta_1}$, P_1 and P_2 are material dependents.

5.8.1.3 Primary and secondary creep of parylene-C

5.8.1.3.1 Sample preparation and the experiments

Parylene-C film was deposited using an SCS (Specialty Coating Systems) parylene deposition machine (i.e., PDS 2010 LABCOTER). The film was coated onto the surface a flat mask glass plate. The parylene-C film was then cut into uniform 5.3 mm wide strips. The length of each testing sample was 15 ± 0.05 mm for the creep test. The tests were done by a dynamic mechanical analyzer, TA instruments DMA Q800. Similar to the previous Section 5.7, eight different parylene-C samples were treated differently by annealing in different conditions to study the oxidation effect, temperature effect, deposition pressure effect, and also annealing time effect. As it has been found in Section 5.6 that the glass transition temperature of the as-deposited parylene-C is about 50°C, 25°C was chosen for tests of creep behavior below T_g; 40°C, and 60°C were chosen to be around T_g, and 80°C, 100°C, 120°C, and 150°C were chosen to be above T_g.

Before the creep test started, the testing chamber was first heated up with the parylene-C sample mounted and then waited for 30 minutes to ensure that the whole system reaches thermal equilibrium with our targeted temperature, as graphically shown in Figure 5-41 (a). Then, a constant stress of 2.43MPa was applied onto the sample for 120 minutes, while the total strain is measured. To observe the recovery behavior of the sample, the stress was then removed and the total strain was continuously recorded for another 60 minutes.

5.8.1.3.2 Results and discussion

As a whole, the results of the creep test and the recovery of eight different pre-treated parylene-C are shown in Figure 5-41 (a) to Figure 5-48 (a). Each figure includes seven curves representing different testing temperatures. Besides, the Burger's model curve fitting results of the creep and recovery are also shown in Table 5-14 to Table 5-21. From these eight figures and tables, several observations and conclusions can be made:

1. It is noted from all figures that there is always little or no primary creep at the temperature lower than the glass transition temperature. For example, from the creep results of as-deposited parylene-C deposited at 35 mTorr shown in Figure 5-42 (a) (one extra curve was performed at 10°C), it can be found that 10° and 25°C, which are significantly below the glass transition temperature (55.1°C in Table 5-11) show no or very little creep. Figure 5-42 (a) further validated that the total strain obtained at 10° C is similar to that at 25° C because the Young's moduli at 10°C and 25 ° C are very close to each other. In addition, there is very little or no permanent strain found after the recovery, meaning that the paryelne-C is in the elastic regime. The second example would focus on the creep results of the parylene-C annealed at 100°C for one day in vacuum as shown Figure 5-45 (a). Tg of this parylene-C sample is found as 113.1°C from Table 5-11. It is observed from Figure 5-45 (a) that there is also no or very little creep found at 25, 40, 60 and 80°C, which are all far below the Tg. Most of the strain remaining measured after the creep tests at these temperatures are also hard to identify. The third example would be aimed at the creep results of parylene-C annealed at 200°C for one day in vacuum as shown in Figure 5-47 (a). As also obtained from

Table 5-11, Tg of this parylene-C cannot be figured out by the experiments as described in Section 5.6. In one of our conclusions in 5.6.3, the measured Tg is found to be always a bit higher than the annealing temperature according to the observed experimental trend of Tg. Therefore the Tg would be expected as higher than 200°C in this parylene-C sample. Therefore, the creep results shown in Figure 5-47 (a) would not be surprising as all seven creep testing temperatures are far lower than 200°C. Consequently this parylene-C behaves like elastic material even at 150°C and thus very little creep is found in the experiment. In addition, also very little permanent strain is found after the recovery.

2. When the creep test started at t=t0=30 minutes, the applied stress suddenly loaded onto the sample and it is shown in eight figures that an instantaneous elastic deformation happens. According to the results, the higher temperature produced the larger instantaneous elastic strain under constant stress. This is explained by the smaller Young's modulus at higher temperature, which agrees well with what we found from our ramping-temperature-dependent modulus experiment and DMA tests shown in Section 5.6. These instantaneous strains at different temperatures were used to calculate the corresponding Young's moduli and the results are shown in the first column of the creep results in Table 5-14 to Table 5-21. It is found that Young's modulus determined at the starting point of the creep test in this section usually differs a bit than what we got from the ramping-temperature-dependent modulus experiment or DMA method. It is likely because of three possible reasons. The first reason would be the thickness variation which inherently comes from the parylene-C deposition. The second reason could be the

thermal history difference. In the DMA method in Section 5.6, the sample is always tested under the oscillatory force at the testing temperature. In this section, however, the Young's modulus is obtained after 30 minutes of annealing. As discussed in Section 5.5, parylene-C might have gone through a long period of crystallization and hence the mechanical properties could be different. The third reason might be the testing strain rate difference. Compared to 1Hz as the oscillation frequency in Section 5.6.1.3, the strain rate at the starting point of the creep test is high enough to cause the strain-rate effect in parylene-C [223]: higher strain rate would introduce higher Young's modulus. Combining these three effects, the measured Young's modulus could sometimes either higher or lower than in Section 5.6. Even though, the values are always very close to each other, and also, the descending trend with respect to the temperature still exists.

3. The Young's modulus at $t=t0+120=150$ min is found using the elastic recovery strain at the time when the applied stress is removed. The results are shown in the first column of the recovery in Table 5-14 to Table 5-21. It can be first seen that with temperatures around or higher than the glass transition temperature, the Young's modulus gets higher after it has being stretched at the constant temperature for 120 minutes. It is also obvious that at temperatures much higher than Tg, the increment can be even more serious. According to what has been demonstrated in the previous few sections, this effect is likely mainly attributed to the crystallization of the parylene-C. In addition, the similar effect can also be found at the temperature lower than Tg, although that as significant as at the temperature higher than Tg. It could be concluded that the pure stretching of the

parylene-C would also increase the Young's modulus either by inducing the crystallization or aligning the polymer chain under the tension force.

4. The primary creep is significant and increases with temperature. The further analysis of the creep needs the help of Burger's model. All creep and the recovery results were curve fitted to the Burger's model, and the results are shown in Table 5-14 to Table 5-21. According to the obtained correlation coefficient, $R2$, the Burger's model explains well with our data whenever the testing temperature is higher than Tg. However, although Burger's model can also be forced to fit with the data lower than Tg, the physical model loses its physical sense because parylene-C showed little or no creep below Tg. This can be verified by the lower correlation coefficients ($R2 < 0.99$) of every creep experiment performed at the temperature lower than Tg. These data are shaded with grey background in the tables. As a result, except at the temperature lower than Tg, it is shown that the retardation time constant, $\tau 1$, decreases with the temperature. Because $\tau 1$ are found to be approximately 6–10 minutes at temperatures higher than Tg no matter what type annealing history of the samples, it is evident that 120 minutes is long enough to make the creep go into secondary region, and the creep strain rates have already reached a steady state, which is shown in Figure 5-41 (a) to Figure 5-48 (a). The steady state slopes, $\frac{\sigma_0}{\eta_0}$, of the creep curves at the temperature higher than Tg increase slightly when creep temperature goes up. Both trends of $\tau 1$ and $\frac{\sigma_0}{\eta_0}$ show that parylene-C creeps more at higher temperature when the temperature is higher than Tg. The phenomenon demonstrates the viscoelastic/viscoplastic behavior of the parylene-C. On the other hand, the creep

performed at the temperature lower than Tg, shows little creep and proves that parylene-C is in the glassy region and thus behaves elastically. Young's modulus of the spring of the Kelvin's element, i.e. E1, can be calculated from $\frac{\sigma_0}{E_1}$ given σ0=2.43MPa. E1 are also generally found to decrease as the testing temperature going up, which is similar to E0.

5. By comparing the creep results of Figure 5-44 (a) (parylene-C pre-annealed at 100°C one day in the air) and Figure 5-45 (a) (parylene-C pre-annealed at 100°C one day in the vacuum), the results show that creep strain of the samples pre-annealed in vacuum has no distinguishable difference to in the air. It infers again that, even after one day of annealing at 100°C in the air, the oxidation has very little effect on parylene-C, which agrees well with the conclusion obtained in Section 5.4. Although the oxidation effect is very little for parylene-C annealed at 100°C in the air, it would be still worthwhile repeating the same creep tests with more parylene-C samples annealed at 100°C but for longer annealing time, such as more than 13 days as predicted in Section 5.4.3.

6. The crystallization effect can be investigated by the creep results as well. By comparing the Figure 5-43 (a) (parylene-C pre-annealed at 100°C 30 min. in the air), Figure 5-45 (a) (parylene-C pre-annealed at 100°C one day in the vacuum), and Figure 5-46 (a) (parylene-C pre-annealed at 100°C two days in the vacuum), it is found that the creep curve of 150°C has a lower total strain after 2 days of annealing. In addition, the parylene-C pre-annealed at 100°C for 30 minutes has very little creep difference to two day annealing in terms of the creep temperatures lower than the Tg. This implies that the crystallization is mostly

done in the first 30 minutes annealing, which has been verified many times in the previous Sections 5.5.2, 5.6.1.3, and 5.7.4. In contrast to the results of 100°C, however, from Figure 5-47 (a) (parylene-C pre-annealed at 200°C one day in the vacuum) and Figure 5-48 (a) (parylene-C pre-annealed at 200°C two days in the vacuum), it can be found that Figure 5-48 (a) generally has a smaller total creep strain than Figure 5-47 (a). It can be explained as the stronger crystallization at 200°C than 100°C. The elastic behavior of the creep results of the parylene-C pre-annealed at 200°C implies that crystallility is much higher than annealed at 100°C.

7. Burger's model also works for the recovery region and the curve fitting results are shown in Table 5-14 to Table 5-21. The retardation time constants are generally larger than those measured from the creep, meaning the recovering behavior progresses slower than the creep. As the time constants of the recovery found from Table 5-14 to Table 5-21 are generally about 10–15 minutes, it can be concluded that 60 minutes recovery time is long enough to decide whether the stain is recovered after the creep or not. As shown in Figure 5-41 (a) to Figure 5-46 (a), a clear permanent strain is generally observed at the testing temperature higher than each corresponding Tg. The permanent remaining strain under the stress of 2.43 MPa implies that parylene-C has gone into plastic region at the testing temperature. It can be seen that the permanent strain is higher when the testing temperature is higher. This would imply that the yield strength is lower as the testing temperature increases, and hence parylene-C deforms more at higher temperature under the same loading.

8. The permanent strain phenomenon after the creep test has been observed by many previous researchers. Many models have been proposed to analyze and predict this irreversible strain. One of the most commonly used models is combine the creep behavior before the recovery, and model the recovery behavior as well as predicting the irreversible strain by powers law. The system constitutive model can be represented as [241–251]:

$$\varepsilon_c = \varepsilon_0 + k\sigma_0 \sum_m C_m \left(1 - exp\left(-\frac{t}{a_\sigma \tau_m}\right)\right) + \varepsilon_{\text{pl}}(t, \sigma_0), \qquad (5\text{-}17)$$

9. where ε_c is the total strain of the material, ε_0 is the elastic strain, k is the stress invariant dependent material property, σ_0 is the applied stress, C_m are constants, a_σ is the stress dependent time-scale factor, which is a function of stress, temperature and also humidity, and ε_{pl} is the viscoplastic strain. The term $k\sigma_0 \sum_m C_m \left(1 - exp\left(1 - \frac{t}{a_\sigma \tau_m}\right)\right)$ in eqn. (5-17) actually represents the generalized Kelvin model, which consists of m series of multiple springs and dashpots in parallel. The viscoplastic strain ε_{pl} accumulated in the time period t1 can also be further modeled by powers law as [242]:

$$\varepsilon_{\text{pl}}(t_1, \sigma_0) = C_{pl}\sigma^{M*m}t_1^m, \qquad (5\text{-}18)$$

where C_{pl}, M, and m must be determined experimentally. It is clearly that the term $C_{pl}\sigma^{M*m}$ would depend on the stress level, and also the testing temperatures.

240
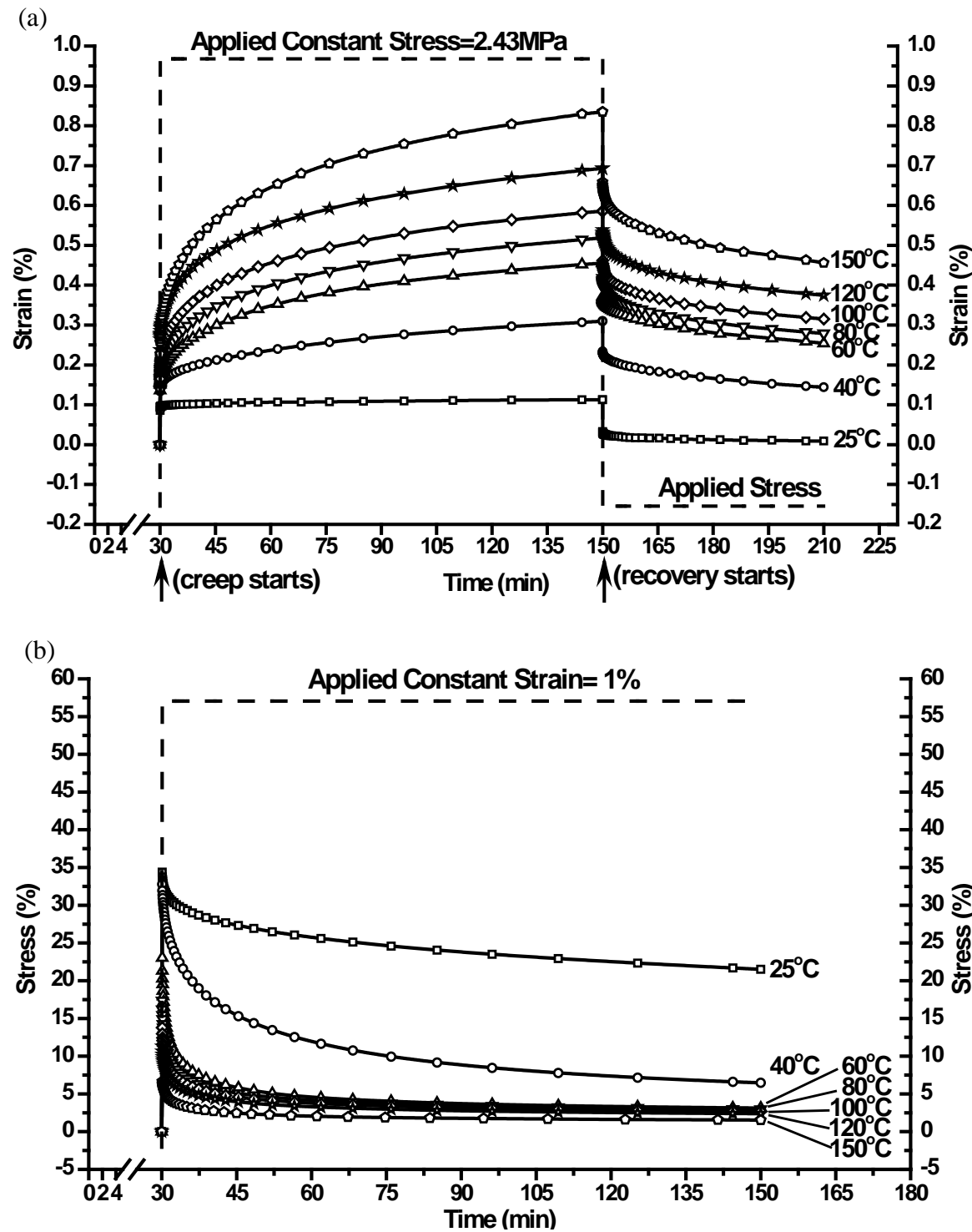
Figure 5-41 (a): Creep results of the as-deposited parylene-C deposited at 22 mTorr (T_g=53.4°C); (b): Stress relaxation results of the as-deposited parylene-C deposited at 22 mTorr (T_g=53.4°C)

Table 5-14: Burger's model curve fitting results of the creep and stress relaxation behaviors of as-deposited parylene-C deposited at 22 mTorr (T_g=53.4°C)

Fitting Results of Parylene-C Creep Behavior						
Temperature (°C)	$E_0(t_0)$ (GPa)	$\sigma_0/E_0 + \sigma_0/E_1$	σ_0/η_0	$-\sigma_0/E_1$	τ_1	R^2
150	0.947	0.586	0.00220	-0.296	7.342	0.992
120	0.918	0.504	0.00167	-0.214	7.334	0.992
100	1.296	0.414	0.00152	-0.203	7.269	0.992
80	1.564	0.362	0.00139	-0.184	7.386	0.992
60	1.615	0.323	0.00116	-0.157	9.472	0.994
40	1.678	0.219	0.00078	-0.068	10.248	0.995
25	2.613	0.103	0.00009	-0.007	4.924	0.976
Fitting Results of Parylene-C Creep Recovery Behavior						
Temperature (°C)	$E_0(t_0+120)$ (GPa)	P_1		P_2	τ_r	R^2
150	1.325	0.473		0.158	12.708	0.966
120	1.511	0.388		0.127	12.081	0.967
100	1.861	0.327		0.112	12.041	0.966
80	2.294	0.290		0.108	12.657	0.966
60	2.796	0.261		0.097	16.108	0.975
40	3.095	0.147		0.077	18.266	0.979
25	2.967	0.011		0.016	8.462	0.947
Fitting Results of Parylene-C Stress Relaxation Behavior						
Temperature (°C)	$E_0(t_0)$ (GPa)	A_1	τ_{sr1}	A_2	τ_{sr2}	R^2
150	0.665	3.450	2.019	2.825	145.960	0.980
120	1.130	5.777	1.800	4.680	130.381	0.978
100	1.379	7.254	1.707	5.549	119.458	0.978
80	1.736	9.759	1.394	6.435	106.734	0.977
60	2.304	13.565	1.294	7.898	82.967	0.977
40	3.279	14.052	4.059	17.038	102.074	0.991
25	3.438	5.106	3.350	28.136	404.606	0.985

(a)

(b)
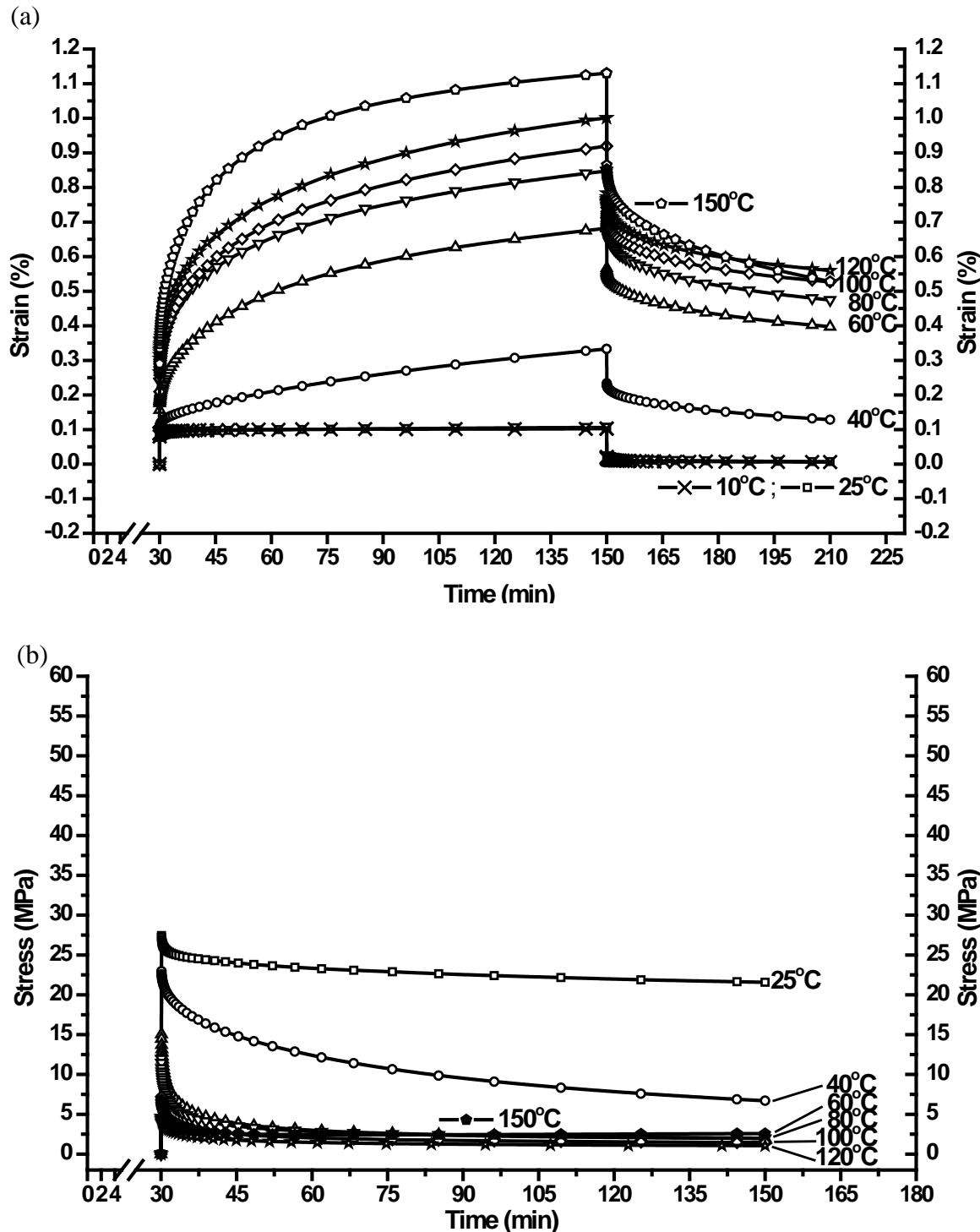
Figure 5-42 (a): Creep results of the as-deposited parylene-C deposited at 35 mTorr (T_g=55.1°C); (b): Stress relaxation results of the as-deposited parylene-C deposited at 35 mTorr (T_g=55.1°C)

Table 5-15: Burger's model curve fitting results of the creep and stress relaxation behaviors of as-deposited parylene-C deposited at 35 mTorr (T_g=55.1°C)

Fitting Results of Parylene-C Creep Behavior						
Temperature (°C)	$E_0(t_0)$ (GPa)	$\sigma_0/E_0 + \sigma_0/E_1$	σ_0/η_0	$-\sigma_0/E_1$	τ_1	R^2
150	0.725	0.878	0.00228	-0.492	7.393	0.992
120	0.795	0.696	0.00270	-0.349	7.964	0.993
100	0.984	0.626	0.00259	-0.338	7.518	0.992
80	0.896	0.591	0.00227	-0.284	7.445	0.992
60	1.380	0.459	0.00193	-0.259	10.816	0.995
40	2.224	0.176	0.00134	-0.059	10.902	0.997
25	2.864	0.096	0.00009	-0.009	4.459	0.983
Fitting Results of Parylene-C Creep Recovery Behavior						
Temperature (°C)	$E_0(t_0+120)$ (GPa)	P_1		P_2	τ_r	R^2
150	0.876	0.548		0.274	15.733	0.971
120	1.064	0.578		0.169	11.119	0.963
100	1.289	0.545		0.160	10.939	0.960
80	1.551	0.494		0.170	11.193	0.960
60	2.011	0.409		0.136	13.842	0.971
40	2.380	0.134		0.088	16.090	0.975
25	2.896	0.009		0.011	4.936	0.935
Fitting Results of Parylene-C Stress Relaxation Behavior						
Temperature (°C)	$E_0(t_0)$ (GPa)	A_1	τ_{sr1}	A_2	τ_{sr2}	R^2
150	0.677	3.579	1.749	2.772	763.768	0.973
120	0.475	2.431	2.033	2.033	137.666	0.980
100	0.721	3.667	1.836	2.979	120.930	0.977
80	1.198	6.603	1.327	4.540	96.500	0.975
60	1.505	8.869	1.391	5.262	78.642	0.979
40	2.297	5.910	4.724	16.209	122.341	0.994
25	2.744	2.479	1.546	24.506	826.375	0.977

(a)
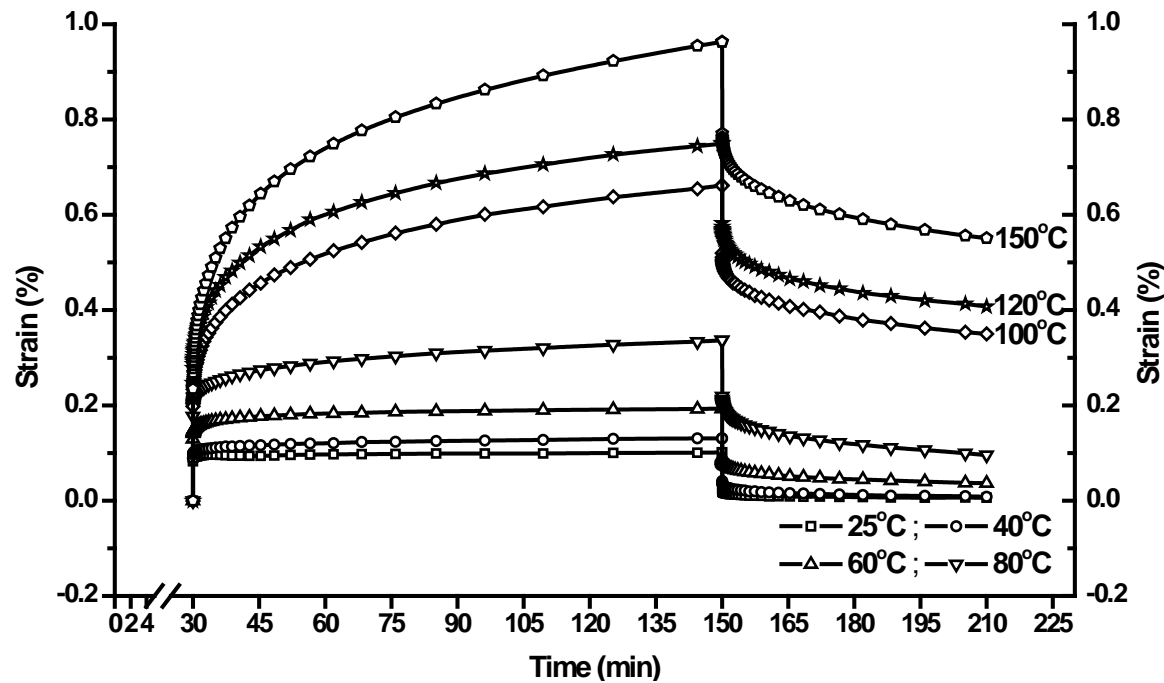
(b)
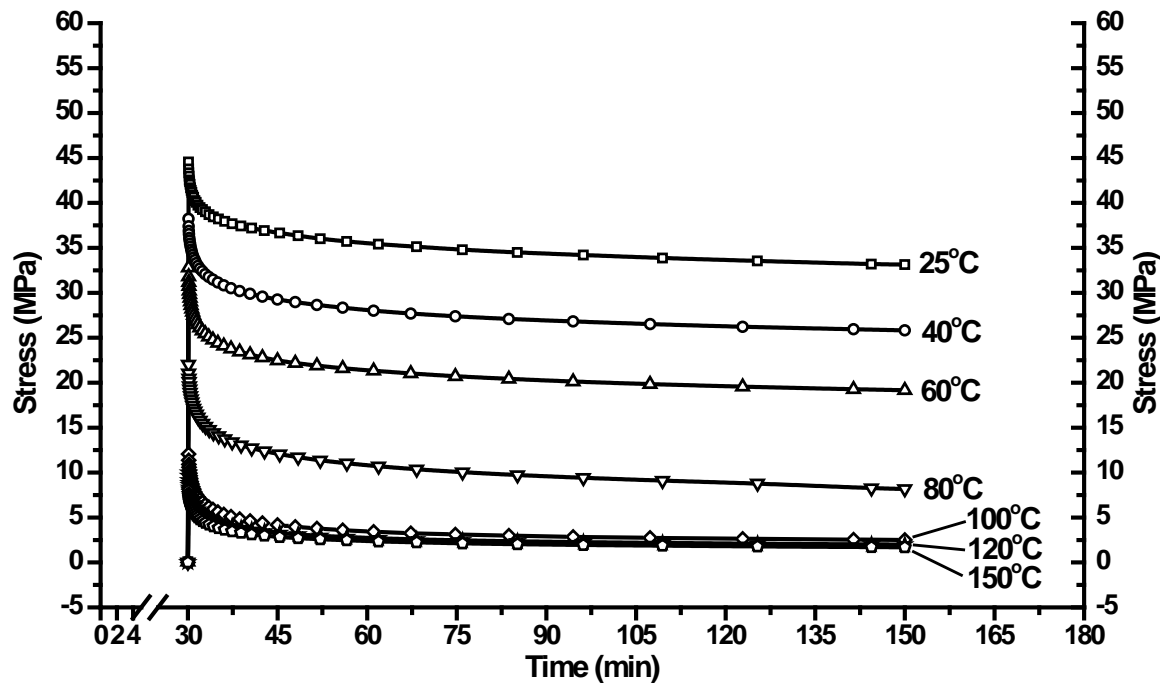
Figure 5-43 (a): Creep results of the parylene-C annealed at 100°C for 30 minutes in the convection oven (T_g=108.2°C); (b): Stress relaxation results of the parylene-C annealed at 100°C for 30 minutes in the convection oven (T_g=108.2°C)

Table 5-16: Burger's model curve fitting results of the creep and stress relaxation behaviors of parylene-C annealed at 100°C for 30 minutes in the convection oven (T_g=108.2°C)

Fitting Results of Parylene-C Creep Behavior						
Temperature (°C)	$E_0(t_0)$ (GPa)	$\sigma_0/E_0 + \sigma_0/E_1$	σ_0/η_0	$-\sigma_0/E_1$	τ_1	R^2
150	0.905	0.662	0.00266	-0.355	6.721	0.993
120	0.873	0.552	0.00175	-0.245	7.401	0.992
100	1.076	0.471	0.00168	-0.218	7.136	0.992
80	1.249	0.270	0.00059	-0.064	4.330	0.986
60	1.721	0.176	0.00016	-0.030	3.604	0.982
40	2.499	0.116	0.00014	-0.015	4.007	0.983
25	2.701	0.095	0.00005	-0.004	0.587	0.906
Fitting Results of Parylene-C Creep Recovery Behavior						
Temperature (°C)	$E_0(t_0+120)$ (GPa)	P_1		P_2	τ_r	R^2
150	1.212	0.568		0.172	12.445	0.966
120	1.381	0.422		0.133	11.599	0.966
100	1.618	0.363		0.129	12.164	0.964
80	1.953	0.107		0.090	10.837	0.956
60	2.323	0.043		0.038	7.222	0.945
40	2.642	0.012		0.021	5.470	0.933
25	3.070	0.008		0.012	3.180	0.929
Fitting Results of Parylene-C Stress Relaxation Behavior						
Temperature (°C)	$E_0(t_0)$ (GPa)	A_1	τ_{sr1}	A_2	τ_{sr2}	R^2
150	0.827	4.217	1.888	3.540	127.971	0.980
120	0.998	5.204	1.768	4.136	125.010	0.979
100	1.206	6.180	1.712	5.011	126.250	0.977
80	2.202	7.515	1.905	13.185	212.748	0.978
60	3.281	7.989	1.775	23.459	494.229	0.974
40	3.824	6.942	2.259	29.976	683.368	0.975
25	4.456	6.067	1.905	37.400	843.503	0.975

(a)

(b)
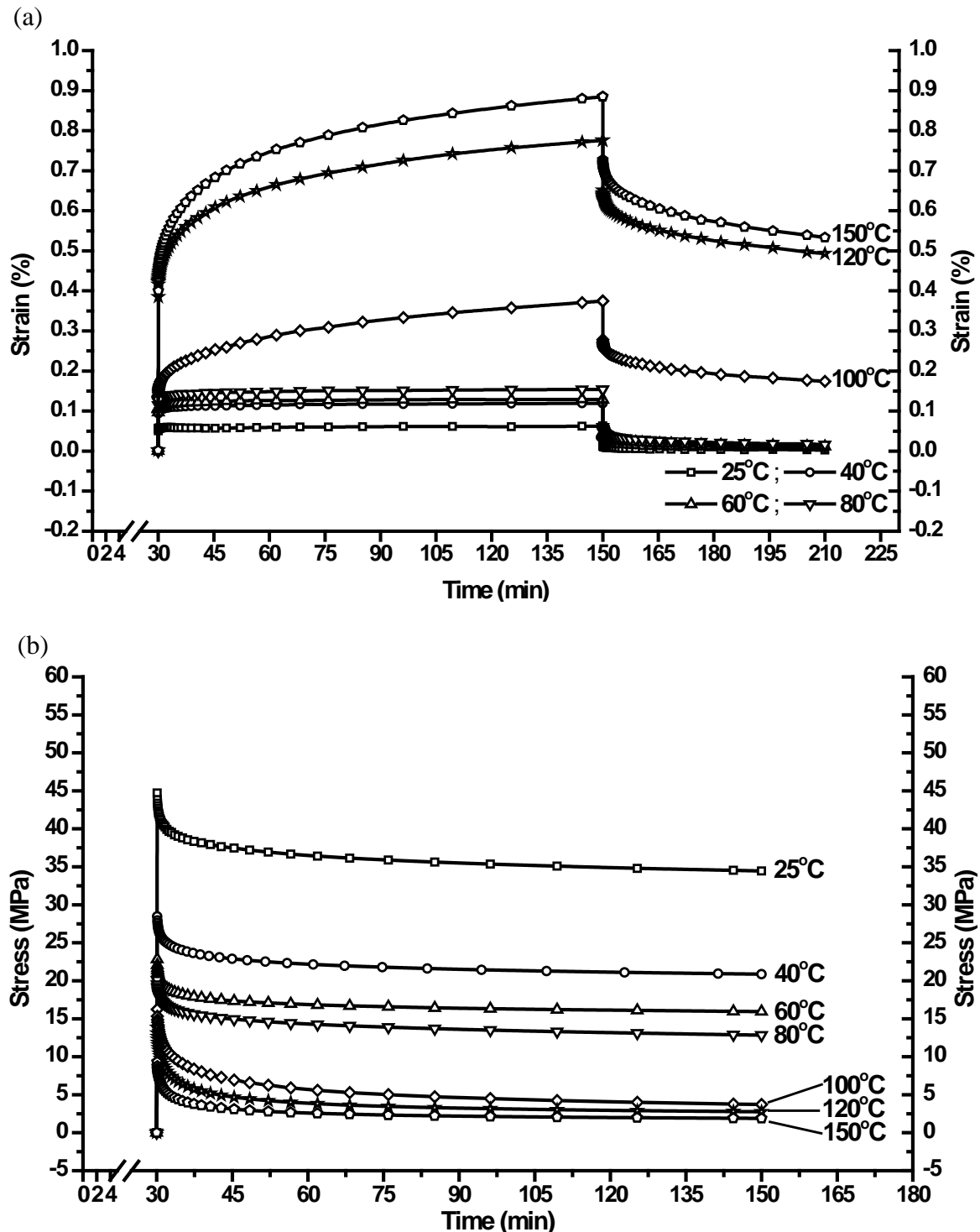
Figure 5-44 (a): Creep results of the parylene-C annealed at 100°C for 1 day in the convection oven (T_g=111.8°C); (b): Stress relaxation results of the parylene-C annealed at 100°C for 1 day in the convection oven (T_g=111.8°C)

Table 5-17: Burger's model curve fitting results of the creep and stress relaxation behaviors of the parylene-C annealed at 100°C for 1 day in the convection oven (T_g=111.8°C)

Fitting Results of Parylene-C Creep Behavior						
Temperature (°C)	$E_0(t_0)$ (GPa)	$\sigma_0/E_0 + \sigma_0/E_1$	σ_0/η_0	$-\sigma_0/E_1$	τ_1	R^2
150	0.560	0.700	0.00164	-0.241	7.003	0.993
120	0.584	0.622	0.00137	-0.185	7.259	0.993
100	1.663	0.257	0.00103	-0.096	7.442	0.992
80	1.957	0.144	0.00009	-0.016	2.394	0.968
60	2.322	0.124	0.00005	-0.016	3.108	0.975
40	2.406	0.112	0.00006	-0.010	3.040	0.984
25	4.493	0.058	0.00004	-0.003	0.201	0.846
Fitting Results of Parylene-C Creep Recovery Behavior						
Temperature (°C)	$E_0(t_0+120)$ (GPa)	P_1		P_2	τ_r	R^2
150	1.487	0.548		0.154	13.031	0.969
120	1.853	0.505		0.124	13.244	0.969
100	2.395	0.183		0.078	11.773	0.961
80	2.478	0.022		0.028	4.806	0.930
60	2.885	0.016		0.023	5.188	0.940
40	2.779	0.011		0.016	5.107	0.936
25	4.980	0.004		0.008	4.058	0.939
Fitting Results of Parylene-C Stress Relaxation Behavior						
Temperature (°C)	$E_0(t_0)$ (GPa)	A_1	τ_{sr1}	A_2	τ_{sr2}	R^2
150	0.932	4.925	1.647	3.740	126.344	0.978
120	1.386	7.334	1.813	5.617	123.350	0.980
100	1.624	6.969	2.435	7.985	123.436	0.981
80	2.010	3.870	1.701	15.492	543.957	0.973
60	2.283	4.186	1.372	17.838	868.723	0.964
40	2.847	4.386	2.175	23.300	907.844	0.973
25	4.472	5.457	1.786	38.130	1005.754	0.971

(a)

(b)
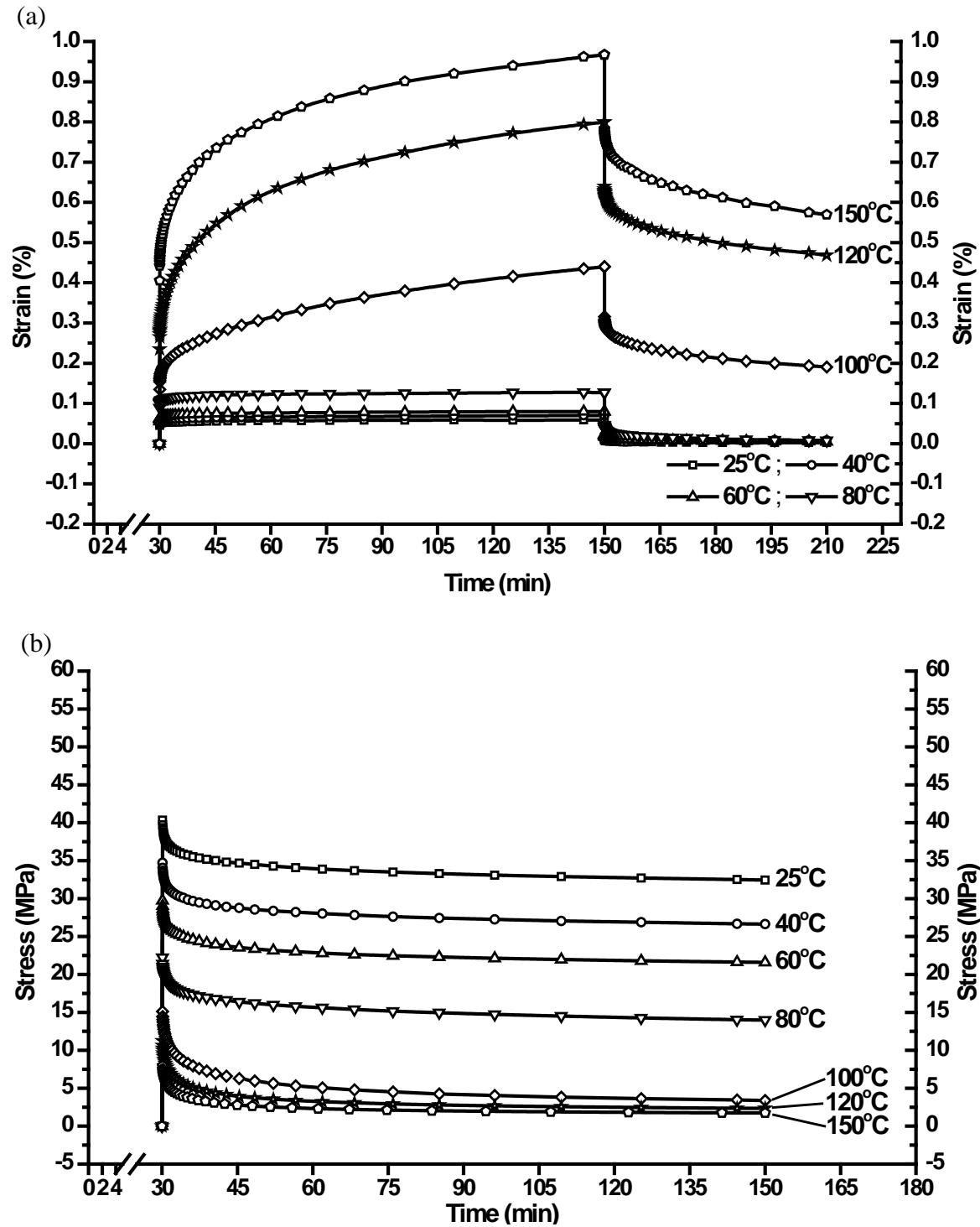
Figure 5-45 (a): Creep results of the parylene-C annealed at 100°C for 1 day in the vacuum oven (T_g=113.1°C); (b): Stress relaxation results of the parylene-C annealed at 100°C for 1 day in the vacuum oven (T_g=113.1°C)

Table 5-18: Burger's model curve fitting results of the creep and stress relaxation behaviors of the parylene-C annealed at 100°C for 1 day in the vacuum oven (T_g=113.1°C)

Fitting Results of Parylene-C Creep Behavior						
Temperature (°C)	$E_0(t_0)$ (GPa)	$\sigma_0/E_0 + \sigma_0/E_1$	σ_0/η_0	$-\sigma_0/E_1$	τ_1	R^2
150	0.549	0.754	0.00190	-0.280	6.804	0.992
120	0.917	0.575	0.00198	-0.279	7.907	0.993
100	1.581	0.275	0.00143	-0.105	7.876	0.993
80	2.460	0.119	0.00008	-0.017	1.983	0.974
60	3.976	0.075	0.00005	-0.011	3.026	0.979
40	4.452	0.064	0.00005	-0.008	3.305	0.983
25	4.868	0.056	0.00003	-0.004	6.095	0.946
Fitting Results of Parylene-C Creep Recovery Behavior						
Temperature (°C)	$E_0(t_0+120)$ (GPa)	P_1		P_2	τ_r	R^2
150	1.285	0.587		0.168	12.718	0.964
120	1.456	0.483		0.132	11.979	0.966
100	1.856	0.202		0.093	10.985	0.960
80	2.882	0.012		0.025	4.977	0.929
60	4.176	0.007		0.012	4.447	0.931
40	4.827	0.010		0.008	3.617	0.899
25	4.915	0.003		0.006	3.066	0.925
Fitting Results of Parylene-C Stress Relaxation Behavior						
Temperature (°C)	$E_0(t_0)$ (GPa)	A_1	τ_{sr1}	A_2	τ_{sr2}	R^2
150	0.798	4.165	1.875	3.267	137.637	0.978
120	1.125	5.793	1.861	4.680	127.073	0.979
100	1.512	6.852	2.306	7.270	121.686	0.982
80	2.224	4.186	1.721	17.016	518.172	0.970
60	2.975	4.638	1.962	24.066	917.710	0.966
40	3.472	4.545	1.891	29.260	1077.451	0.972
25	4.035	4.340	1.678	35.202	1242.959	0.970

(a)
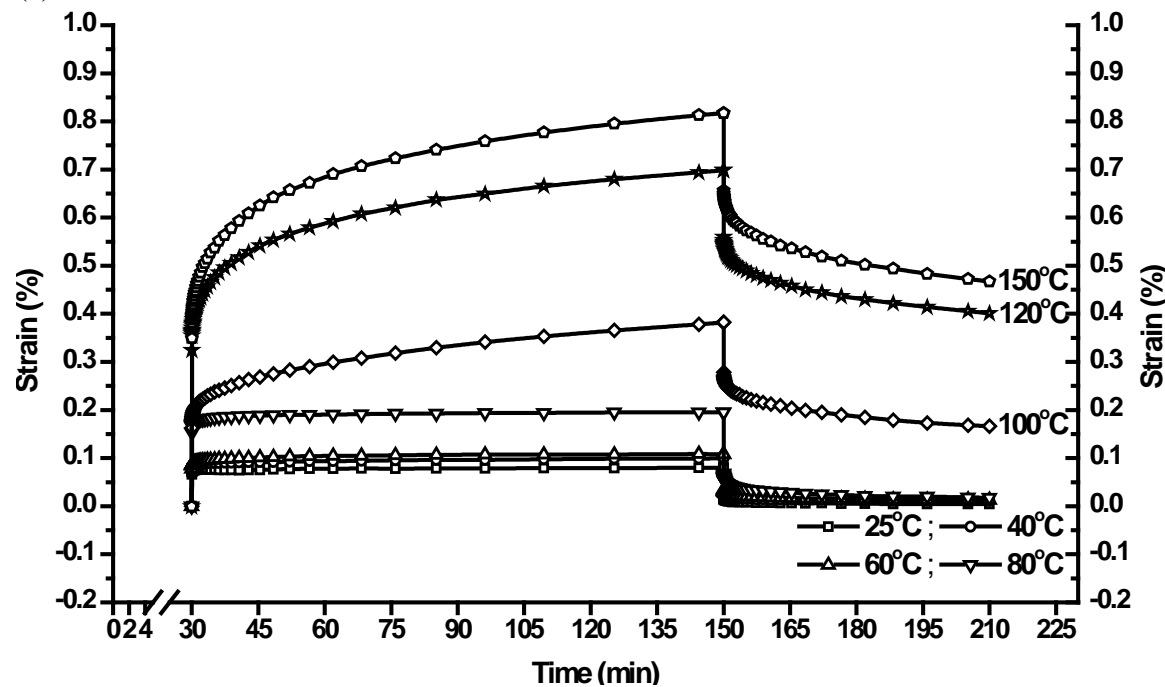
(b)
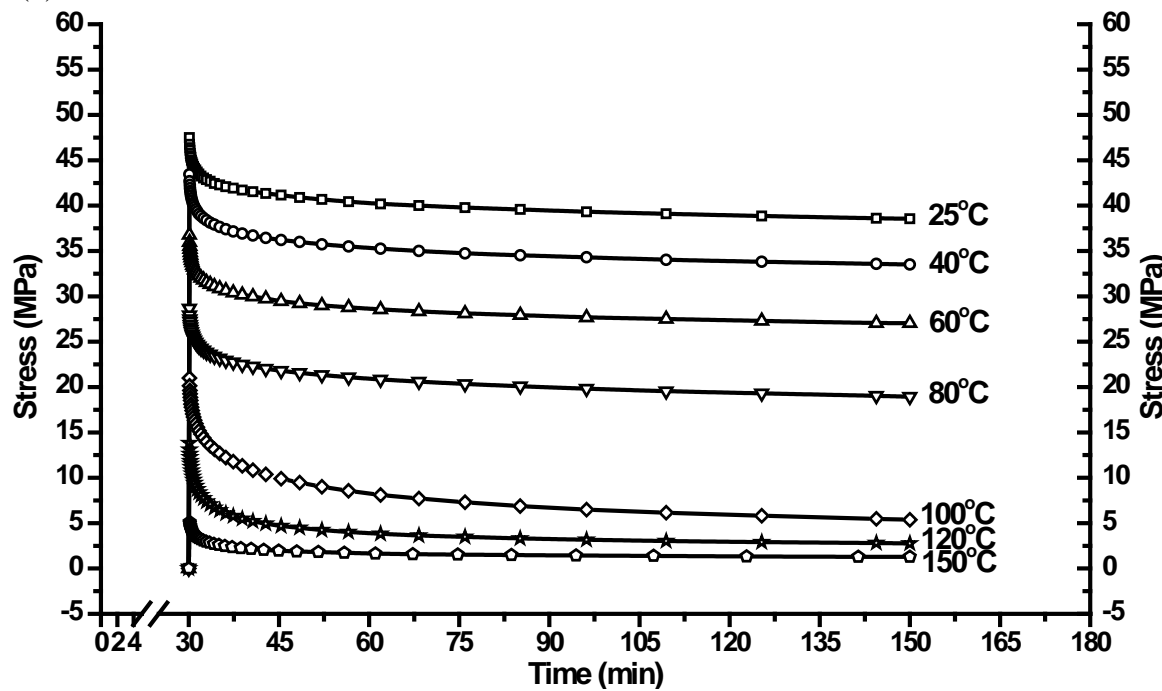
Figure 5-46 (a): Creep results of the parylene-C annealed at 100°C for 2 days in the vacuum oven (T_g=115.2°C); (b): Stress relaxation results of the parylene-C annealed at 100°C for 2 days in the vacuum oven (T_g=115.2°C)

Table 5-19: Burger's model curve fitting results of the creep and stress relaxation behaviors of the parylene-C annealed at 100°C for 2 days in the vacuum oven (T_g=115.2°C)

Fitting Results of Parylene-C Creep Behavior						
Temperature (°C)	$E_0(t_0)$ (GPa)	$\sigma_0/E_0 + \sigma_0/E_1$	σ_0/η_0	$-\sigma_0/E_1$	τ_1	R^2
150	0.638	0.637	0.00160	-0.229	6.647	0.992
120	0.686	0.549	0.00133	-0.175	6.535	0.992
100	1.352	0.267	0.00101	-0.074	6.695	0.992
80	1.465	0.187	0.00008	-0.017	2.058	0.967
60	2.876	0.102	0.00006	-0.014	3.760	0.976
40	2.978	0.091	0.00008	-0.008	2.624	0.984
25	3.407	0.076	0.00003	-0.005	0.241	0.900
Fitting Results of Parylene-C Creep Recovery Behavior						
Temperature (°C)	$E_0(t_0+120)$ (GPa)	P_1		P_2	τ_r	R^2
150	1.455	0.482		0.149	12.553	0.967
120	1.662	0.413		0.123	12.596	0.967
100	2.216	0.175		0.084	11.763	0.961
80	1.846	0.023		0.032	4.598	0.930
60	3.249	0.016		0.014	3.669	0.929
40	3.309	0.012		0.011	2.919	0.938
25	3.821	0.006		0.008	2.744	0.921
Fitting Results of Parylene-C Stress Relaxation Behavior						
Temperature (°C)	$E_0(t_0)$ (GPa)	A_1	τ_{sr1}	A_2	τ_{sr2}	R^2
150	0.511	2.654	2.111	2.208	164.820	0.979
120	1.382	7.294	1.789	5.635	123.023	0.980
100	2.099	8.433	2.669	11.187	133.011	0.983
80	2.866	5.154	1.847	22.502	593.552	0.973
60	3.677	5.595	1.857	30.103	924.254	0.970
40	4.345	5.563	2.082	36.799	1085.072	0.973
25	4.751	4.874	1.668	41.734	1281.668	0.972

(a)
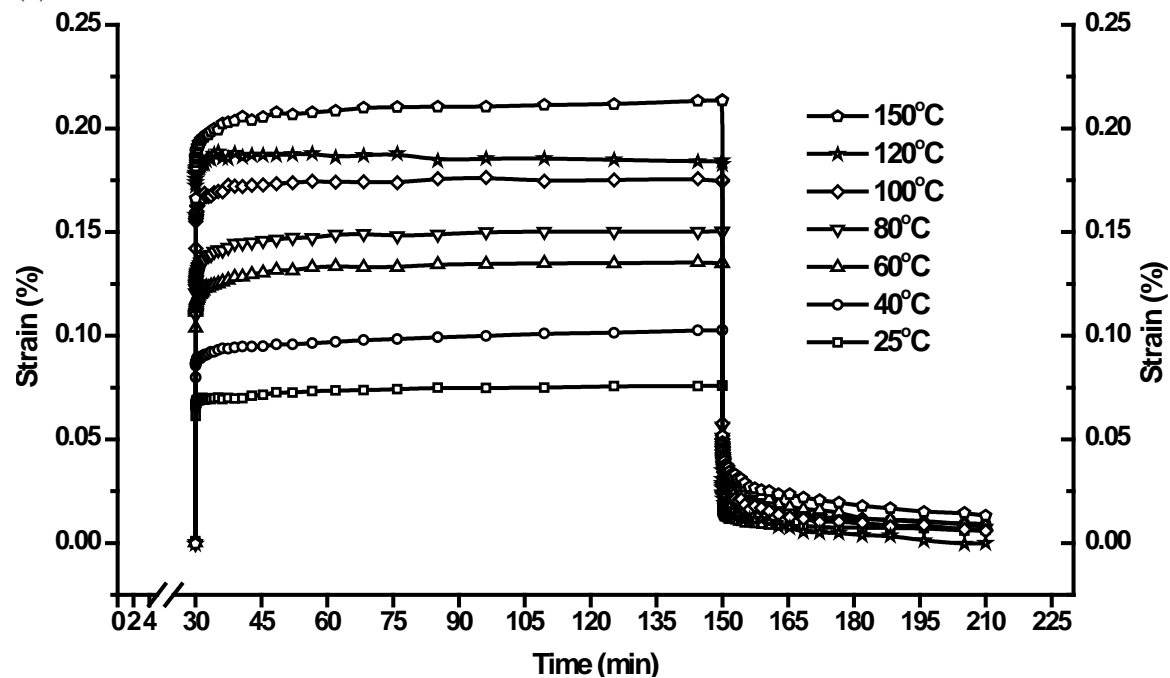
(b)
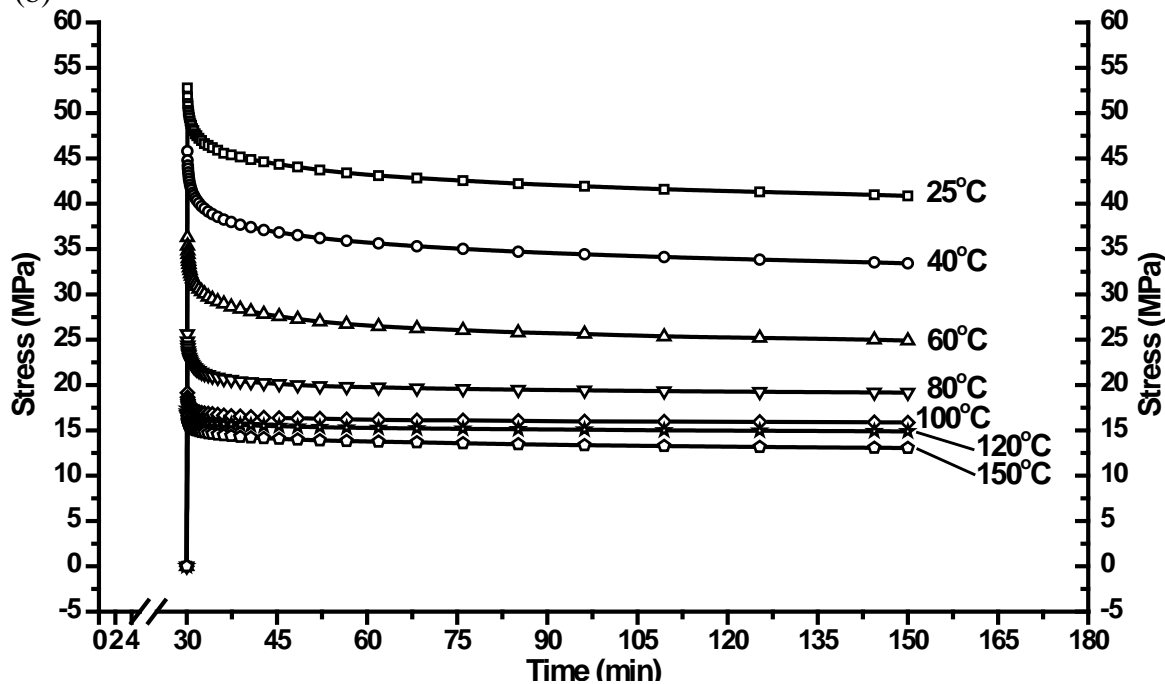
Figure 5-47 (a): Creep results of the parylene-C annealed at 200°C for 1 day in the vacuum oven (T_g>200°C); (b): Stress relaxation results of the parylene-C annealed at 200°C for 1 day in the vacuum oven (T_g>200°C)

Table 5-20: Burger's model curve fitting results of the creep and stress relaxation behaviors of the parylene-C annealed at 200°C for 1 day in the vacuum oven ($T_g>200°C$)

Fitting Results of Parylene-C Creep Behavior						
Temperature (°C)	$E_0(t_0)$ (GPa)	$\sigma_0/E_0 + \sigma_0/E_1$	σ_0/η_0	$-\sigma_0/E_1$	τ_1	R^2
150	1.338	0.205	0.00008	-0.019	2.963	0.974
120	1.410	0.187	-0.00003	-0.011	1.264	0.871
100	1.566	0.171	0.00004	-0.015	1.131	0.937
80	2.014	0.145	0.00006	-0.019	2.013	0.963
60	2.180	0.130	0.00005	-0.016	3.643	0.964
40	2.839	0.094	0.00007	-0.007	3.393	0.984
25	3.666	0.074	0.00002	-0.006	17.304	0.921
Fitting Results of Parylene-C Creep Recovery Behavior						
Temperature (°C)	$E_0(t_0+120)$ (GPa)	P_1		P_2	τ_r	R^2
150	1.474	0.018		0.025	6.511	0.938
120	1.600	0.004		0.021	4.815	0.900
100	1.971	0.012		0.031	1.891	0.908
80	2.447	0.011		0.033	3.389	0.942
60	2.812	0.012		0.030	6.498	0.947
40	3.310	0.012		0.014	5.379	0.928
25	4.094	0.007		0.008	4.357	0.944
Fitting Results of Parylene-C Stress Relaxation Behavior						
Temperature (°C)	$E_0(t_0)$ (GPa)	A_1	τ_{sr1}	A_2	τ_{sr2}	R^2
150	1.639	1.692	2.060	14.278	1153.461	0.972
120	1.738	1.397	1.447	15.628	2066.978	0.958
100	1.914	2.179	0.819	16.644	1973.455	0.951
80	2.563	4.378	1.055	20.580	1316.844	0.960
60	3.630	6.736	1.884	28.259	782.956	0.969
40	4.579	6.826	1.975	37.590	865.992	0.972
25	5.277	6.295	1.792	45.117	1034.578	0.971

(a)

(b)
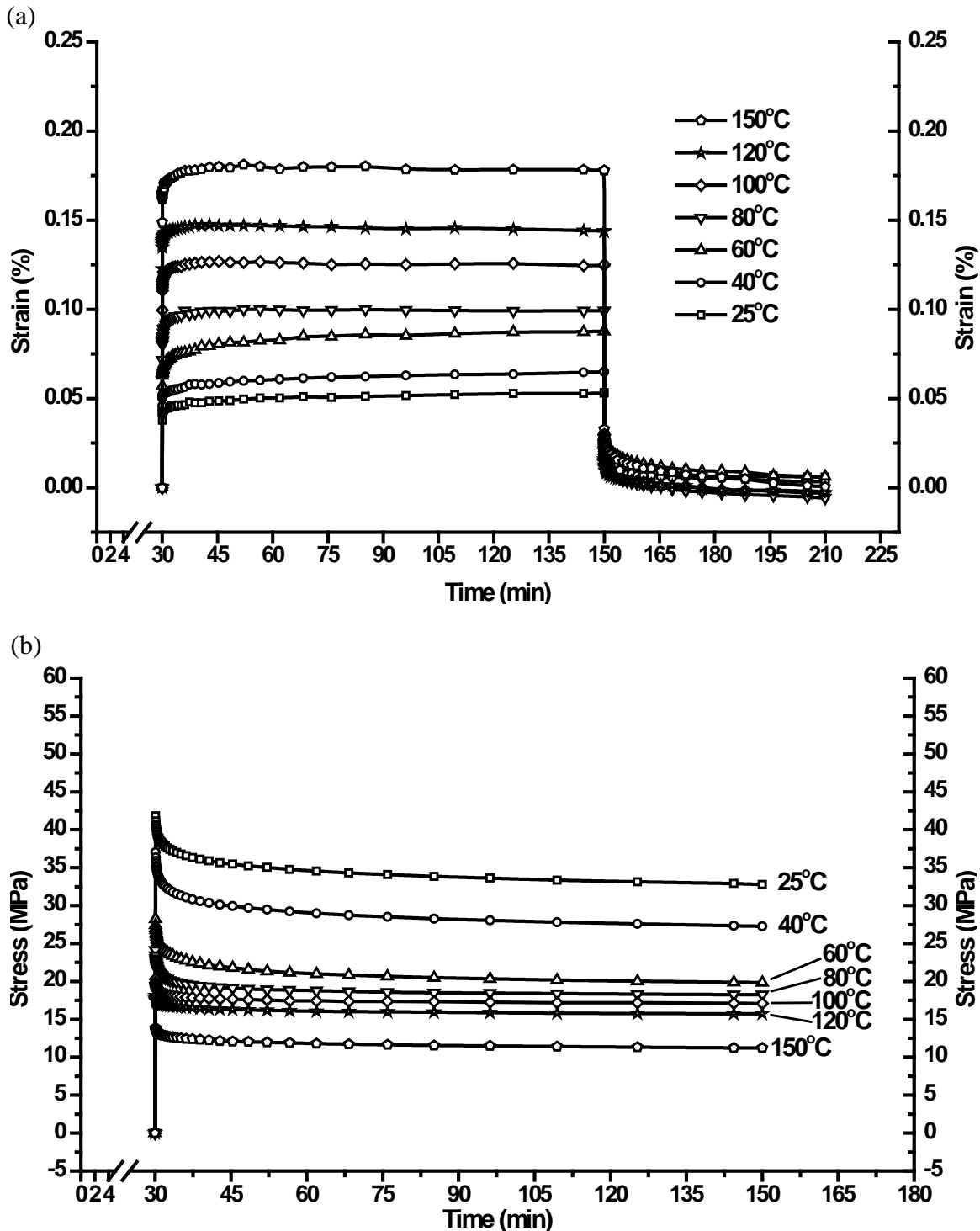
Figure 5-48 (a): Creep results of the parylene-C annealed at 200°C for 2 days in the vacuum oven (T_g>200°C); (b): Stress relaxation results of the parylene-C annealed at 200°C for 2 days in the vacuum oven (T_g>200°C)

Table 5-21: Burger's model curve fitting results of the creep and stress relaxation behaviors of the parylene-C annealed at 200°C for 2 days in the vacuum oven (T_g>200°C)

Fitting Results of Parylene-C Creep Behavior						
Temperature (°C)	$E_0(t_0)$ (GPa)	$\sigma_0/E_0 + \sigma_0/E_1$	σ_0/η_0	$-\sigma_0/E_1$	τ_1	R^2
150	1.502	0.179	-0.00001	-0.015	2.114	0.961
120	1.803	0.147	-0.00002	-0.009	1.002	0.919
100	2.200	0.125	0.00000	-0.012	1.004	0.926
80	3.034	0.098	0.00001	-0.016	1.297	0.970
60	3.862	0.080	0.00007	-0.014	4.095	0.975
40	4.833	0.059	0.00005	-0.007	6.798	0.983
25	5.787	0.049	0.00004	-0.006	6.073	0.975
Fitting Results of Parylene-C Creep Recovery Behavior						
Temperature (°C)	$E_0(t_0+120)$ (GPa)	P_1		P_2	τ_r	R^2
150	1.645	0.005		0.021	5.552	0.923
120	1.925	0.000		0.013	3.700	0.891
100	2.430	0.001		0.019	1.750	0.912
80	3.261	-0.002		0.021	3.299	0.934
60	4.187	0.009		0.017	5.497	0.946
40	4.793	0.005		0.008	4.699	0.927
25	5.930	0.007		0.004	2.800	0.926
Fitting Results of Parylene-C Stress Relaxation Behavior						
Temperature (°C)	$E_0(t_0)$ (GPa)	A_1	τ_{sr1}	A_2	τ_{sr2}	R^2
150	1.386	1.350	2.632	12.238	1194.563	0.978
120	1.813	1.323	1.594	16.456	2154.843	0.956
100	2.030	2.133	0.880	17.877	2167.343	0.958
80	2.411	3.972	1.109	19.528	1386.513	0.962
60	2.822	4.909	1.847	22.285	844.266	0.967
40	3.702	5.514	2.007	30.504	906.889	0.974
25	4.183	4.834	2.125	36.010	1104.291	0.973

5.8.1.4 Summary

In this section, creep tests are performed with eight differently pre-annealed parylene-C samples. As it has been found in Section 5.6 that the as-deposited parylene-C starts to crystallize at the temperature higher than 50°C and thus the T_g changes, the parylene-C samples are annealed at different temperatures prior the creep tests to achieve different T_g. Creep tests at different temperatures correspond to the creep study of different crystallinity of the parylene-C. The testing temperatures are chosen to cover before and after the glass transition temperatures. The primary, secondary creep and recovery behavior are all investigated in this section. The results show that parylene-C has very little or no creep below T_g, but has increasing creep and creep rate above T_g. The Young's modulus at t=30 min and t=150 min of each samples are calculated, and it shows that the Young's modulus increases during the creep, implying that the crystallization takes place during the creep either due to thermal annealing or mechanical stretching.

As aforementioned, most of the parylene-C crystallization is done in the first minute once the annealing temperature reaches over the T_g. It turns out that the creep results shown in Figure 5-41 (a) cannot be fully regarded as the creep results of the "as-deposited" parylene-C. Because it takes the first 30 minutes to thermally stabilize the testing chamber, the parylene-C sample had been treated in the elevated temperature for 30 minutes in the testing chamber and crystallized during this thermal stabilization. Therefore, the strain level of the creep results at 100°C, 120°C, and 150°C show similar results in Figure 5-43 to Figure 5-46. As long as the temperature of the pre-annealing treatments of the parylene-C sample is less than its creep temperature, the parylene-C

sample also experiences further crystallization at the creep temperature during the 30 minutes stabilization. To overcome this problem, the best way to do is place the sample in a pre-heated and thermally stabilized chamber and starts the creep test right after the placement. The temperature profile of this experiment can be treated as a step function. As the crystallization time constant is found to be about 0.845 minute, some of the creep in this experiment happens before the first time constant of its crystallization. Unfortunately, DMA Q800 does not provide this kind of function due to its sample loading limitation. An alternate approach was proposed and performed to fulfill this idea, which will be discussed in Section 5.8.2.

A 4-element Burger's model is utilized in this section to curve fit our results and the model agrees well with our creep data according to the obtained correlation coefficients, with the exception of the results obtained at the temperature lower than T_g. The derived T_g is generally in between 7-10 minutes for the creep, meaning that 30 minutes, i.e. 3 time constants, is long enough for parylene-C to finish the primary creep behavior. As the permanent viscoplastic strain is found after the creep test at the temperature higher than T_g, it is believed that the yield point could be even less than 2.43 MPa at these temperature levels. The future work would focus on the study of this irreversible strain and also the yield strength of differently pre-annealed parylene-C at different temperatures. In addition, as only primary and secondary creep behavior have been studied here, it worth a study of the investigation of the tertiary region of the parylene-C creep, which leads to the rupture as shown in Figure 5-39 (b). This study can be achieved by either longer creep with 2.43 MPa, which might take a long time, or a higher creep loading stress to shorten the testing time.

5.8.2 As-deposited parylene-C creep study under a step temperature profile

5.8.2.1 Experimental setup

To solve the problem of the parylene-C's crystallization occuring during the first 30 minutes of the testing chamber's thermal stabilization prior to the creep test, a convection oven is pre-heated at the targeted temperature and thermally stabilized prior to the real creep tests. The testing setup is shown in Figure 5-49 (a)
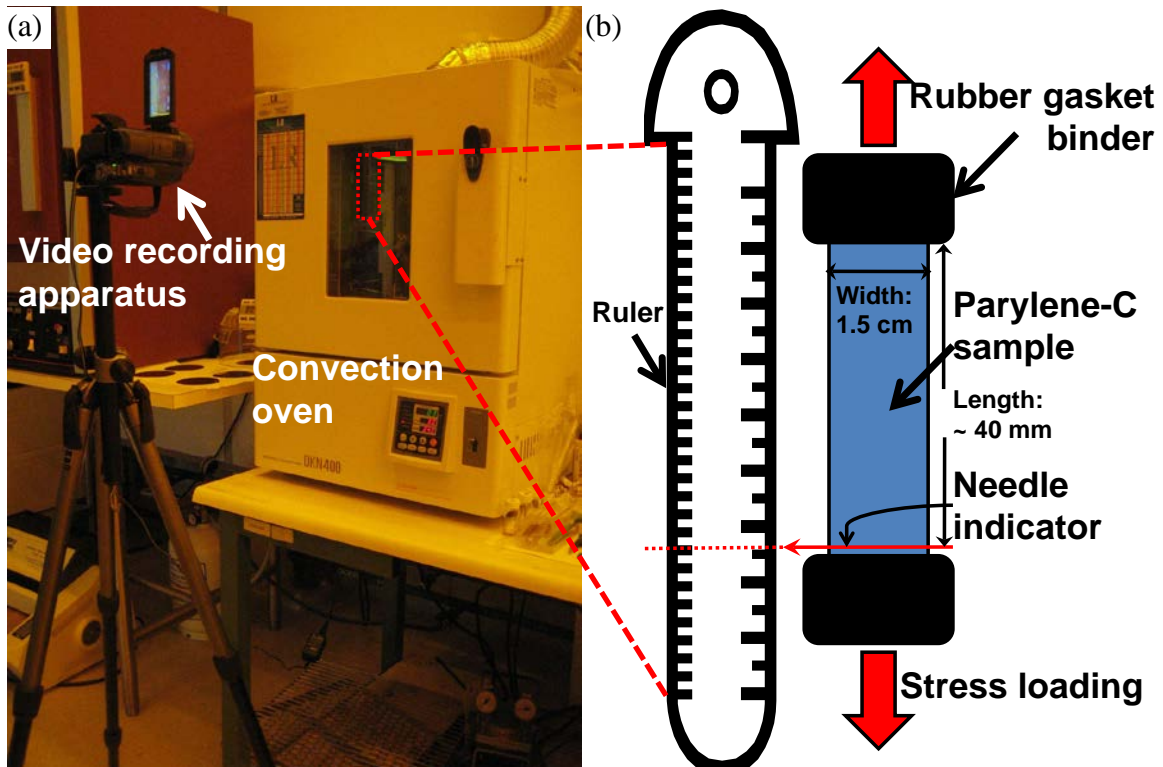
Figure 5-49: The testing setup of parylene-C creep with Heaviside temperature profile: (a) convection oven setup with a video recording apparatus, (b) parylene-C sample mounting configuration in the convection oven

Parylene-C film was deposited 11.25 µm thick and then cut into uniform 15-mm-wide strips, each with a length of more than 40 mm, facilitating later binding onto the

testing clamps. One third of the as-deposited samples were treated in a convection oven, and one third in a vacuum oven, all at 100°C for 30 minutes. A needle indicator was glued onto the bottom of the sample for convenient data reading, as can be seen in Figure 5-50. As shown in Figure 5-49 (b), the finished samples were clamped using two flat rubber gaskets to prevent the sample from sliding inside the clamp and ensure the uniform distribution of the tensile stress. A constant tensile stress of 2.43 MPa, which is the same as in Section 5.8.1, is applied to the samples by gravitational loading. The testing temperature was chosen as 80°C, 100°C, 120°C, and 150°C, which are all higher than the T_g of as-deposited parylene-C (~ 50°C).
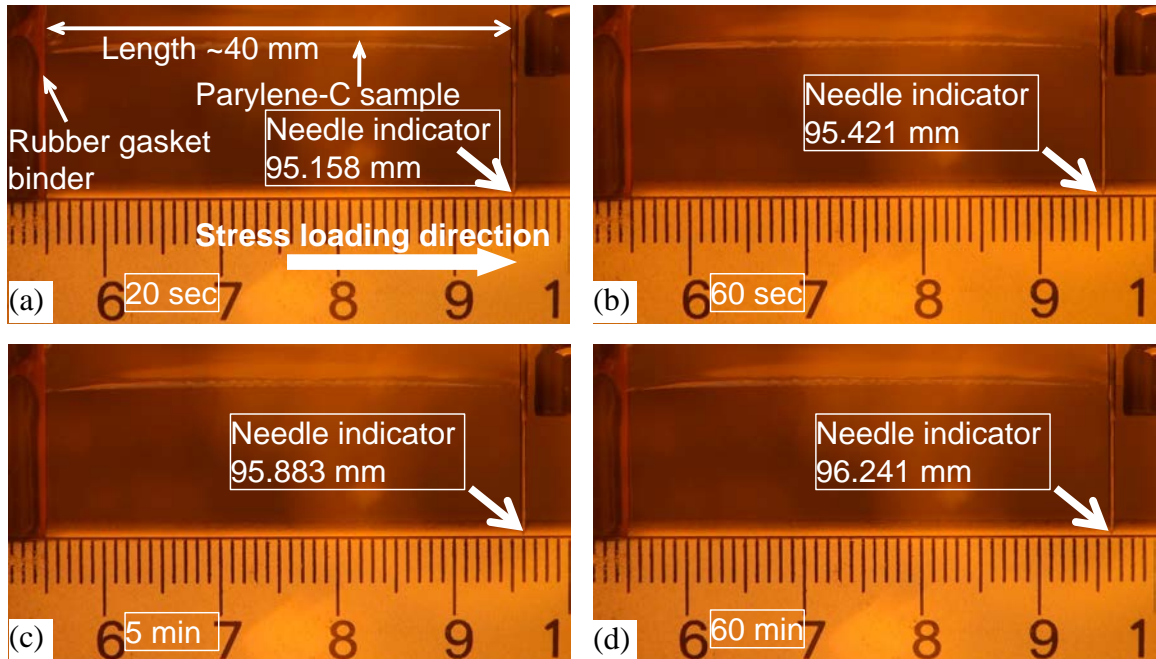
Figure 5-50: Typical capture photos of the parylene-C creep test (as-deposited parylene-C tested at 120°C) after (a) 20 sec, (b) 60 sec, (c) 5 minutes, and (d) 60 minutes. (Numbers shown on the measuring ruler represent centimeters.)

The convection oven was first pre-heated to the target temperature. Once the oven's temperature was stabilized, the parylene-C sample was placed in the oven and the door was closed immediately. As the Biot number is much less than one, the temperature distribution is assumed to be uniform within the samples [252]. The theoretical heat flux was also calculated and verified that the sample was in thermal equilibrium with the oven's inner ambient temperature in less than one second. Therefore, parylene-C film is assumed to fully experience the target temperature right after placement into the oven, and the samples can be mathematically assumed to experience a Heaviside temperature profile in this creep test.

The creep test was performed under the previous mentioned temperatures for longer than 60 minutes, while the location of the needle indicator was filmed by the video recording apparatus through the observing window of the convection oven, as shown in Figure 5-49 (a). A picture was first taken prior the sample placed in the oven so that the original length extension of the sample under the stress of 2.43 MPa can be first measured. Photos at several critical time intervals during the creep test were then captured from the video, enhanced by Photoshop and run through a Matlab program to determine the sample length as a function of time, as shown in Figure 5-50. Thermal expansion effect of the samples was also considered and eliminated during the data analysis.

5.8.2.2 Experimental results and discussions

The obtained creep curves of three different pre-annealed parylene-C samples are shown in Figure 5-51 to Figure 5-53. By comparing Figure 5-51 (the results of as-deposited parylene-C) and Figure 5-41 (a) (creep results of as-deposited parylene-C pre-

annealed for 30 minutes during the chamber thermal stabilization), it is found that the creep strain obtained under Heaviside temperature profile (Figure 5-51) is much higher than in Figure 5-41. Take the sample tested at 150°C for an example, the strain in Figure 5-51 is found to be 7% after 60 minutes of creep, while the strain in Figure 5-41 (a) is found to be only 0.7%. Because the creep temperature profile during the creep test in this section is a step function, the creep initiated right after the parylene-C sample was placed in the oven. Therefore, although the crystallization time constant is found less than one minute in Section 5.5.2, it still has lots of amorphous molecules when it starts to creep. As a result, the parylene-C tested in this section can extend much longer than in Section 5.8.1.
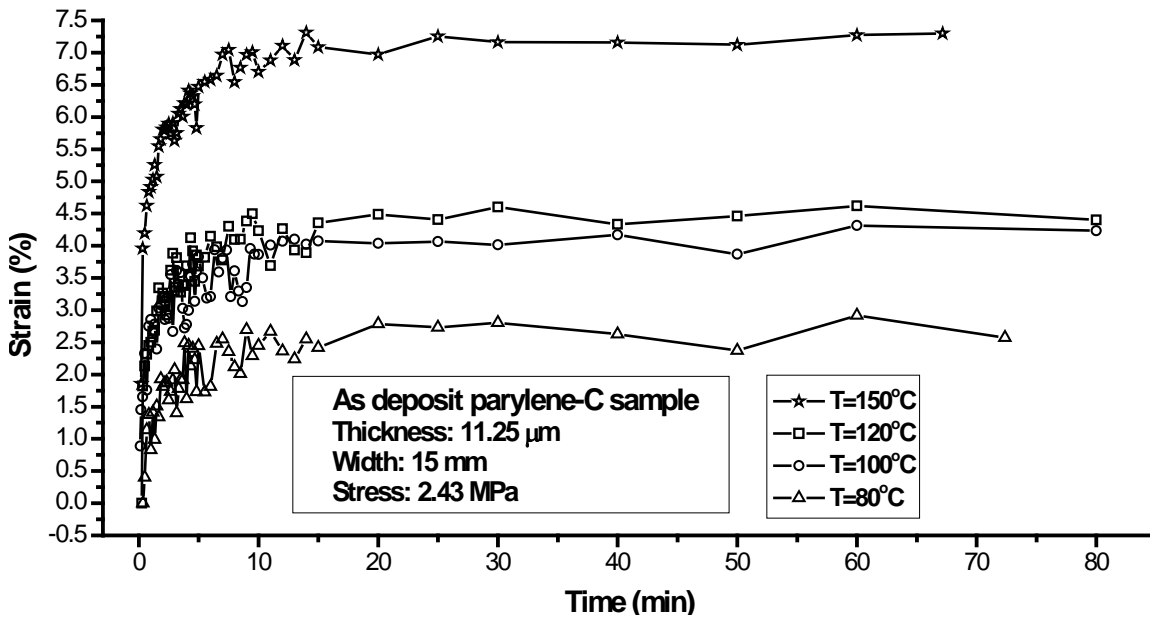
Figure 5-51: Creep results of as-deposited parylene-C performed at 80°C, 100°C, 120°C, and 150°C with a Heaviside temperature profile

It is also found that the creep saturates quickly in less than 10 minutes. However, unlike the curve shown in Figure 5-41 (a), which keeps expanding with a constant rate, the strain obtained in this section remains pretty flat afterward. The Burger's model is also used to curve fit the as-deposited data and the dominant time constants are extracted. The obtained time constants are shown in Table 5-22. It is found from Table 5-22 that the time constants also possess a descending trend as the temperature increases.

Table 5-22: Time constant of as-deposited parylene-C samples tested at different temperatures

Time constants subjected to different testing temperatures				
Temperature (°C)	80	100	120	150
Time constant τ (min)	5.34	4.29	3.48	2.21

Figure 5-52 shows the creep results of parylene-C annealed at 100°C in the air for 30 minutes. Compare to the as-deposited parylene-C results in Figure 5-51, it can be seen that the samples pre-processed in the 100°C convection oven showed no significant signs of creep at temperatures of 80°C and 100°C, while it shows a creep similar to those found in as-deposit samples at the temperatures of 120°C and 150°C at a decreased rate and lesser overall displacement. This phenomenon is believed to be caused by the crystallization and the oxidation of the parylene-C that occurred when it was annealed in the 100°C convection oven. To understand the reliability of the creep test performed in this section, the creep curve representing pre-annealed parylene-C tested at 100°C shown in Figure 5-52 is compared to the curve representing as-deposited parylene-C thermally treated at 100°C for 30 minutes during the system thermal stabilization shown in Figure

5-41 (a). From Figure 5-41 (a), the sample tested at 100°C extends to about 0.5% after 60 minutes of creep, while the curve shown in Figure 5-52 has a strain ranging bout 0.5% to 1%. Due to the low resolution of the method provided in this section, which is about 0.5%, these two strains do not show a significant difference and therefore the comparison verifies that the testing method performed in this section is a reliable approach.
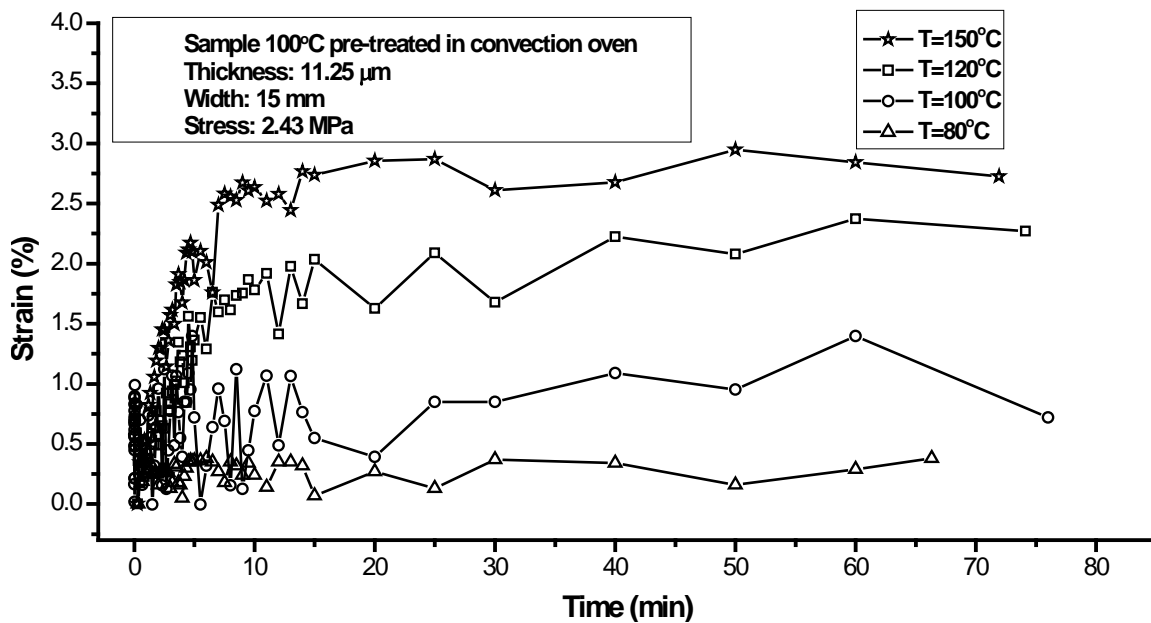
Figure 5-52: Creep results of parylene-C pre-annealed at 100°C in the air, performed at 80°C, 100°C, 120°C, and 150°C with a Heaviside temperature profile

As shown in Figure 5-53, the creep results of parylene-C samples pre-annealed in the 100°C vacuum oven show a similar behavior to the as-deposit samples at all four temperatures, but with a smaller creep strain. The lesser overall strain of the samples treated at 100°C in vacuum implies the intrinsic polymer transformation, which is mainly due to the crystallization.

The oxidation results can also be studied by comparing Figure 5-52 and Figure 5-53. It is found that the strain of the creep curves shown in Figure 5-53 is always higher than in Figure 5-52 at all four testing temperatures. As two samples are both pre-annealed at 100°C, in addition, the crystallization effect can be ignored at the time of instantaneous stain applied, it is evident that the oxidation does happen at 100°C and dominates the creep results in this study. It is believed that the oxygen atom embedded in the parylene-C sample deters the polymer movement during the creep tests. The results verify that annealing of parylene-C in vacuum keeps the sample oxygen-free and does preserve its properties.
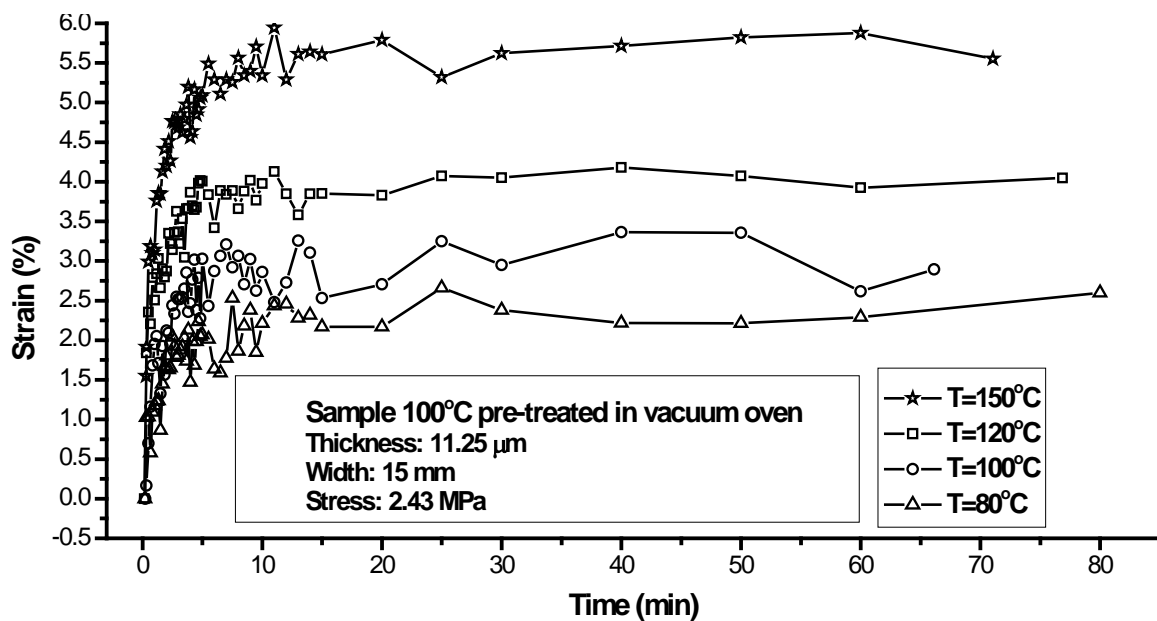
Figure 5-53: Creep results of parylene-C pre-annealed at 100⁰C in the vacuum, performed at 80⁰C, 100⁰C, 120⁰C, and 150⁰C with a Heaviside temperature profile

5.8.3 Stress relaxation of parylene-C

5.8.3.1 Stress relaxation overview

Stress-relaxation is another experiment which is also commonly used to find the time-dependent mechanical behavior of the materials. The concept of the stress relaxation experiment is shown in Figure 5-54. As shown in Figure 5-54 (a), the stress relaxation test measures the stress evolution under a constant strain. The environmental temperature is generally constant. The corresponding output of the applied strain is shown in Figure 5-54 (b). The stress is first induced by the initial instantaneous strain at $t=t_0$. Both induced stress relaxes and the relaxing rate decrease gradually with respect to the time. A permanent stress could be found depends on the type of material tested. The induced stress of the thermoplastic polymer is generally relaxed to zero while a permanent stress is generally found with the thermoset polymer [239].
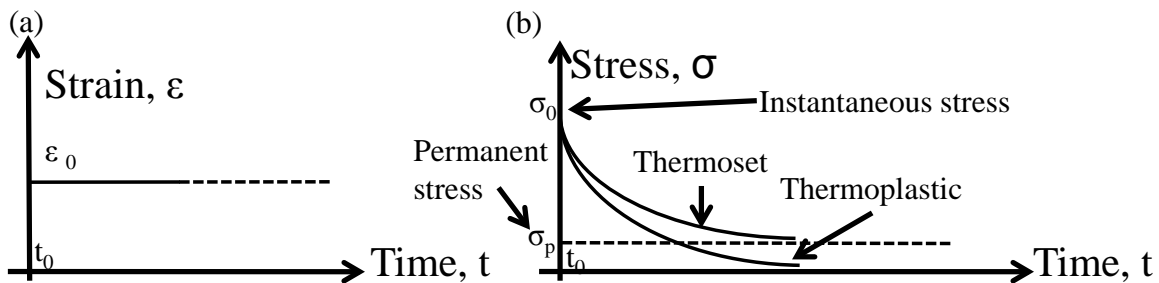
Figure 5-54: The stress relaxation test of polymers: (a) constant applied strain during the stress relaxation test at a constant temperature, (b) the corresponding stress output versus time

Similar to the creep tests of the parylene-C, stress relaxation tests are also of great importance as the implantable parylene-C MEMS devices would face the body

temperature, i.e., 37°C, during its operation, and the built-in stress might dominate the device's life. On the other hand, with the knowledge of the stress relaxation of parylene-C, the residual stress of parylene-C MEMS devices after the fabrication can be relaxed by treating in a proper post-annealing temperature and time.

5.8.3.2 Solution of the Burger's model for stress relaxation

With a proper initial condition, the constitutive equation of Burger's model expressed in eqn. (5-12) can be solved for stress relaxation. Rewrite eqn. (5-12) as:

$$\sigma_0 + p_1\dot{\sigma} + p_2\ddot{\sigma} = q_1\dot{\varepsilon} + q_2\ddot{\varepsilon}, \tag{5-19}$$

where

$$p_1 = \frac{\eta_0}{E_0} + \frac{\eta_0}{E_1} + \frac{\eta_1}{E_1},$$

$$p_2 = \frac{\eta_0\eta_1}{E_0E_1},$$

$$q_1 = \eta_0, \tag{5-20}$$

$$q_2 = \frac{\eta_0\eta_1}{E_1}.$$

To solve eqn. (5-19) for stress relaxation behavior, the initial strain conditions are expressed as $\varepsilon(0) = \varepsilon_0 H(t)$, where $H(t)$ is the Heaviside function, $\dot{\varepsilon}(0) = \varepsilon_0\delta(t)$ and $\ddot{\varepsilon}(0) = \varepsilon_0\frac{\delta(t)}{dt}$. Applied $\varepsilon(0)$, $\dot{\varepsilon}(0)$, $\ddot{\varepsilon}(0)$ into eqn. (5-19), the solution of the obtained stress can be solved as [239, 253, 254]:

$$\sigma = \frac{\varepsilon_0}{\sqrt{p_1^2 - 4p_2}}[(q_1 - q_2r_1)\exp^{-r_1 t} - (q_1 - q_2r_2)\exp^{-r_2 t}], \tag{5-21}$$

or for simplicity:

$$\sigma = A_1\exp^{-r_1 t} + A_2\exp^{-r_2 t}, \tag{5-22}$$

In eqn. (5-21), r_1 and r_2 are expressed as:

$$r_1 = \frac{p_1 - \sqrt{p_1^2 - 4p_2}}{2p_2}, \text{ and } r_2 = \frac{p_1 + \sqrt{p_1^2 - 4p_2}}{2p_2}. \tag{5-23}$$

The values of four physical elements of the Burger's model can be calculated by the following expressions:

$$E_0 = \frac{q_2}{q_1},$$

$$\eta_0 = q_0,$$

$$E_1 = \frac{E_0 \eta_0^2}{p_1 E_0 \eta_0 - \eta_0^2 - q_2 E_0}, \tag{5-24}$$

$$\eta_1 = \frac{q_2 E_1}{\eta_0}.$$

In addition, the two time constants τ_{sr1}, and τ_{sr2} can be obtained by the reciprocal of r_1 and r_2 as:

$$\tau_{sr1} = \frac{1}{r_1}, \text{ and } \tau_{sr1} = \frac{1}{r_2}. \tag{5-25}$$

5.8.3.3 Stress relaxation experiment

5.8.3.3.1 Sample preparation and the experiments

In this section, the stress relaxation was performed with eight parylene-C samples treated/annealed the same as in Section 5.8.1, as well as with the same geometry. Seven testing temperatures were also chosen the same as in Section 5.8.1 for comparison. During the stress relaxation experiment, an instantaneous strain of 1% was applied onto the sample and the corresponding stress relaxation was monitored for two hours. Similarly, the system was pre-heated to the target temperature for 30 minutes before the stress relaxation test.

5.8.3.3.2 Results and discussion

The results of the stress relaxation test of eight different pre-treated parylene-C samples are shown in Figure 5-41 (b) to Figure 5-48 (b) on pages 240 to 254. Similar to the figures of creep tests, each figure has seven curves corresponding to seven different testing temperatures. The Burger's curve fitting results are also shown in the stress relaxation parts in Table 5-14 to Table 5-21 on pages 241 to 255. From the results shown in those figures and tables, several founds can be made as follows:

1. It is found that the stress always demonstrates a descending trend at whatever temperature, and a permanent stress is always found as long as the 1% strain is applied to the samples. The permanent stress level depends on the testing temperature. The remaining permanent stress becomes much less when the testing temperature is higher than Tg. In this case, the higher the testing temperature, the lesser the permanent stress obtained. It implies the high mobility of the parylene-C polymer chain at higher temperature. The descending rate generally also increases as the testing temperature increases. However, when the testing temperature is lower than Tg, very little descending rate observed and the permanent stress is relatively higher. It is evident that the glass transition temperature is a very important indicator that divides the results into two parts: very little stress is relaxed and also at slower rate with temperature lower than Tg, while more stress is relaxed and at faster relaxing rate at the temperature higher than Tg.

2. It is found from Burger's model expressed in eqn. (5-21) that the solution model has two time constants: τsr1 and τsr2. The results of the first time constant, τsr1,

in Table 5-14 to Table 5-21 generally fall in the range of 1–5 minutes. However, the value of τsr1 spreads arbitrary and no obvious trend can be found. On the other hand, according to Table 5-14 to Table 5-21, the values of τsr2 are found ranging from about 100 up to 2150 minutes, which is much larger than the first time constant τsr1. Another trend also can be found that τsr2 generally decreases as the testing temperature increases, with the exception of samples pre-annealed at 200ºC (Table 5-20 and Table 5-21). Again, this infers that the parylene-C is softer at higher temperature and the polymer chain is easier to deform. The stress relaxation results of samples pre-annealed at 200ºC all show very large τsr2, implying very little stress relaxation. Therefore the parylene-C annealed at 200ºC for either one or two days are very close to elastic material, which has also been predicted in Section 5.8.1. Because the annealing of parylene-C at 200ºC was performed in the vacuum oven, it is believed that the oxidation effect can be ignored during the sample preparation, and thus this material property change (from viscoelastic to elastic) is attributed to the crystallization of the parylene-C. As the second time constant is usually longer than 120 minutes, the effect of the second time constant cannot be seen in the figures shown in this section. Further study needs to be done to verify the accuracy of model.

3. As aforementioned, it can be graphically found that the remaining permanent stress decreases as the testing temperature increases. In addition, more stress is relaxed when the testing temperature gets higher than Tg, which has been found usually close but a bit higher than the annealing temperature in Section 5.6. It infers that the parylene-C residual stress resulting from the clean room fabrication

can be relaxed by annealing the parylene-C at a temperature higher than the maximum processing temperature. It turns out that monitoring the temperature history of the parylene-C fabrication process is helpful in predicting and reducing its residual stress after the device is done. In our clean room, the temperature generated in most processes is generally controlled less than 200ºC. Therefore, to relax the residual stress of the parylene-C-based device, it is suggested to anneal the device at 200ºC in the vacuum oven. As aforementioned, the time first time constant τsr1 is generally in the range of 1–5 minutes, it can be concluded that the residual stress can be mostly relaxed in 15 minutes (3 time constants). Therefore, two-hours annealing would be long enough to relax most of the residual stress in the parylene-C device, according to what we have just found in this section.

4. It is also found that the remaining permanent stress is higher as the pre-annealing temperature gets higher. For example, at the testing temperature of 150ºC, parylene-C pre-annealed at 200ºC (shown in Figure 5-47 and Figure 5-48) has the highest stress remaining among all eight different parylene-C samples. This is likely due to the highest crystallinity coming from the high pre-annealing temperature. High crystallinity also results in slower stress relaxing rate. This means parylene-C annealed at 200°C behaves similar to an elastic material, which is also concluded in Section 5.8.1.

5. From Figure 5-41 (b) to Figure 5-48 (b), it can be seen that the stress is introduced immediately after the instantaneous 1% strain is applied. The level of the stress response depends on the Yong's modulus at the testing temperature. Similar to the Young's modulus calculation in Section 5.8.1, the Young's modulus can be

obtained by the measured stress divided by 1% of strain. The results of calculated Young's modulus are shown in the first column of the stress relaxation part in Table 5-14 to Table 5-21. As expected, the obtained Young's modulus decreases as the testing temperature increases. As expected, it is found that the Young's modulus obtained from stress relaxation experiments are close to the values obtained from creep experiments. The minor difference is likely attributable to thickness variation and clamping variations.

5.8.3.4 Summary

A series of stress relaxation experiments at seven different testing temperatures has been done with eight differently pre-treated parylene-C samples. The stress relaxation experiments performed at temperatures higher than T_g have faster stress relaxation rates and less residual stress after 120 minutes than experiments performed below T_g. The Burger's model solution for stress relaxation behavior is a solution with two-time-constants. The curve fitting results show that the first time constant is generally in the range of 1–5 minutes but no trend could be observed from the current data obtained in our tests. The second time constant is always found much larger than the first time constant, falling in the range of ~ 100–2150 minutes. In general the second time constant decreased with increasing testing temperature, except when parylene-C was pre-annealed at 200⁰C, which behaved elastically at the temperatures lower than 200⁰C. Because the second time constants are usually larger than 120 minutes, the effect of the second time constant cannot be clearly observed in our results in the Figure 5-41 (b) to Figure 5-48 (b). More stress relaxation experiments with longer testing time are needed to understand the second time constant behavior.

From the stress relaxation results, it is suggested that, in order to relax the residual stress of a parylene-C-based device, the device can be placed at the temperature which is higher than the highest temperature that the device had experienced during its fabrication. The time should be longer than three times the first time constant for complete relaxation. In our experience, annealing the device at 200⁰C in vacuum for two hours is preferable.

It is also found that the parylene-C pre-annealed at higher temperature has higher remaining permanent stress than at lower temperature after two hours of stress annealing experiment. This is due to the high crystallinity of the parylene-C generated during its pre-annealing process. Whether the remaining permanent stress is helpful depends on the devices' application. If the remaining permanent stress is not required in its final application, the device can be annealed at the elevated temperature. If the remained stress is necessary in the device, the parylene-C is suggested to be pre-annealed at a higher temperature than its final operational temperature to tailor the T_g to a higher value. By increasing T_g, it prevents the stress loss in the final application at the operational temperature and therefore the device's lifetime can become longer.

5.8.4 Summary

In this section, the creep and the stress relaxation behavior, which represent the time-dependent behavior of the parylene-C were investigated. This work provides useful information to help researchers design and make the parylene-C based devices. According to what has been found in this section, parylene-C is a very thermal-sensitive material and it takes a lot care to fabricate it carefully in the right temperature. In order to minimize or reduce the residual stress, the temperature needs to be carefully selected

during the device fabrication. The fabrication thermal history has to be monitored to prevent unpredicted device function behavior.

For example, it is recommended that the device should be pre-annealed at a temperature higher than its designed operation temperature to stabilize the parylene-C mechanical properties. In addition, by properly designing the fabrication temperatures and procedures, the required built-in stress of the device won't be relaxed during later clean room fabrication and its normal operations.

On the other hand, if it is necessary to eliminate residual stress or it is necessary to thermally deform and mold the parylene-C device, the temperature experienced during the device fabrication needs to be monitored. In such cases, a higher temperature than the temperature the device has experienced is required.

It is well known that high temperature could be introduced during the parylene-C fabrication or post fabrication. By understanding the relationship between the mechanical properties of parylene-C with respect to the temperature, people can design parylene-C devices to maintain functionality and extend lifetime.

5.9 Viscoplasticity of Parylene-C Film at Human Body Temperature

5.9.1 Overview of parylene-C viscoplasticity study

Due to its superior biocompatibility, parylene-C has been a prominent protective coating material for many biomedical devices since the 1950s [255]. In addition, there is a fast development of parylene-C bioMEMS technology with many potential applications, such as, spinal cord implant, glaucoma drainage device and cochlear implant [238, 255, 256]. However, there were reports on the aging degradation of parylene-C in animal body fluid. For an example, it was found that the as-deposited parylene-C showed long-term degradation in the monkey brain two years after the implantation [257]. Although there is suspicion that the plastic or viscoplastic behavior of parylene-C is part of the degradation mechanism, this has never been systematically studied. Therefore, there is concern that the lack of understanding of parylene-C's plastic behavior can lead to wrongful use of it, especially for long-term implant devices.

The creep behavior, i.e. total strain change with time under a constant loading stress, and the stress relaxation behavior, i.e., total stress change with time under a constant strain, of parylene-C film at different temperatures have been studied in Section 5.8.1. The testing results showed that as-deposited parylene-C film can have plastic deformation at 37°C as its glass transition temperature range is 35–60°C [258]. Therefore, this work is focused on the plastic, or more accurately, viscoplastic, behaviors of parylene-C film at 37°C due to its growing population in implantations. To understand the viscoplastic behaviors of parylene-C film, uniaxial tensile tests under various conditions are performed including tests under different strain rates, cyclic

loading/unloading tests, abrupt strain rate change tests, creep-recovery tests, and stress-relaxation tests [259, 260]

5.9.2 Sample preparation and viscoplastic experiments

5.9.2.1 Sample preparation and testing environment setup

The testing parylene-C samples were prepared at the same deposition condition by the same coating system as described in previous few sections. The as-deposited film was then cut into strips with 5.3 mm in width and 10 mm in length. All tests were performed in the DMA Q800 by TA instruments at 37°C. Similarly, the testing chamber was first ramped to 37°C, and waited until the whole system reached thermal equilibrium before the tests started.

5.9.2.2 Testing results

All testing results from the machine are nominal stresses or strains. In this section, all nominal stresses and strains are readily converted to the true stresses and strains unless otherwise specified. (Strain rate tests) 5 different strain rates were chosen from 8.33×10^{-6} s^{-1} to 8.33×10^{-2} s^{-1} (i.e., the highest strain rate Q800 can apply), each of which has one order of magnitude jump, as shown in Figure 5-55. (Cyclic loading/unloading tests) The cyclic loading/unloading tests were done at the strain rate of 8.33×10^{-5} s^{-1} (as shown in Figure 5-56). The first loading/unloading was done at 22.92 MPa and the second done at 32.92 MPa. (Abrupt strain rate change tests) The abrupt strain rate change test was done by changing strain rate from 8.33x10-5 S-1 to 8.33x10-6 S-1 during the uniaxial tensile tests. Two abrupt strain rate change tests were performed. One was done at the strain of 0.9% and the other at 1.1%, as shown in Figure 5-57.

(Creep tests) For creep tests, five stresses were applied: 2.5 MPa, 10 MPa, 20 MPa, 30 MPa, and 40 MPa. These stresses were applied for 120 minutes during the creep tests and then removed to observe the creep recovery for another 60 minutes. The creep results are shown in Figure 5-58 and fitted with Burger's model (discussed below). (Stress relaxation tests) The stress relaxation tests were performed under 6 different strains: 0.25%, 0.5%, 0.75%, 1%, 1.5%, and 2%. These constant strains were applied onto the samples for 120 minutes to observe the stress relaxation behaviors of the parylene-C film. The stress relaxation results are shown in Figure 5-59, which are also fitted with Burger's model.

5.9.2.3 Discussion

In this section, the Burger's model is still used to analyze all the results shown below due to its simplicity. Similar to Section 5.8, eqn. (5-14) is used for the creep strain analysis; eqn. (5-16) is used for the creep recovery analysis; and eqn. (5-22) is used for stress relaxation stress analysis.

Figure 5-55 shows the experimental results of uniaxial tensile tests under different strain rates and it clearly shows a rate-dependent behavior. The higher the strain rate, the larger the yield strength is. Note that, for the strain rates 8.33×10^{-2} s^{-1}, 8.33×10^{-3} s^{-1} and 8.33×10^{-4} s^{-1}, the end points of the three data curves are the sample fracture points. It is found that the parylene-C film tends to break more easily when the applied strain rate is higher. At strain rates higher than 8.33×10^{-4} s^{-1}, the parylene-C film behaves like a brittle material. The Young's modulus is found to be about 3GPa for all five curves in the early linear region, which agrees well with the result found in Sections 5.6, 5.7, and 5.8.
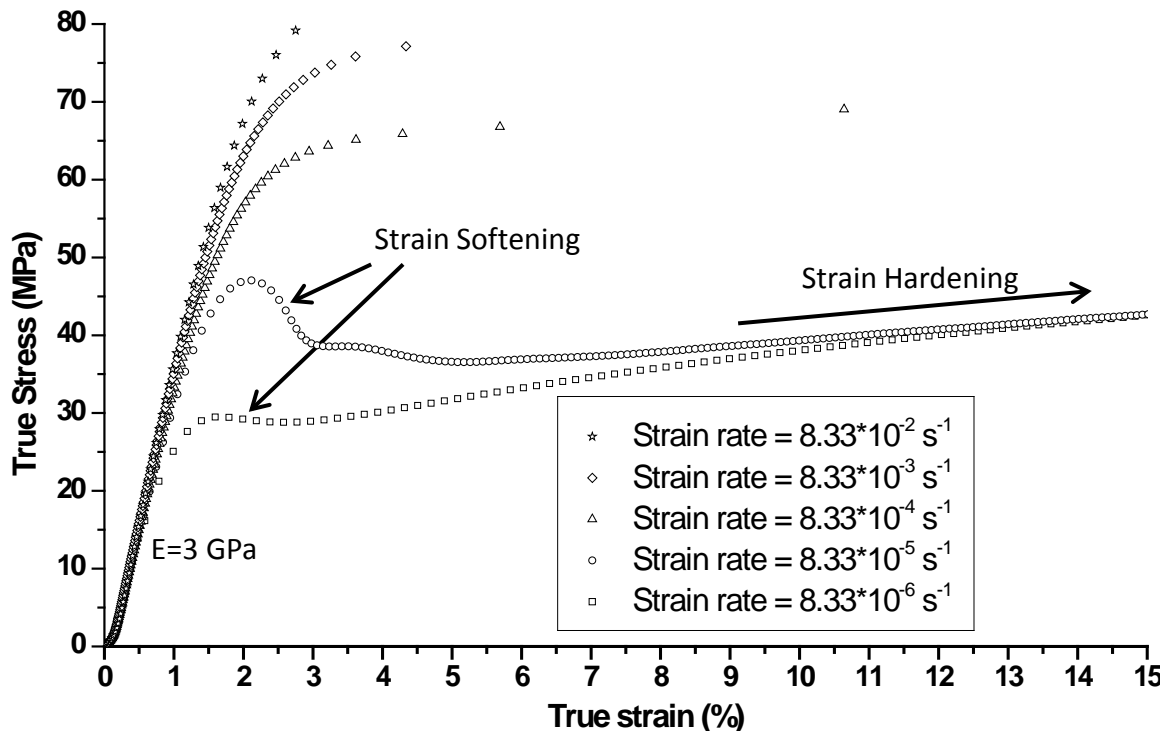
Figure 5-55: The results of constant strain-rate tests

Figure 5-56 shows the cyclic loading/unloading test results, where a permanent strain deformation of 0.09% of parylene-C remains after a stress of 22.92 MPa is loaded and then unloaded. When the stress is reloaded again, the stress-strain curve shows a hysteresis, which is another evidence of the creep recovery. However, after a while, the curves do approach the monotonic curve of the standard uniaxial tensile test without unloading.

Figure 5-57 is the results from the abrupt strain rate change experiments. It is found that when the strain rate abruptly decreases from 8.33×10^{-5} s^{-1} to 8.33×10^{-6} s^{-1}, the stress drops and gradually coincides with the lower strain rate curve. This means that, with a strain rate under 8.33×10^{-5} s^{-1}, the Young's modulus is strain-rate dependent but not strain-rate-history dependent.
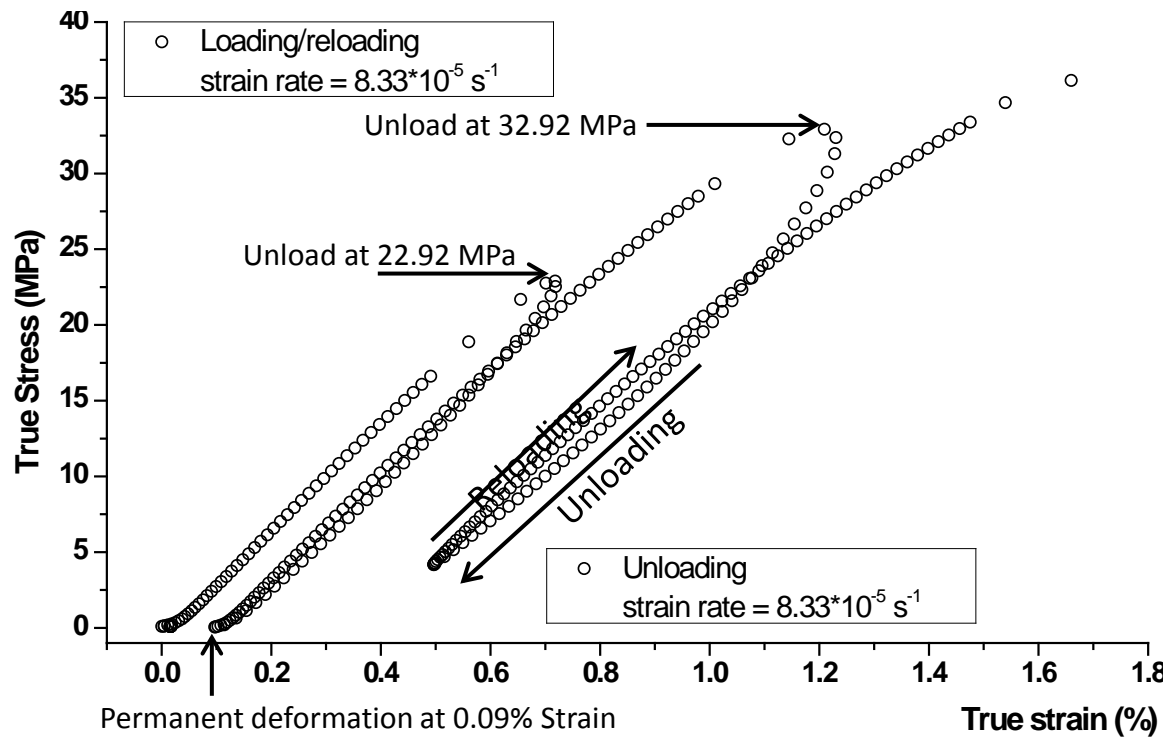
Figure 5-56: The results of cyclic loading/unloading tests
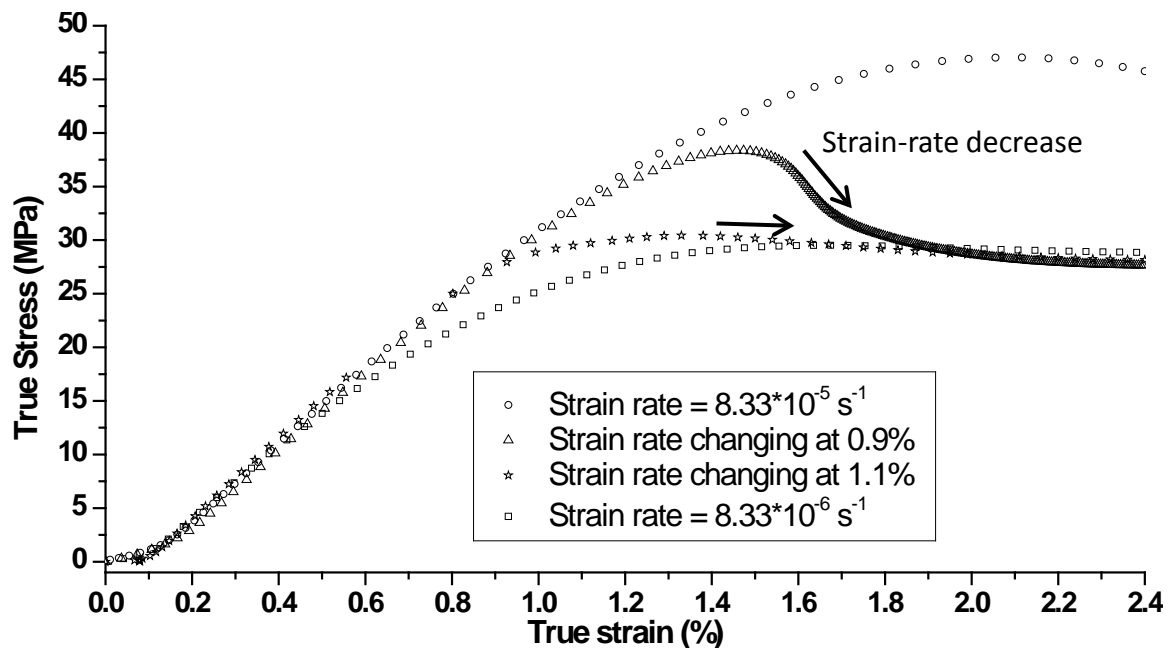
Figure 5-57: The results from the abrupt strain-rate change tests

Figure 5-58 shows the results of creep tests. Burger's model is used to fit the data curve for four different applied stresses (2.5 MPa, 10 MPa, 20 MPa, and 30 MPa). At applied stress lower than 30 MPa, the Burger's model fits well with the experimental results. The time constant is bigger for larger stress as shown in Table 5-23. At 40 MPa, the specimen simply breaks so no reliable creep data is recorded. The fitting parameters of the Burger's model for creep recovery are shown in Table 5-24. In comparison, the time constant for the creep recovery increases with decreasing loading stress, which is different from the creep case. When the applied stress is 2.5 MPa, it is found that the creep slope, σ_0/η_0, is very small so that the parylene-C film shows little or no creep behavior.
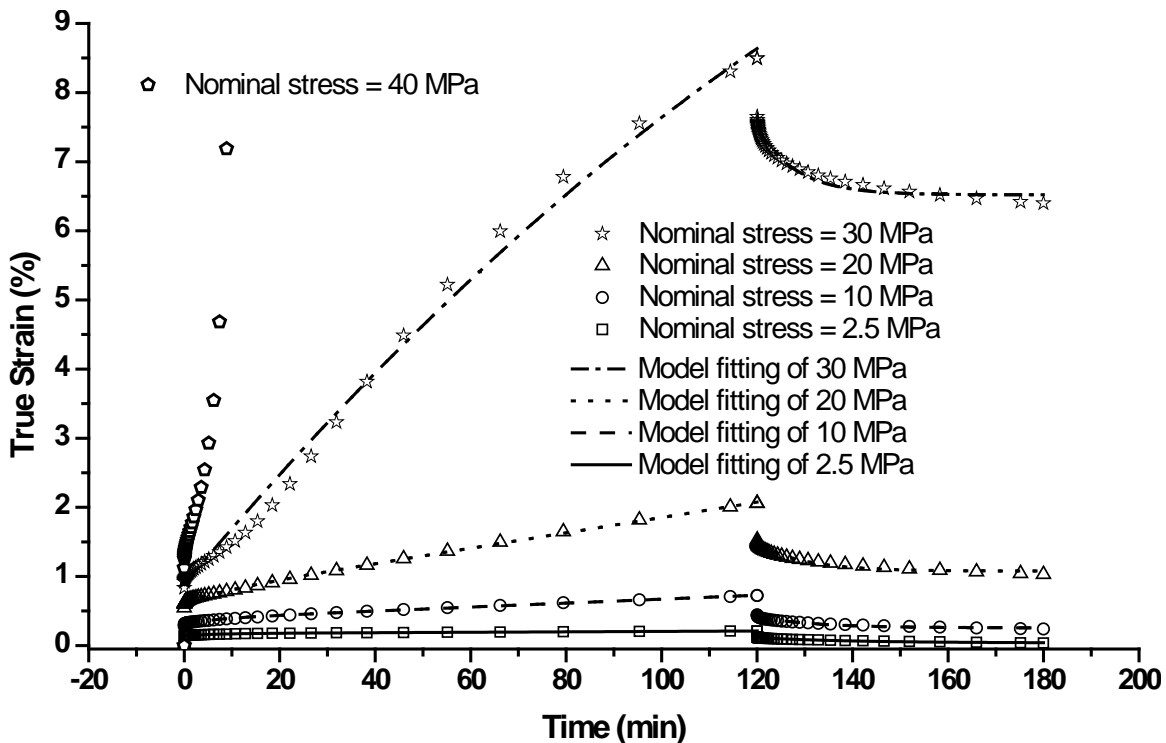
Figure 5-58: The results of creep tests of parylene-C film under different loading stresses: Theoretical Burger's model shows good fitting for the applied stress less than 30 MPa.

Figure 5-59 shows the results and the modeling of the stress relaxation tests. Note that the stress relaxation solution of the Burger's model inherently give two time constants, hence Table 5-25 shows two time constants for each test. The first (and smaller) time constant is identified as the dominant time constant and it decreases as the applied strain increases. The second time constant is always at least an order of magnitude larger than the first time constant. Therefore, the second time constant will not be observed in our experiments due to a limited time span. Accordingly, the stress relaxation data is consistent with the creep data in the sense that parylene-C exhibits a significantly stronger plastic flow when the applied stress is higher than 35 MPa (corresponding to 1% strain). In addition, the stress is relaxed faster with higher stress loading.
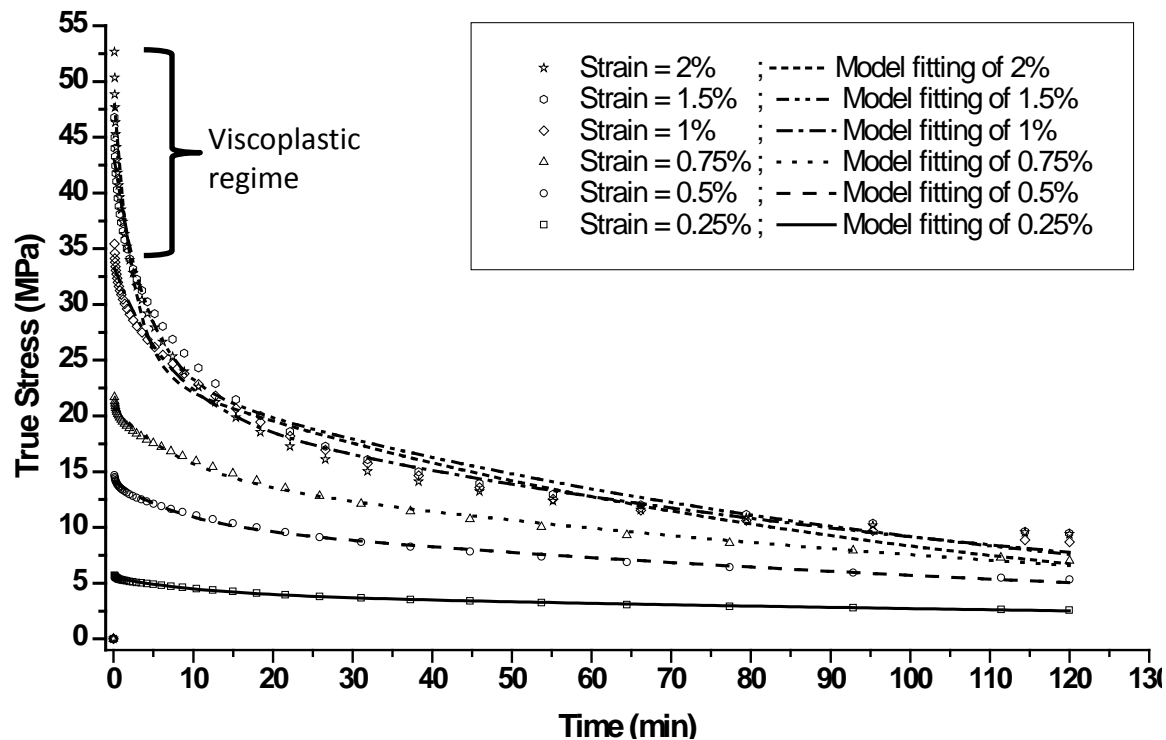
Figure 5-59: The results of stress relaxation tests. Stress relaxation is observed for all the chosen strains. Higher strain gives faster stress relaxation.

Table 5-23: Parameters of Burger's model for creep. At 40 MPa, the sample breaks and no creep could be recorded.

Applied Stress (MPa)	$\sigma_0/E_0 + \sigma_0/E_1$	σ_0/η_0	σ_0/E_1	τ_c (min)
2.5	0.00174	$3.096*10^{-6}$	$-3.062*10^{-4}$	7.522
10	0.00385	$2.861*10^{-5}$	$-6.980*10^{-4}$	7.512
20	0.00743	$1.109*10^{-4}$	-0.0012	10.982
30	4.882	-0.00589	-14.873	2214.1
40	NA	NA	NA	NA

Table 5-24: Parameters of Burger's model for creep recovery

Applied Stress (MPa)	P_1	P_2	τ_r
2.5	3.766*10-4	7.707*10-4	20.510
10	0.00256	0.00161	12.168
20	0.0108	0.00385	10.051
30	0.0652	0.00972	8.127
40	NA	NA	NA

Table 5-25: Parameters of Burger's model for stress relaxation

Applied Strain (%)	P_3	τ_{sr1}(min)	P_4	τ_{sr2}(min)
0.25	1.475	11.373	4.034	253.611
0.5	3.637	8.033	10.514	163.596
0.75	5.780	8.249	14.971	146.124
1	12.446	7.107	20.989	120.705
1.5	19.500	3.987	23.851	104.838
2	24.778	2.366	24.177	93.888

In summary, it is found that the time constants of creep, creep recovery and stress relaxation are functions of applied stress (or strain), as well as temperature found in [257]. Besides, above a small strain around 0.1% (~ 2.5 MPa), the parylene-C is clearly plastic and rate-dependent, hence viscoplastic.

5.9.3 Summary

Five different uniaxial tensile tests under different testing conditions were performed to study the viscoplastic behaviors of as-deposited 20-μm-thick parylene-C films. The results show that, above about 0.1% of strain (~ 2.5 MPa) parylene-C is a strain (or stress) and strain-rate-dependent material. Burger's model is adequate to describe its creep and stress relaxation behaviors. Future work would focus on a more delicate viscoplastic model, e.g., Bodner-Partom model, to analyze parylene-C viscoplastic behavior [259–266].

5.10 Summary and Conclusion

Several mechanical properties and polymer properties of parylene-C are investigated in this chapter. The simplest densification experiment is first demonstrated. It shows that as-deposited parylene-C first extends at temperature lower than ~ 50°C and starts to shrink at higher temperature, implying that the parylene-C starts to crystallize at ~ 50°C. This assumption was verified by repeating the testing on the same sample with the same temperature profile. It is found that the parylene-C length does not shrink until the previous testing temperature, implying the thorough crystallization during the previous thermal annealing. The thermal coefficient of as-deposited parylene-C is found as 35.5 ppm/°C, which agrees very well with the available literature value.

Oxidation of parylene-C is investigated qualitatively by XPS and FTIR. The results show that the oxidation of parylene-C is very little at 100°C while it becomes serious at 200°C. This agrees with the prediction by Nowlin's neutron activation oxygen analysis. In contrast to the XPS's scanning only the surface of the materials, the FTIR results can prove that the oxidation of parylene-C actually happens through the specimen thickness. After annealed in air at 200°C, FTIR result also show that the oxidized parylene-C is composed of CO double bond and CO single bond, and the observed broad OH spectrum also indicates the likely decomposition and hydrolysis of parylene-C at high temperature.

Crystallization of parylene-C is studied by using x-ray diffraction technology. Crystallinity, d-spacing, and crystallite size are all investigated according to the XRD data. The crystallinity of as-deposited is reported in the literature as 60% to which all XRD results are calibrated accordingly. It is shown that the paryelne-C crystallinity and crystallite size increase rapidly when the specimens experience the high testing temperature. The crystallite size gets bigger with the progression of the annealing time and also as the annealing temperature increases. The time constant is found as 0.845 minutes according to the pre-annealed parylene-C crystallite size data. It also shows that the crystallization does not happen until temperature reaches ~ 50°C, which is strong evidence of showing parylene-C's glass transition temperature at 50°C. The d-spacing of (020) plane of parylene-C remains constant at around 6.31 Å during the isothermal XRD scanning at 100°C.

The glass transition temperature is investigated by using DMA scanning. Different pre-treated parylene-C specimens are prepared to study the oxidation effect,

influences of annealing temperature and of the annealing time. The glass transition temperature of as-deposited parylene-C is obtained as 53.4°C with glass transition range as 50.2–57°C. It is found that the glass transition temperature keeps up with the pre-annealing temperature higher than 60°C, while no T_g shift is found after pre-annealed at 40°C for 30 minutes. On the other hand, the glass transition range gets broader as the pre-annealing temperature increases. T_g is always obtained as the temperature close to and a bit higher than the pre-annealing temperature. No T_g difference is found regardless whether the specimen is pre-annealed in air or in vacuum oven at 100°C. Therefore, it can be concluded that the T_g is not seriously influenced by oxidation, or the oxidation effect is not the dominant effect at 100°C. T_g slightly increases with the longer pre-annealing time at the same annealing temperature. According to the T_g results, it is found that the T_g is very sensitive to the pre- annealing temperature. Combined with the crystallization study of the parylene-C, the T_g results can lead to the conclusion that the crystallization would be the main factor that causes the shift of the glass transition temperature. It is found that the glass transition temperatures previously reported by different groups vary widely from room temperature to 150°C. It is likely due to the non-standardized preparation of parylene-C samples which might have experienced different thermal processes prior to the glass transition temperature testing, causing difference in levels of crystallinity among the specimens.

The uniaxial tensile tests are performed on differently pre-annealed parylene-C samples in this chapter to investigate the influence of the crystallinity on the uniaxial tensile test results. It is found that parylene-C with higher crystallinity results in larger Young's modulus, tensile strength and less percent of elongation, which correspond to

stiffer, stronger and more brittle results. In addition, uniaxial tensile tests are also performed at different temperatures higher than 20°C. It shows that the Young's modulus decreases as the testing temperature increases, indicating the softening of the material and also proves parylene-C as the thermoplastic material.

Viscoelastic and viscoplastic properties of parylene-C have never been studied before and very rare papers about them are published. In this chapter, the viscoelastic and viscoplastic properties of parylene-C are first ever explored. It shows that the creep and stress relaxation results highly depend on the pre-annealing temperature. It is attributed to the T_g shift after the pre-annealing which renders the crystallinity change at the temperature for the pre-annealing processes. The creep results of parylene-C demonstrate a permanent strain remaining after the test, indicating that the parylene-C is a viscoplastic material. The conclusion can also be derived from the remaining permanent stress obtained after the stress-relaxation test. The remaining permanent strain or stress indicating that the yielding point of the parylene-C has changed at the elevated temperature, and cannot be found just by the regular point where the strain increases with no stress increase. Therefore, the loading/unloading experiment is performed at 37°C to understand this phenomenon. With the widely used parylene-C in the development of the biomedical devices, the viscoelastic and viscoplastic properties of parylene-C at 37°C need to be understand in more detail to avoid the unwanted device behavior happening in the human body after the devices implanted.

In summary, all experimental results presented in this chapter suggest that parylene-C film is a highly temperature-dependent polymer. With all the knowledge obtained in this chapter, people can tailor parylene-C's properties in order to satisfy their

needs for different applications. Because the CVD as-deposited parylene-C is deposited at the metastable state, it tends to crystallize immediately at the temperature higher than T_g and then transforms itself to a more stable state. In order to have devices with more stable parylene-C mechanical properties, it is suggested to pre-anneal the parylene-C at the temperature higher than the device's designed operation temperature prior to the usage of the devices to prevent the occurrence of the crystallization during its real operation.